REGULATION OF SMALL GTPASES IN EPITHELIAL CELL COLLECTIVE MIGRATION

A Dissertation

Presented to the Faculty of the Weill Cornell Graduate School

of Medical Sciences

in Partial Fulfillment of the Requirements for the Degree of

Doctor of Philosophy

by

Yun-Yu Tseng

January 2017

REGULATION OF SMALL GTPASES IN EPITHELIAL CELL COLLECTIVE MIGRATION

Yun-Yu Tseng, Ph.D.

Cornell University 2016

Collective migration is a complex process in which cells migrate together with multicellular polarity while connected with each other through cell-cell junctions. Epithelial collective migration is a fundamental process in development, and occurs in many contexts, from formation of ducts and glands to tissue homeostasis and regeneration. Small GTPases, including members of the Ras and Rho subfamilies, have been reported to be involved in migration. However, the detailed mechanism of how these small GTPases regulate collective migration remains unknown.

Rap1 GTPase, which belongs to the Ras subfamily, functions in cell-cell and cell-ECM connections, two important characteristics related to epithelial collective migration. I have shown that Rap1 activates Cdc42 in controlling epithelial collective migration, which may occur through a Cdc42 GEF, β-PIX, and a scaffold protein, IQGAP1.

In addition to Rap1, depletion of Rho, Rac, and Cdc42 induced collective migration defects in the human bronchial epithelial cell line (16HBE cells). Since RhoGTPases are activated by guanine nucleotide factors (GEFs) and inactivated by GTPase-activating proteins (GAPs), to understand which GEFs control RhoGTPases in epithelial collective

migration, I performed a small hairpin RNA screen targeting GEFs in 16HBE cells. Combining biological approaches and computational analysis, we discovered that SOS1, a Rac/Ras dual GEF, mediates Ras pathway in controlling epithelial collective migration. In addition to SOS1, we also found that ARHGEF18 controls RhoA and its downstream effector, myosin, in epithelial collective migration. Additionally, depletion of ARHGEF3, ARHGEF11, and ARHGEF28, Rho specific GEFs, also induced migration defects that were different from those induced by RhoA-depletion. Finally, depletion of several GEFs caused tight junction defects and also induced migration defects, which suggests that intact tight junctions may be required for epithelial collective migration. Overall, this study provides a potential mechanism by which Rap1 regulates epithelial collective migration and a comprehensive analysis of Rho GEFs involved in epithelial collective migration.

BIOGRAPHICAL SKETCH

Yun-Yu Tseng was born in Taiwan and earned her Bachelor of Science degree in agricultural chemistry at National Taiwan University and her Master of Science degree in biopharmaceutical sciences at National Yang-Ming University.

In 2009 Yun-Yu was enrolled in the doctoral program in Biochemistry, Cell, and Molecular Biology at the Weill Cornell Graduate School of Medical Sciences in New York and did her graduate research in Dr. Alan Hall's laboratory at Memorial Sloan-Kettering Cancer Center. Her graduate studies focused on the regulation of epithelial collective migration. During her graduate research in Dr. Hall's laboratory, Yun-Yu presented her research at the 2015 Annual Meeting of the American Society for Cell Biology. Her future goals include pursuing a career in the biopharmaceutical industry as a scientist.

DEDICATION

I dedicate my thesis to my beloved mentor, Dr. Alan Hall, who guided and supported me during my PhD study.

ACKNOWLEDGEMENTS

I would like to thank my mentor, Dr. Alan Hall for all his guidance and genuine advice. His passion and dedication to science have been my constant source of support and inspiration. I was extremely fortunate to have the opportunity to work and learn from him. To me, Alan was not only one of the greatest scientists, but also the greatest person that I have ever met. I will always remember him in this way.

I would also like to thank Dr. Michael Overholtzer, who unconditionally helped me finish my PhD study after Alan's untimely passing. I am very grateful for his guidance and support during this difficult time. In addition, I would like to thank my committee members, Dr. Jennifer Zallen and Dr. Antony Brown, for their time and precious suggestions throughout years.

I would like to thank Dr. Gaudenz Danuser and Dr. Assaf Zaritsky at UT Southwestern for their cooperation in analyzing the migrating behaviors of cells. I would also like to thank past and present members of the Hall laboratory, especially Dr. Angeles Rabadan, for her help in the collective migration screen, and Dr. Tatiana Omelchenko, Dr. Joanne Durgan, Dr. Sean Wallace, and Dr. Dan Jin for their generous support during my PhD study.

Finally, I would like to thank my family for their unconditional love and support over the years. None of this would have been possible without them.

TABLE OF CONTENTS

LIST OF FIGURES

LIST OF TABLES

Chapter 1 – Introduction

1.1 Overview

Coordinated cell movement, or collective cell migration, is a critical process involved in many stages of metazoan life. During development, collective migration contributes to the morphogenesis of several tissues and organs, such as mammary gland development, blood vessel sprouting and neural crest cell migration. In adult tissues, collective migration facilitates wound closure after injury, and is involved in the pathogenesis of diseases such as cancer. Cancer cells can spread or metastasize through a process called collective invasion, where cells disseminate in groups away from primary tumor sites.

Small GTPases control many cellular behaviors, such as proliferation, differentiation, adhesion, and migration. The Ras superfamily is divided into Ras, Rho, Rab, Ran, and Arf subfamilies based on their different sequences, structures, and functions (Goitre, Trapani et al. 2014). Among these, the Ras and Rho subfamilies have been shown to be important controllers of cell migration, involved in driving the migration of single cells and the collective migration of cell groups. How the many GTPases comprising these subfamilies coordinately regulate these complex processes remains poorly understood.

In this dissertation, I present my research into the regulation of epithelial collective migration. My research identified a role for the Rap1 GTPase in controlling collective migration and uncovered novel Rho Guanine nucleotide exchange factors (GEFs) that regulate this process. The role of collective migration in development and cancer progression, as well as the different small GTPase families and their functions in collective migration will be discussed.

1.2 Collective migration

Collective cell migration is defined as the ability of a group of cells to move together. The behaviors of the individual cells can affect the others, through stable or transient cell-cell interactions (Friedl and Gilmour 2009, Rorth 2012). For example, collective migration occurs in epithelial cells populations, where cells have strong cell-cell interactions, or in mesenchymal cells, that have looser cell-cell connections. Despite the difference in the strength of interaction, both epithelial and mesenchymal cells require these interactions to link individuals together and influence each other's migrating behavior. Cell-cell connection is mediated by homophilic interactions, such as those mediated by cadherin-based adherens junction proteins, including E-cadherin in epithelial cells, or N-cadherin in neural cells, together with tight junction proteins, desmosomal proteins and gap junction proteins (see section 1.5). Connections between cells can also form through heterophilic interactions, such as immunoglobulin superfamily members, including nectin and nectin-like families (Shimono, Rikitake et

al. 2012). While cadherin-based junctions are important for collective migration that occurs during development, such as branching morphogenesis of the mammary gland and trachea, blood vessel sprouting, or neural crest cell migration, whether other forms of cell-cell connections also play a role in collective migration is not clear.

Cells within adherent, collectively migrating groups also exhibit multicellular polarity and use "supracellular" actin organization to generate retraction forces and protrusion for migration (Friedl and Gilmour 2009). As for single cells, the front row cells generate actin-rich lamellipodia and pseudopodia to lead the migration, while the back row cells form cryptic lamellipodia beneath the proceeding cells, in the direction of migration (Farooqui and Fenteany 2005). Thus, cells co-regulate their cytoskeleton dynamics within the migrating group and coordinate each other's behavior to function like a single cell for efficient migration. Little is known about how cells form this supracellular cytoskeletal organization, but it is probably related to the cadherin-based or other junctional proteins-based cell-cell coupling (Friedl and Gilmour 2009).

Another characteristic of collective migration is that the migrating group can modify the extracellular matrix (ECM) as it moves, to clear a track to facilitate migration. For example, in 3D tissues, migrating cell groups encounter higher space restriction compared to single cell migration. Collective cell migration relies on the leader cells expressing membrane-type-1 matrix metalloproteinase (MT1-MMP) to create microtracks while the follower cells expand the track by lateral ECM degradation for generating a clear path of reduced mechanical resistance (Wolf, Wu et al. 2007). In

addition to ECM degradation, collective migrating cells also produce and assemble ECM materials, such as fibronectin, to provide a cohesive substrate that bridges neighboring cells and facilitates collective migration or invasion (Serres, Debarbieux et al. 2014). In some cases, collective migrating cells cooperate with the surrounding cells to generate the tracks for collective migration for example migrating epidermal keratinocytes and their neighboring dermal fibroblasts. Only in the keratinocyte and fibroblast co-culture system, collagen IV and laminin-1 deposition occurs to build the basal membrane (Smola, Stark et al. 1998). In collective invasion, stromal fibroblasts generate tracks to facilitate the following cancer cell movements (Gaggioli, Hooper et al. 2007).

In summary, collective migration depends on cell-cell adhesions, polarized actin cytoskeleton, and dynamic ECM modification within the migrating group, and may be facilitated by the surrounding environment. These collective migration events are involved in embryonic morphogenesis, tissue regeneration, and cancer invasion.

1.2.1 Collective migration in development and regeneration

Collective migration is one of the fundamental processes for embryonic morphogenesis and tissue regeneration in different animal models. Here, I describe the collective migration process in border cells in *Drosophila*, lateral line development in zebrafish, as well as mammary gland morphogenesis, vascular sprouting, and neural crest migration in mammals.

1.2.1a Border cell migration in Drosophila

One of the well-studied models of collective migration is the migration of border cells in *Drosophila.* The border cells contain four to eight migratory follicle cells and two less motile polar cells in the center (Montell, Rorth et al. 1992, Han, Stein et al. 2000). The polar cells secrete the cytokine Unpaired, which activates the JAK/STAT pathway in the neighboring follicle cells and induces them to detach from the follicular epithelium (Silver and Montell 2001, McGregor, Xi et al. 2002). The border cells migrate through the nurse cells to the anterior dorsal border of the oocyte, where they form the micropyle for sperm entry (Rorth 2002, Montell 2003). The oocyte secretes EGF (epidermal growth factor) and PVF1 (platelet-derived growth factor and vascular endothelial growth factor-related factor 1) and PVF2 to guide border cell migration (McDonald, Pinheiro et al. 2003, Bianco, Poukkula et al. 2007). While the activity of the Rac GTPase is highest in the leader cells and sets the direction of migration (Murphy and Montell 1996, Wang, He et al. 2010), live imaging of border cells migration reveals the leader and follower cells are also interchangeable during the period of migration (Prasad and Montell 2007). Between border cells and their substrate, the nurse cells, E-cadherin mediated adhesion functions in a positive feedback loop with Rac activity in the leader cells to stabilize forward-directed protrusion and directionality during movement. On the other hand, E-cadherin mediated adhesion between individual border cells facilitates direction communication in the leader and the follower cells, holds the cluster together, and polarizes the

individual border cells to have forward protrusions. Thus, E-cadherin is an integral component in border cell collective migration (Cai, Chen et al. 2014).

1.2.1b Literal line development in zebrafish

The zebrafish posterior lateral line (pLL) is a sensory system that comprises the mechanosensory organs, neuromasts, which contain sensory hair cells for water flow sensing. The neuromasts are deposited by the migrating posterior lateral line placode (primordium), which contains a cluster of more than 100 cells, from the anterior trunk to the tail of fish larvae (Haas and Gilmour 2006). The directional migration of placode cells is guided by the chemokine, Cxcl12a (also known as Sdf1a), which is expressed along the myoseptum. The migrating primordium expresses Cxcl12a receptor, Cxcr4b, in the leading edge and downregulates its expression in cells about to be deposited from the trailing edge (David, Sapede et al. 2002). Subsequently, another Cxcl12a receptor, Cxcr7, was discovered that is expressed in trailing cells of the primordium. The polarized expression of Cxcr4b and Cxcr7 is required for collective migration of the primordium (Dambly-Chaudiere, Cubedo et al. 2007, Valentin, Haas et al. 2007). Depletion of Cxcr4 impairs primordium migration, while depletion of Cxcr7 results in stretching of the trailing cells and impairs migration (Haas and Gilmour 2006, Valentin, Haas et al. 2007). Furthermore, these experiments suggest that Cxcr7 functions as a sink for Cxcl12a, sequestering Cxcl12a to generate the gradient for directional migration (Dona, Barry et al. 2013).

1.2.1c Mammary gland morphogenesis

Mammary gland development can be divided into three phases, embryonic mammary development and postnatal branching morphogenesis that start in puberty and then continue in the pregnancy/lactation period. In mice, the embryonic mammary gland originates as an epidermal placode, which then forms a stratified organization and invades into the mesenchyme. Upon late fetal development, the mature lumen forms, with cytokeratin 8-expressing luminal epithelial cells and basally positioned cytokeratin 14-expressing cells, which differentiate to myoepithelial cells during puberty (Hogg, Harrison et al. 1983, Sun, Yuan et al. 2010, Moumen, Chiche et al. 2011). At the onset of puberty, with stimulation from several steroid hormones, the simple quiescent mammary duct forms stratified terminal end buds (TEBs), which have multiple layers of epithelial cells and are surrounded by a basally positioned cap cell layer (Williams and Daniel 1983). TEBs elongate and form secondary branches to build bilayered ducts. During pregnancy/lactation, the mammary gland forms tertiary branches and the luminal epithelium goes through rapid cell proliferation and differentiation to form the secretory alveoli (Watson and Khaled 2008).

Many research studies utilize mammary glands at the puberty stage as material for studying epithelial branching morphogenesis. Moreover, the development of organotypic culture techniques has facilitated the establishment of mammary gland morphogenesis models *in vitro* within 3D ECM gels (Simian, Hirai et al. 2001, Fata, Mori et al. 2007). With long-term confocal imaging or transmission electron

microscopy-based imaging of primary organotypic 3D cultures of mouse mammary glands, mammary ducts were observed to elongate using collective migration without leading cell extensions or leading actin-rich protrusions (Ewald, Brenot et al. 2008, Ewald, Huebner et al. 2012). On the contrary, the interior epithelial cells within the stratified epithelium are highly protrusive and motile and have selective protrusions toward the direction of elongation (Ewald, Huebner et al. 2012, Huebner, Neumann et al. 2016). Further studies have demonstrated that Rac1 and MAPK signaling are required for cell migration and branch elongation in mammary gland development (Huebner, Neumann et al. 2016), but how these signaling pathways coordinate cell movements is poorly understood. Overall, the current data suggest that mammary gland elongation could be the consequence of a pushing, rather than a pulling, mechanism. Whether cell-cell adhesions could be involved in propagating these movements in concert with Rac and other GTPases awaits further mechanistic studies.

1.2.1d Vascular sprouting

Vascular sprouting occurs in both morphogenesis and tissue regeneration. Two phenotypically distinct cell types are primarily involved in vascular sprouting, namely "tip cells" and "stalk cells", defined by their gene expression profiles and endothelial cell functional specifications within the newly formed sprout. The tip cell, the leading cell, is migratory and polarized, and has multiple extended filopodia that determine the direction of the newly formed blood vessel. The stalk cell, the following cell, proliferates during sprout extension and forms the nascent inner lumen (Gerhardt,

Golding et al. 2003). A fine-tuned feedback loop between vascular endothelial growth factor (VEGF) and delta-like ligand 4 (DLL4)/Notch signaling establishes a "salt and pepper" distribution of tip and stalk cells within the activated endothelium. VEGF is essential for induction of tip cells, however, not all the cells with VEGFR expression can become tip cells. The cells which have high DLL4, and less notch activity, will be selected as the tip cells. Notch activation in the neighboring cells inhibits VEGFR2 expression and indirectly inhibits DLL4 expression, and therefore reinforces the dominance of the selected tip cell and limits the number of tip cells induced by VEGF (Hellstrom, Phng et al. 2007). However, tip cells and stalk cells are interchangeable during the elongation of the vessel, while stalk cells continuously migrate to the tip and change their phenotype to become tip cells, and tip cells can intercalate into the stalk (Jakobsson, Franco et al. 2010).

1.2.1e Neural crest migration

During vertebrate development, the neural crest cells emerge from the neural plate and undergo differentiation and epithelial-to-mesenchymal transition (EMT) before migration. Neural crest cells travel long distances throughout the developing embryo to nearly every major organ. They form streams or chains while migrating and are loosely connected with their neighbors through cadherins, tight junctions, gap junctions, and other cell-cell adhesion molecules (McKeown, Wallace et al. 2013, Kulesa and McLennan 2015).

Several *in vivo*, *in vitro* studies and computational analyses have addressed the mechanisms of neural crest migration. Two models are provided to answer the migratory behaviors of neural crest cells: the leaders and followers model, and the co-attraction and contact inhibition of locomotion (CIL) model (Szabo and Mayor 2016). VEGF, one of the chemotactic factors, is involved in neural crest cell migration. The leader cells migrate up VEGF gradients, while the followers migrate through the direct or indirect connection of leader cells, which is independent of VEGF gradient (McLennan, Teddy et al. 2010, McLennan, Schumacher et al. 2015). The leaders and followers are interchangeable; a follower turns in to a leader when it is exposed to a detectable VEGF gradient for a sufficiently long time while a leader cell changes to a follower once it fails to sense the VEGF gradient or when the VEGF gradient is lost (McLennan, Dyson et al. 2012, McLennan, Schumacher et al. 2015).

A second model of neural crest migration is the co-attraction and CIL model. In this model, co-attraction and CIL are coordinated to maintain a desired cell density for efficient collective migration. Neural crest cells secrete the complement factor C3a as a neural crest chemoattractant, which can counterbalance the tendency of neural crest cells to scatter via CIL or EMT (Carmona-Fontaine, Theveneau et al. 2011, Broders-Bondon, Paul-Gilloteaux et al. 2016). The polarity protein Par3 is required for CIL by inhibiting the Rac-GEF Trio and Trio-mediated Rac activation at cell-cell contacts (Moore, Theveneau et al. 2013). In summary, two models have been proposed to explain of the mechanisms of neural cell migration. A combination of *in vivo* and *in*

vitro experiments and computational simulations could provide more detailed mechanisms about neural crust cell migration.

1.2.2 Collective invasion of cancer

Collective migration behavior is not only found during embryonic development or tissue regeneration but also can be found in pathological states, such as collective invasion during cancer progression. One popular hypothesis to explain the mechanism of cancer cell metastasis is called epithelial to mesenchymal transition or EMT, a process whereby the epithelial-origin tumor cells change their identities from polarized, non-motile cells to unpolarized, highly motile mesenchymal cells that can invade into surrounding tissue as single cells (Christiansen and Rajasekaran 2006; Hanahan and Weinberg 2011). However, due to a lack of morphological evidence in human cancer tissue, this concept is debatable among clinical pathologists (Tarin, Thompson et al. 2005; McDonald, Maitra et al. 2012). Recent experimental evidence utilizing lineage tracing to track cancer cells that have undergone EMT also suggests that some cancers, for example breast carcinoma, can undergo metastatic spread in the absence of EMT induction (Fischer, Durrans et al. 2015). In addition to the EMT model, several researchers and clinical pathologists have found that cancer cells can also invade collectively into surrounding stroma, indicating the cancer cells still maintain cell-cell connections, expressing E-cadherin or other cell-cell adhesion molecules during invasion (Nabeshima, Inoue et al. 1999; Friedl and Wolf 2003; Bronsert, Enderle-Ammour et al. 2014). Notably, in addition to being present in

differentiated cancer types, cell-cell connections can also be found in poorly differentiated tumor cells. These cells form loosely attached small streams as they invade into the stroma (Wang, Enomoto et al. 2016). Those observations are in line with recent experimental evidence from breast cancer models demonstrating that distant metastases frequently arise from multicellular clusters that emerge from primary tumors by collective invasion, enter the blood stream as clusters, and extravasate to colonize distant sites as multiclonal seeds (Cheung, Padmanaban et al. 2016). Therefore, collective invasion may be one of the important mechanisms that initiate tumor metastasis.

Cancer cells use a leader-follower mechanism for collective invasion. The invading groups are connected through E-cadherin, and the leader cells express integrin β1 and podoplanin (Brockbank, Bridges et al. 2005; Wicki, Lehembre et al. 2006). Moreover, using three-dimensional (3D) organoid assays, researchers found that the leader cells in a tumor undergoing collective invasion express several basal epithelial genes, such as keratin 14 (K14), K5, P-cadherin and p63. Furthermore, K14+ cells were found in the leading edge of tumors undergoing collective invasion in the major human breast cancer subtypes. Moreover, luminal cancer cells convert to invasive basal cells by induction of basal epithelial genes. While few luminal cancer cells express basal epithelial genes, depletion of K14 or p63 was sufficient to block collective invasion in both in 3D culture and *in vivo*, which suggested that basal epithelial gene induction is required for collective invasion (Cheung, Gabrielson et al. 2013).

1.3 Ras GTPases family and collective migration

1.3.1 Ras superfamily of small GTPases

The Ras superfamily of small guanosine triphosphatases (GTPases) is composed of more than 150 members in humans, with evolutionarily conserved orthologs found in flies, fungi, yeast, worms, and plants (Rojas, Fuentes et al. 2012). They share a conserved structure and biochemical properties and act as a binary molecular switches, despite the divergences in sequence and function among the family members (Vetter and Wittinghofer 2001). Based on their sequences and functional similarities, the Ras superfamily can be divided into five families, include Ras, Rho, Rab, Ran, and Arf. With variation in structure, post-translational modifications that determine the subcellular localization, and different regulators and effectors, these small GTPases regulate a wide range of fundamental cellular process, including proliferation, differentiation, morphogenesis, polarization, adhesion, migration, survival and apoptosis (Goitre, Trapani et al. 2014).

The Ras superfamily proteins function as GTP/GDP molecular switches, cycling between the inactive GDP-bound form and active GTP-bound form. Guanine nucleotide exchange factors (GEFs) promote GDP dissociation and GTP binding to form the active GTP-bound form, while GTPase-activating proteins (GAPs) increase the intrinsic GTPase activity to promote the formation of the inactive GDP-bound form (Figure 1.1).

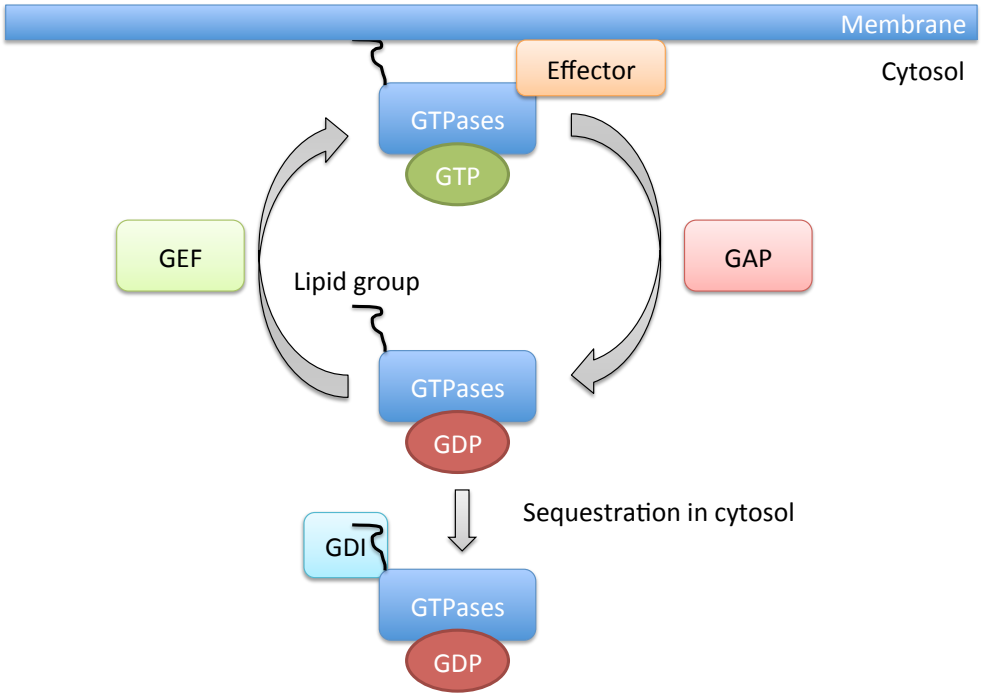

Figure 1.1 Regulation of Ras GTPases by GEFs, GAPs, and GDIs.
Ras GTPases are activated by GEFs, which promotes the release of GDP from GTPases, and inactivated by GAPs, which catalyze the intrinsic GTPase activity. The active GTPases bind to membranes and interact with downstream effectors for signal transduction. For Rho GTPases, Rho GDIs sequester the inactive GTPases in the cytoplasm by masking the lipid modification sites on the GTPases.

Structurally, the Ras superfamily members share a set of conserved sequence motifs at the N-terminus, named "G boxes" (G1 through G5). Together with five alpha helices (A1-A5) and six beta-strands (B1-B6), these motifs make up a ~20 kDa "G domain" (Ras residues 5-166) that process the basic function of guanine nucleotide binding and hydrolysis. The major conformational differences between GTP-bound and GDP-bound GTPases are in switch I (Ras residues 30-38) and switch II (Ras residues 59-67), where the core effector domain (Ras residue 32-40, includes switch I) is critical

for target effectors binding to GTP-bound GTPases (Figure 1.2) (Wennerberg, Rossman et al. 2005, Goitre, Trapani et al. 2014).

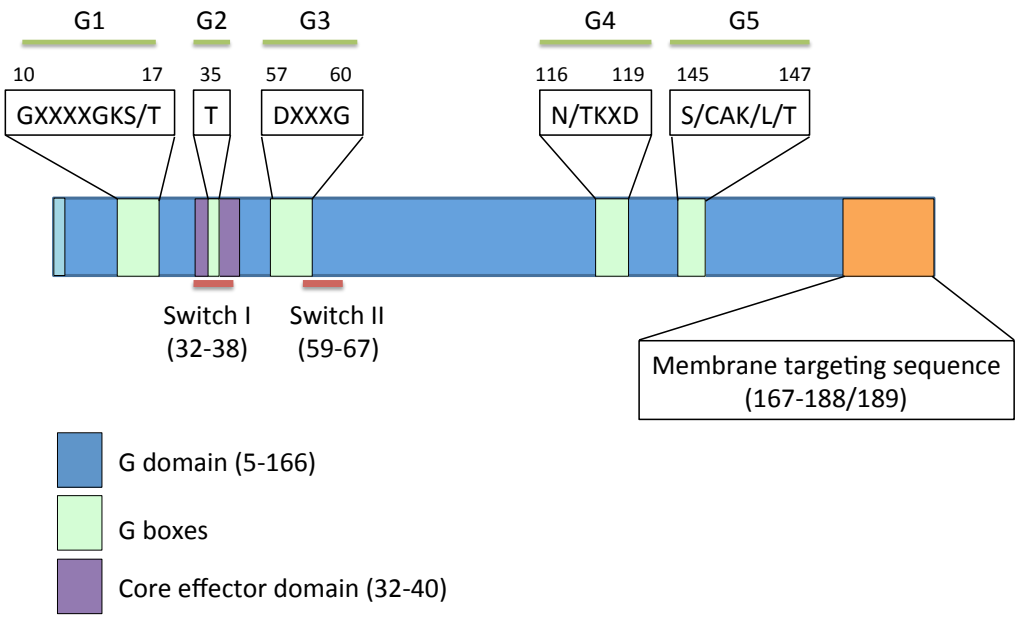

Figure 1.2 Ras functional domains
Ras family proteins contain common motifs with conserved sequence, named G boxes (G1 to G5) at N-terminus and post modification site at C-terminus for membrane targeting. Switch I and switch II are the regions where have the major structural difference between GTP-bound (active) and GDP-bound (inactive) GTPase. The core effector domain is important for the binding of effectors and GTP-bound GTPases.

Post-translational modifications of Ras proteins are important for determining their subcellular localization. The majority of Ras and Rho subfamily members terminate in a CAAX sequence, where C is cysteine, A is an aliphatic amino acid, and X is any amino acid. The CAAX motif is recognized by farnesyltransferase and geranylgeranyltransferase I, which catalyze the addition of a farnesyl or geranylgeranyl isoprenoid, respectively, to the cysteine residue of CAAX motif. When

coupled with a palmitoylated upstream residue, cysteine, the CAAX motif composes the membrane-targeting sequence that directs the interaction between different membrane compartments and controls subcellular localization. Other than GEFs and GAPs, Rho family proteins are regulated by the third class of proteins, guanine nucleotide dissociation inhibitors (GDIs), which sequester inactive Rho GTPases in the cytoplasm by masking the prenyl modification site and therefore inhibiting Rho GTPase activation (Ahearn, Haigis et al. 2012).

Although all the Ras superfamily members share a core structure which contains the conserved G box involved in guanine nucleotide binding and GTP hydrolysis, they have specific functions which result in multiple and divergent roles. Here I will focus on the Ras and Rho family among the Ras superfamily and their relationships with collective migration.

1.3.2 Ras GTPase family and collective cell migration

The Ras family is composed of more than 36 members and divided into Ras, Ral, Rap, Rad, Rheb, and Rit subfamilies based on their structural and functional differences. The Ras subfamily functions in cell proliferation, differentiation, survival, apoptosis, and gene expression(Goitre, Trapani et al. 2014). The Ral subfamily functions in GTP-dependent exocytosis. The Rap subfamily functions in cell-cell and cell-matrix adhesion. The Rad subfamily functions in cell shape remodeling and cell-cycle checkpoint. The Rheb subfamily functions in the mTOR pathway, cell growth and

cell-cycle progression. And finally, the Rit subfamily functions in neuronal differentiation and survival (Goitre, Trapani et al. 2014). Among these subfamilies, members of the Ras and Rap subfamily have been shown to play a role in collective migration. Here, I will focus on these two subfamilies.

1.3.2a Ras subfamily

The Ras sarcoma (Ras) oncoproteins are one of the most studied members of the Ras family because of their critical roles in human oncogenesis. The K-Ras and H-Ras genes and their transforming properties were identified in 1982 while another related transforming gene, N-RAS, was identified in 1983 (Der, Krontiris et al. 1982, Goldfarb, Shimizu et al. 1982, Parada, Tabin et al. 1982, Santos, Tronick et al. 1982, Shih and Weinberg 1982, Hall, Marshall et al. 1983). Gain-of-function missense mutations in Ras genes (K-RAS, N-Ras, and H-Ras) are found in 27% of all human tumors, with hotspot mutations at G12, G13, and Q61. Despite 82-90% identical amino acid sequences between Ras genes, K-Ras is the predominantly mutated isoform (85%), followed by N-Ras (11%) and H-Ras (4%) in human cancers (Hobbs, Der et al. 2016).

Ras proteins act as signaling hubs by responding to extracellular stimulation and propagating signals into cells (Wennerberg, Rossman et al. 2005). Activated Ras interacts with multiple and functional distinct downstream effectors, which control gene transcription and regulate cell proliferation, differentiation, and survival. The

best characterized Ras signaling pathway is activation of Ras by epidermal growth factor (EGF). Activated Ras then stimulates Raf, which turns on the ERK mitogen-activated protein kinase (MAPK) cascade. Once the EGF receptor binds to EGF, the receptor undergoes a conformational change, dimerization, and activation of its tyrosine kinase activity, which recruits the adaptor molecule growth-factor-receptor-bound protein 2 (GRB2). GRB2 links the receptor to the Ras exchange factor SOS, which activates Ras (Egan, Giddings et al. 1993, Gale, Kaplan et al. 1993, Li, Batzer et al. 1993, Rozakis-Adcock, Fernley et al. 1993). Activated Ras recruits Raf serine/threonine kinase to the plasma membrane and then promotes Raf activation (Leevers, Paterson et al. 1994). Raf phosphorylates and activates the MEK1/2 dual specificity protein kinase, which phosphorylates and activates ERK1/2 mitogen-activated protein kinase (Gomez and Cohen 1991). Finally, ERK phosphorylates and activates a variety of substrates, including transcription factors, protein kinases and phosphatases, cytoskeletal elements, signaling molecules, and apoptotic proteins. (Yoon and Seger 2006). Other than the Raf-MEK-ERK cascade, Ras also activates other downstream pathways, including phosphatidylinositol 3-kinase (PI3K), the RalGDS family of exchange factors, and the phospholipase C epsilon (PLCε) pathway (Goitre, Trapani et al. 2014).

"Leaders and followers" is one of the mechanisms for collectively migrating cells. Usually, leader cells express "guidance receptors", such as receptor tyrosine kinases (EGFR, PDGFR, and VEGFR) which activate downstream pathways. Studies using migrating MDCK epithelial sheets indicated the cells close to the wound edge display

elevated Erk1/2 activity, suggesting these cells represent a spatially distinct population of leader cells (Matsubayashi, Ebisuya et al. 2004, Nikolic, Boettiger et al. 2006). Other studies using transforming growth factor β (TGFβ) to induce collective migration of keratinocytes also showed that MEK/ERK activity is required for sheet migration (Chapnick and Liu 2014). However, the detailed mechanism of how the Ras pathway regulates collective migration still needs further investigation. Interestingly, it was recently reported by the Hall lab that Ras signaling is also required for the establishment of epithelial cell-cell adhesions, suggesting that Ras signaling could also influence collective forms of migration by coordinating cell-cell junctions (Durgan, Tao et al. 2015).

1.3.2b Rap subfamily

The subfamily of Rap proteins were first cloned based on the homology between the K-Ras and Rap proteins, which share about 50% identical sequences (Pizon, Chardin et al. 1988). The Rap subfamily includes two Rap1 (Rap1A and Rap1B) and three Rap2 (Rap2A, Rap2B, and Rap2C) proteins in mammals. They have 60% amino acid sequence homology, but can signal through distinct downstream pathways. While depletion of both Rap1 isoforms (Rap1A and Rap1B) in mice is embryonic lethal, the single deletions of each isoform alone only cause partial lethality indicating the functional redundancy of Rap1A and Rap1B isoforms (Chrzanowska-Wodnicka, White et al. 2015). On the other hand, Rap2 knockout mice have not been reported.

Several studies indicate Rap1 mainly functions in regulating cell adhesion. Rap1 regulates β1, β2, and β3 integrin subunits, which are connected to the actin cytoskeleton, to affect both integrin activity (affinity) and integrin clustering (avidity) depending on the integrin and the cell type (Bos 2005). Rap1 promotes integrin activation through its effectors, RapL and RIAM, depending on the cell type. In T-lymphocytes, RapL is recruited by Rap1 to activate αLβ2 integrin (Katagiri, Maeda et al. 2003). In other cell types that lack RapL, activated Rap1 interacts with RIAM, and then RIAM recruits talin to the plasma membrane where it activates integrin (Watanabe, Bodin et al. 2008, Lee, Lim et al. 2009). Other than mediating cell-ECM adhesion, Rap1 also functions in regulating cell-cell adhesion. The first indication that Rap1 regulates adherens junctions comes from research in *Drosophila*. Rap1 mutant cells condense their adherens junctions to one side of the cell, different from wild type cells where the adherens junctions are evenly distributed around the cell (Knox and Brown 2002). In MDCK cells, inhibition of Rap1 impedes E-cadherin expression on the cell surface (Price, Hajdo-Milasinovic et al. 2004). Depletion of several Rap-specific GEFs, such as C3G, PDZ-GEFs, and Epac, disrupts junctions in endothelial and epithelial cells (Hogan, Serpente et al. 2004, Cullere, Shaw et al. 2005, Dube, Kooistra et al. 2008). Rap1 may be involved at different steps of junction formation. The Rap GEF, C3G, directly binds to E-cadherin in immature junctions, but is mutually exclusive to the binding of β-catenin to E-cadherin (Hogan, Serpente et al. 2004). Therefore, this indicates that Rap activity is required for junction formation. However, another Rap GEF, PDZ-GEF2, is required for junction maturation, since depletion of PDZ-GEF2 causes zipper-like junctions, in which E-cadherin is recruited

to the cell-cell contacts but these fail to proceed to maturation (Dube, Kooistra et al. 2008).

Rap1 has been shown to regulate actin cytoskeleton organization and migration. Several actin modulating proteins, such as Rho, Rac, and Cdc42, have been linked to Rap activation. For example, Rap1 is directly linked to RacGEFs Vav2 and Tiam1 (Arthur, Quilliam et al. 2004), and RhoGAPs Arap3 and RA-RhoGAP (Yamada, Sakisaka et al. 2005, Krugmann, Andrews et al. 2006). Rap1 induces the translocation of Vav2 to localize Rac activity to sites of cell spreading (Arthur, Quilliam et al. 2004). Moreover, Rap1 interacts with Arap3 and affects PDGF-induced lamellipodia formation (Krugmann, Andrews et al. 2006). In *Dictyostelium discoideum*, Rap1 controls cell motility through regulation of myosin II (Jeon, Lee et al. 2007). The Rap1 GEF, Epac1, activates Rap1, β1 integrin-dependent cell adhesion, cell polarization, and enhances chemotaxis of monocytes (Lorenowicz, van Gils et al. 2006). Furthermore, several Rap1 effectors, such as Afadin/AF-6 and RIAM, directly interact with actin binding proteins, like profilin and Ena/VASP (Boettner, Govek et al. 2000, Lafuente, van Puijenbroek et al. 2004). Currently, it is not known whether Rap1 regulates collective migration. However, based on Rap1 functions both in cell-cell and cell-ECM adhesion, a role for Rap1 in this process seems likely.

1.4 Rho GTPase family and collective migration

The Rho family of small GTPases is composed of 20 members, including the best characterized Rho, Rac, and Cdc42 (Ridley 2015). Similar to Ras GTPases, Rho GTPases act as molecular switches which cycle between an active GTP form and an inactive GDP form. Activation of Rho GTPases is mediated by a family of approximately 80 GEFs, while the inactivation is performed by a family of approximately 70 GAPs (see section 1.3.1). Active Rho GTPases have been reported to interact with more than 100 downstream effectors, including serine/threonine kinases, tyrosine kinases, lipid kinases, lipases, oxidases, and scaffold proteins, and are involved in actin and microtubule cytoskeleton dynamics, gene expression, regulation of enzymatic activities, cell cycle progression, and cell morphogenesis (Jaffe and Hall 2005, Hall 2009). The existence of multiple GEFs, GAPs, and effectors of Rho GTPases suggests that the Rho signaling pathway is complex and the activity of the pathway depends on the spatiotemporal context in the cell.

1.4.1 Rho GTPases in migration

The concept that Rho GTPases are involved in migration was built by a series of landmark findings from Hall, Ridley and Nobes in the 1990s. They showed that Rac promotes lamellipodia formation upon growth factor stimulation (Ridley, Paterson et al. 1992), while Rho is required for stress fiber formation and focal adhesion assembly

downstream of growth factor stimulation (Ridley and Hall 1992). Cdc42 was later found to promote filopodia formation and to activate Rac (Nobes and Hall 1995). Both lamellipodia and filopodia are actin-rich membrane protrusions formed as a result of actin polymerization. While lamellipodia are broad protrusions formed by a branched actin filament network, filopodia are finger-like extensions containing parallel bundles of actin filaments (Ridley 2011). Stress fibers are large bundles of actin filaments extending across a cell, which are anchored by focal adhesions and cross-linked by a periodically distributed a-actinin and myosin II (Burridge and Wittchen 2013). Further studies showed the complexity of Rho GTPases signaling pathways in controlling migration. Rac binds to WAVE1, which leads to Arp2/3 complex activation and actin assembly (Eden, Rohatgi et al. 2002). Rac1 also controls cofilin activity via the Rac-PAK-LIMK pathway (Arber, Barbayannis et al. 1998, Yang, Higuchi et al. 1998). Cofilin severs actin filaments at protrusions and provides free barbed ends of existing actin filaments, which promotes Arp2/3 binding and stimulates branching. Cdc42 interacts with N-WASP, which also promotes the activation of the Arp2/3 complex (Miki, Sasaki et al. 1998), and mDia2, which nucleates and elongates actin filaments (Peng, Wallar et al. 2003). RhoA is known to provide contractility and promote tail retraction during migration. Rho activates ROCK, which activates myosin light chain kinases and myosin II for actomyosin contraction (Totsukawa, Yamakita et al. 2000), and mDia1, which promotes actin polymerization (Watanabe, Kato et al. 1999). Recently biosensor studies suggest that Rho is also activated at the leading edge during migration, and indicates that RhoA is involved in the initiation of protrusions, whereas Rac1 and Cdc42 facilitate the reinforcement and stabilization of newly

expanded protrusions (Machacek, Hodgson et al. 2009). Together, Rho GTPases control migration through protrusion formation, front-back polarity, actomyosin contractility, and the turnover of the cell-matrix and cell-cell adhesion, which together regulate the different aspects of cell migration (Figure 1.3).

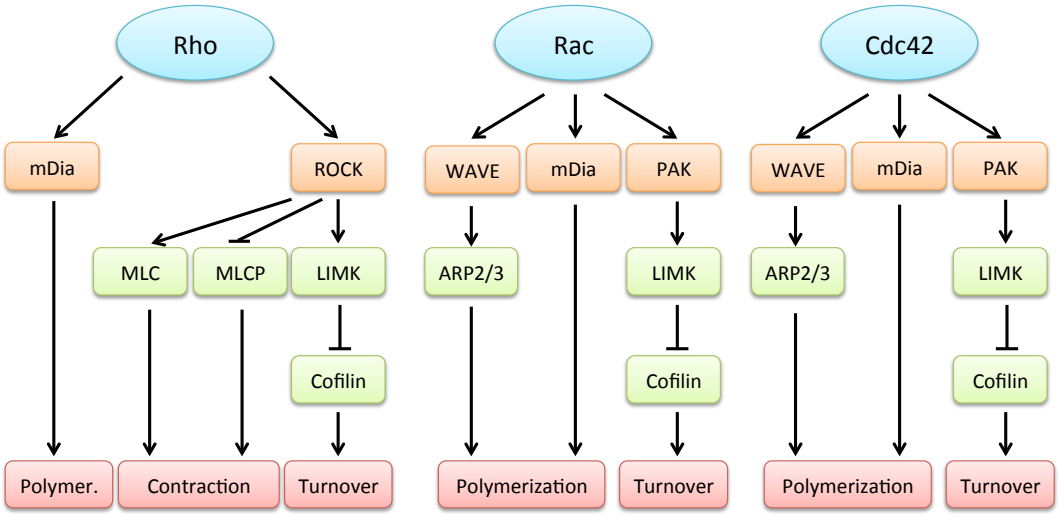

Figure 1.3 Rho GTPase signaling in controlling the actin cytoskeleton.
Active Rho, Rac, and Cdc42 interact with downstream effectors including kinases, ROCK and PAK, and nucleation promoting factors, mDia, WAVE and WASP, to control the dynamics of the actin cytoskeleton structure. After mDia induces actin nucleation to produce unbranched actin filaments, WASP and WAVE bind to the ARP2/3 complex and this leads to actin polymerization. PAK phosphorylates LIMK, which in turn phosphorylates and inhibits cofilin activity, thereby regulating actin turnover. Rho activates ROCK and ROCK phosphorylates MLCK and MLCP, which increases the phosphorylation of myosin light chain and contribute to the contractility. Abbreviation: mammalian Diaphanous-related formins (mDia), Rho-associated protein kinase (ROCK), WASP-family verprolin-homologous protein (WAVE), p21-activated kinase (PAK), myosin light chain (MLC), myosin light chain phosphatase (MLCP), LIM-kinase (LIMK), and actin-related protein-2/3 (ARP2/3).

1.4.2 Rho GTPases in cell-cell adhesion

For collectively migrating cells, each cell needs to maintain stable or transient cell-cell adhesion during movement (see section 1.2). Cell-cell adhesion in epithelial cells is mediated by the apical junctional complex, which includes tight junctions, adherens junctions, and associated actin filaments, desmosome, and gap junctions. The establishment and maintenance of the apical junctional complex are mediated by Rho GTPases.

Rac1-WAVE-Arp2/3 and Cdc42-N-WASP-Arp2/3 pathways are required for actin polymerization in the initial formation of junctions to facilitate E-cadherin engagement at the primordial junctions (Ehrlich, Hansen et al. 2002). Rho-mDia dependent actin polymerization, which generates linear F-actin filaments, also stabilizes the primordial junctions (Kobielak, Pasolli et al. 2004). Moreover, Rho-mediated actomyosin contractility and Rac/Cdc42 mediated actin polymerization provide the mechanical force to seal the neighboring membranes and result in expansion/linearization of adherens junctions (Vasioukhin, Bauer et al. 2000, Ehrlich, Hansen et al. 2002, Sahai and Marshall 2002). As junctions mature, cells elongate and generate distinct tight junctions that include claudins and ZO proteins (ZO-1, ZO-2, and ZO-3), occludin, JAM-A and other proteins. Cdc42 promotes the formation of the Par6-aPKC-Par3 complex, which activates aPKC activity and phosphorylates several tight junction proteins to facilitate the establishment of apical-basal polarity and the segregation of apical tight junctions (Suzuki, Ishiyama et al. 2002, Wallace, Durgan et

al. 2010, Quiros and Nusrat 2014). Furthermore, the established adherens junctions undergo continuous remodeling by endocytosis and recycling of cadherins (de Beco, Gueudry et al. 2009) and Rho, Rac, and Cdc42 contribute to both the stabilization and the turnover of junctional proteins (Quiros and Nusrat 2014). Therefore, the activities of Rho, Rac, and Cdc42 regulate junction establishment, maturation, and stabilization.

1.4.3 Rho GTPases in collective migration

Together, Rho GTPases regulate general cell migration and cell-cell adhesion, the two important components in collective migration, which suggests they also function in collective migration. For the leader and follower mode of collective migration, where the leader cells form filopodia and lamellipodia at the front and are connected to the follower cells at the rear, the initial formation of protrusions in the leading edge depends on Rac- and Cdc42-mediated actin polymerization and polarization. In *Drosophila* border cell migration, E-cadherin mediated adhesions between leaders and followers provide a feedback loop with Rac signaling to stabilize the forward-directed protrusions and generate a stable front (Cai, Chen et al. 2014). During vascular sprouting in zebrafish, ARHGEF9b activates Cdc42 to bind to Formin-like 3, which induces the extension of endothelial filopodia and migration (Wakayama, Fukuhara et al. 2015). Moreover, in endothelial cell culture, Angiopoietin-1 promotes the formation of an atypical protein kinase C (PKC)-ζ and β-catenin complex at the leading edge of migrating endothelial cells, which brings Par3, Par6 and adherens junction proteins at the front to locally activate Rac1 and facilitates collective

migration (Oubaha, Lin et al. 2012). During neural crest cell migration, N-cadherin inhibits protrusion and Rac1 activity at the cell-cell contacts, and in turn promotes protrusion and Rac1 activation at the front edge (Theveneau, Marchant et al. 2010). RhoA also contributes to the formation of leader cells during collective migration. Cultured MDCK cells form finger-like structures during collective migration, where the leader cells drag its followers by mechanical force generated in the leader. Addition of Y27632, that inhibits Rho-kinases, blebbistatin that is an inhibitor of myosin-II contraction, or C3 transferase that inhibits RhoA-C GTPases, inhibits the finger structure formation. Therefore, Rho signaling controls the development of the finger structure via mechanical cues, through which leader cells drag the migrating structure while the peripheral actomyosin cable prevents the initiation of new leader cells (Reffay, Parrini et al. 2014). Furthermore, both pushing and pulling mechanotransduction forces are transmitted between the migrating cells and between the cells and the substrates, suggesting Rho-mediated actomyosin contractility is important in the regulation of collective migration (Tambe, Hardin et al. 2011, Ng, Besser et al. 2012).

1.5 RhoGEFs and collective migration

The activation of Rho GTPases is mediated by RhoGEFs, which catalyze the exchange of GDP to GTP. Once Rho GTPases are activated, they interact with several downstream effectors that modulate distinct cellular activities (see section 1.3.1).

There are approximately 80 RhoGEFs in the human genome, encoded by two gene families: the Dbl family, which contains 69 members in humans, and the DOCK family, which is composed of 11 members. It remains unclear why these two subfamilies coexist, and whether they conduct signals at the same time under some conditions.

Since there are approximately four times more Rho GEFs than Rho GTPases, this suggests that a single Rho GTPase can be regulated by several Rho GEFs and there may be functional redundancy amongst the Rho GEFs. Furthermore, a single Rho GEF can activate more than one GTPase, and thus the actual number of GEFs that can act on a single Rho GTPase is even higher. It is believed that Rho GEFs provide the spatial and temporal control of Rho GTPase activity, and therefore they contribute to specificity, as well as the complexity of Rho GTPase signaling.

1.5.1 Dbl family

The first mammalian Rho GEF was identified as a transforming gene from diffuse B-cell-lymphoma cells, and therefore named Dbl (Eva, Vecchio et al. 1988, Hart, Eva et al. 1991). Dbl contains a region of about 240 residues that is homologous with Cdc24, a Cdc42 GEF in budding yeast. Since then, 69 distinct members of the Dbl family have been identified in humans. The Dbl family is characterized by a Dbl homology (DH) catalytic domain, followed by an adjacent C-terminal pleckstrin homology (PH) domain, and the DH-PH domain is essential for GEF activity *in vivo*. Outside the DH-PH domain, Dbl family members show great diversity and contain different protein

domains that contribute to the specificity of GEFs under different cellular conditions (Rossman, Der et al. 2005).

The DH domain, composed of about 200 amino acids, is the minimal region required for nucleotide exchange activity *in vitro*. DH domains contain three conserved regions, CR1, CR2, and CR3. CR1, CR3, and conserved residues within the C terminus of the domain (helix α6) constitute the GTPase binding surface. Switch 1 of Rho GTPases interacts with CR1 and CR3, while switch 2 of Rho GTPases predominantly contacts with CR3 and helix a6 region. Furthermore, part of the Rho GEF and GTPase interface is formed by the seatback region of the DH domain on the GEF and β2, β3 strands of switch regions on the GTPase. These interaction regions are highly variable between different GEFs and GTPases, and are important for determining the specificity. Interactions between the GEF DH domain and the GTPase cause the rearrangement of the GTPase structure and induce the dissociation of GDP. As GTP is more abundant than GDP in the cells, the dissociation of GDP allows the rebinding of GTP to the GTPase. Binding of GTP causes the dissociation of the GEF from the GTPase, which leaves the GTPase in the active form for interacting with downstream effectors (Rossman, Der et al. 2005).

PH domains, composed of about 100 amino acids, are found C-terminal to the DH domains, and facilitate the activation of Rho GTPases. In contrast the structural similarity between the DH domains of different GEFs, the PH domains are positioned differently relative to the DH domain. For example, the DH and PH domains of Dbs

directly interact with Cdc42, and the interaction is required for efficient Rho GTPase activation (Rossman, Worthylake et al. 2002). However, PH domains of other GEFs, such as Tiam1 that forms complex with Rac and ITSN-L that forms complex with Cdc42, do not directly interact with the DH domain-bound GTPase (Karnoub, Worthylake et al. 2001, Pruitt, Karnoub et al. 2003). Therefore, direct binding of the GTPase is not a general mechanism for the function of PH domains. PH domains have also been proposed to facilitate the interaction of GTPases with the plasma membrane. The interaction of PH domains with phosphoinositides on the membrane could orientate the DH domain so it can properly bind to Rho GTPases. Other than the interaction with the lipid bilayer, the PH domain also been proposed to function as a docking site for the downstream effectors of Rho GTPases. For example, the PH domain of Dbl directly binds to ezrin, which is activated by Rho GTPases to link the plasma membrane and the actin cytoskeleton (Vanni, Parodi et al. 2004). Although the functions of the PH domains are distinct in different Dbl GEFs, the fact that Dbl family members invariably contain a PH domain adjacent to their DH domain suggests that it plays an important role in GEF function.

1.5.2 DOCK family

The second GEF family, the Dock family, contains 11 members. Lacking sequence homology to DH domains in the Dbl family, they are characterized by the presence of two evolutionarily conserved domains: Dock homology region-1 and -2 (DHR-1 and DHR-2). The DHR-1 domain of Dock GEFs directly interacts with PIP3, and therefore

facilitates their membrane recruitment; while the DHR-2 domain of Dock GEFs is sufficient for promoting guanine nucleotide exchange *in vitro* (Brugnera, Haney et al. 2002). A distinct characteristic of Dock GEF members is the specificity of activating Rac or Cdc42, but not Rho or other members of the Rho GTPase family (Cote and Vuori 2002, Cote and Vuori 2006).

Based on the similarity of protein sequences and the presence of different functional domains, Dock family members are divided into four subgroups: Dock-A (Dock1, 2, and 5) and Dock-B (Dock3 and 4), which have specific GEF activity toward Rac; Dock-C (Dock 6, 7, and 8), which has Rac/Cdc42 dual GEF activities; Dock-D (Dock 9, 10, and 11), which has specific GEF activity toward Cdc42. The N-terminus of Dock-A/B GEFs mediates their interaction with Elmo scaffolding proteins, which is required for Rac-dependent actin cytoskeleton remodeling (Komander, Patel et al. 2008), while the C-terminus PxxP region facilitates interactions between SH3-containing adaptor proteins, such as Crk and Grb2. Dock-D members contain PH domain at their N-terminus, which is involved in binding phosphoinositides for membrane targeting (Laurin and Cote 2014). For the Dock GEF family, most studies have characterized the function of the DHR-1 and DHR-2 domains. It is possible that other regions in those GEFs provide scaffolding or regulatory functions in Rho GTPase signaling, which requires further investigation.

1.5.3 Rho GEFs and migration

One of the key events for cell to migrate is the formation of lamellipodia or filopodia in the direction of cell movement, and that requires Rac or Cdc42 activation for establishing and maintaining polarized protrusion (see section 1.4.1). Dock1 (also named Dock180), a Rac GEF, and β-PIX, a Rac/Cdc42 dual GEF, have been reported to activate Rac or Cdc42 at the front of migrating cells (Kiyokawa, Hashimoto et al. 1998, Li, Hannigan et al. 2003). Both Dock1 and β-PIX are localized to sites of adhesion near the leading edge of protrusions. The paxillin-p130Cas-CrkII complex brings Dock1 to these focal adhesions, while the paxillin-GIT-PAK complex recruits β-PIX to the adhesion site to activate Rac or Cdc42 (Kiyokawa, Hashimoto et al. 1998, Li, Hannigan et al. 2003). In addition to Dock1 and β-PIX, Tiam1, a Rac GEF, and Asef1 and Asef2, Rac/Cdc42 dual GEFs, have also been implicated in the regulation of cell migration (Kawasaki, Sato et al. 2003, Bristow, Sellers et al. 2009, Wang, Watanabe et al. 2012).

RhoA is believed to contribute to contractility through tail retraction, and may be involved in the formation of protrusions during cell migration (see section 1.4.1). Knockout of Lsc (p115RhoGEF), a Rho-specific GEF, is unable to generate and sustain a single-dominant pseudopod in neutrophils. Moreover, loss of Lsc causes cells to become loosely attached compared to wild type cells. As a result, they migrate faster but with reduced directionality, which suggests Lsc is involved in the regulation of cell migration (Francis, Shen et al. 2006). Similarly, knockdown of Syx1

(PLEKHG5), a Rho-specific GEF, in breast and brain tumor cells fails to form lamellipodia in the direction of migration (Dachsel, Ngok et al. 2013). Furthermore, depletion of PDZ-RhoGEF (ARHGEF11) or Net1 inhibits tail retraction and affects focal adhesion turnover during lysophosphatidic acid (LPA)-stimulated migration (Iwanicki, Vomastek et al. 2008, Carr, Zuo et al. 2013). Together, several Rho GEFs regulate RhoA activity during different steps of migration.

Several studies have implicated Rho GEFs in the regulation of single cell migration, however it remains largely unknown which Rho GEFs control GTPase activity during collective migration. β-PIX has been shown to be involved in both single cell migration and collective migration. Depletion of β-PIX disrupts epithelial collective migration *in vitro* and collective anterior visceral endoderm (AVE) cell migration in the early mouse embryo (Omelchenko, Rabadan et al. 2014). The expression and activities of Rho GEFs are cell-type specific and may be different in various culture conditions or distinct migration modes. Therefore, whether the same Rho GEFs involved in single cell migration also play a role in collective migration is unknown and requires future investigation.

1.6 Thesis objective

Collective migration is a coordinated movement of physically connected cells, which is required for proper metazoan development and also contributes to disease

progression in cancer. Rho GTPases regulate both single cell and collective migration. However, whether other small GTPases are involved and how Rho GTPases are regulated in epithelial collective migration are still unknown. I used 16HBE, a human bronchial epithelial cell line as a model, to study epithelial collective migration. In Chapter 3 of this dissertation, I identified Rap1, a Ras-family GTPase, as a regulator of epithelial collective migration. In Chapter 4 of this dissertation, I discovered several Rho GEFs related to epithelial collective migration by screening a shRNA library, which targets 80 Rho GEFs in the human genome.

Chapter 2 - Materials and Methods

2.1 Reagents

2.1.1 DNA constructs

The DNA constructs used are listed in Table 2.1. All constructs were verified by sequence analysis (MSKCC sequencing facility).

Table 2.1 DNA expression constructs

Plasmid name	Description and source
pQCXIP-HA-Rap1A WT	Rap1A WT was applified from pMT-mycRap1A WT construct by PCR and add HA tag on the N-terminal site using the following primers. Forward: 5'-CGCGCACCGGTGCCACCATGTACCCATACGATGTTCCAGATTACGCTCG TGAGTACAAGCTAGTGGTCCTTGGT-3' Reverse: 5'-GCGCGGAATTCCTAGAGCAGCAGACATGATTTCTTTTT -3' AgeI/EcoRI fragment coloned into AgeI/EcoRI pQCXIP.
pQCXIP-HA-Rap1A V12	Rap1A V12 was applified from pRK5-mycRap1A V12 construct by PCR and add HA tag on the N-terminal site using the following primers. Forward: 5'-CGCGCACCGGTGCCACCATGTACCCATACGATGTTCCAGATTACGCTCG TGAGTACAAGCTAGTGGTCCTTGGT-3' Reverse: 5'-GCGCGGAATTCCTAGAGCAGCAGACATGATTTCTTTTT -3' AgeI/EcoRI fragment coloned into AgeI/EcoRI pQCXIP.
pQCXIP-HA-Rap1A N17	Rap1A N17 was applified from pRK5-mycRap1A N17 construct by PCR and add HA tag on the N-terminal site using the following primers. Forward: 5'-CGCGCACCGGTGCCACCATGTACCCATACGATGTTCCAGATTACGCTCG TGAGTACAAGCTAGTGGTCCTTGGT-3' Reverse: 5'-GCGCGGAATTCCTAGAGCAGCAGACATGATTTCTTTTT -3' AgeI/EcoRI fragment coloned into AgeI/EcoRI pQCXIP.
pEGFP-bPIX	EGFP-tagged human β-PIX was from Dr. Tatiana Omelchenko
pEGFP-myc-βPIX	Myc and EGFP tagged human β-PIX was from Dr. Tatiana Omelchenko
pEGFP-IQGAP1	EGFP-tagged human IQGAP1 was from Addgene plasmid 30112

2.1.2 shRNA library

An shRNA library was constructed in pSUPERpuro. This library contains at least 3 hairpins per gene for 80 predicted human Rho GEFs. Cdc42 shRNA was cloned into pSUPERpuro construct and made by Dr. Tatiana Omelchenko. ARHGEF3 and Rho shRNAs were obtained from the TRC library collection in pLKO.1 construct (MSKCC RNAi core facility). The selected shRNA sequences are listed in Table 2.2.

Table 2.2 shRNA reagents

Gene Name	shRNA number	TRC number	Sequence
BCR	sh126	-	AGGATCCAACGACCAAGAA
PLEKHG2	sh127	-	GGACCTCAATCACTGAAGA
	sh129	-	AGCGCATTCTCAAGTACCA
PLEKHG6	sh147	-	GTGAGGCTGCACACTTTCA
ARHGEF11	sh181	-	GAACCTGCCTGAACTCATA
	sh182	-	GGAACTCGGTACTGTCAGA
ARHGEF18	sh172	-	GAAGCTGTTAGTCATTACA
	sh174	-	GGCTACGACTGCACAAACA
β-PIX	sh190	-	GGATATTAGTGTCGTGCAA
	sh192	-	AGACTGTGCTTTCAACGTA
ARHGEF28	sh232	-	ACTCAGTTCTCATGATGTA
	sh234	-	GAGGACTAGTGAACATCAA
SOS1	sh199	-	ACAGTTGAGTGGCATATAA
	sh201	-	GGCAGAAATTCGACAATAT
ARHGEF3	sh543	TRCN0000047543	GCCTAGTAATAAACGGGTCAA
	sh546	TRCN0000047546	CGCAAACTAGATCTCTGGAAT
	sh547	TRCN0000047547	CCCATGCTGAAACTCTCCATA
Rho	sh1	TRCN0000047710	GTACATGGAGTGTTCAGCAAA
	sh2	TRCN0000047711	CGATGTTATACTGATGTGTTT
Cdc42	sh1	-	GATGACCCCTCTACTATTG

2.1.3 Antibodies

Primary antibodies used for western blot include β-actin (A5316, Sigma) at 1:50000, ARHGEF18 (EB06163, Everest) at 1:500, BCR (N-20, sc-885, Santa Cruz Biotechnology) at 1:1000, Cdc42 (610929, BD Transduction) at 1:1000, E-cadherin (13-1900, Invitrogen) at 1:1000, ERK1/2 (M5670, Sigma) at 1:2000, phospho-ERK (M8159, Sigma) at 1:1000, HA (clone 12CA5, CRUK) at 1:1000, Intersectin 2 (H00050618-A01, Abnova) at 1:1000, LARG (N-14, sc-15439, Santa Cruz Biotechnology) at 1:1000, Myosin Light Chain 2(3672S, Cell Signaling) at 1:1000, phospho-myosin light chain 2 (3675S, Cell Signaling) at 1:500, α-PIX (4573S, Cell Signaling) at 1:1000, β-PIX (07-1450, Millipore-Chemicon) at 1:2000, Rac1 (23A8, Abcam) at 1:2000, RhoA (sc-418, Santa Cruz Biotechnology) at 1:500, RhoA/C (sc-179, Santa Cruz Biotechnology) at 1:500, SOS1 (C-23, sc-256, Santa Cruz Biotechnology) at 1:1000, SOS2 (C-19, sc-258, Santa Cruz Biotechnology), Taim1 (C-16, sc-872, Santa Cruz Biotechnology), Trio (D-20, sc-6060) at 1:500, α-tubulin (MCA77S, Serotec) at 1:2000. Secondary polyclonal antibodies conjugated with HRP for western blot were from Dako and used at 1:5000.

Primary antibodies used for immunofluorescence include E-cadherin (13-1900, Invitrogen) at 1:100, ZO-1 (61-7300, Invitrogen) at 1:100. Secondary antibodies conjugated with Alexa 488 or Alexa 568 (Invitrogen) at 1:400.

2.1.4 Primers for PCR and qPCR

The primers for PCR and qPCR detection were designed using NCBI Primer-Blast. The primers were selected because: first, they must be specific to the target gene and be able to detect all transcription variants of the gene; second, the primers span exon-exon region to avoid amplifying the genomic DNA; third, the PCR product size was between 70-150 base pairs for qPCR detection; and fourth, the primer melting temperature (Tm) was between 57°C to 63°C, with optimization at 60°C. Two sets of primers were selected for each gene. After testing the primer efficiency using qPCR, the suitable primer was selected for experiments.

2.1.5 Other reagents

Other reagents used include Alexa Fluor 488 phalloidin (A12379, Invitrogen) at 1:200, Hoechst 33342 (Sigma) at 1 μg/ml, Y27632 (HA139, Sigma) at 10 μM, Blebbistatin (203391, Calbiochem) at 10μM, ERKi (SCH772984, provided by Neal Rosen Lab, MSKCC) at 1μM, GSK1120212 (S2673, Selleckchem) at 500 nM, PD0325901 (S1036, Sellleckchem) at 500 nM.

2.2 Cell Biology

2.2.1 Cell culture conditions

The human bronchial epithelial cell line, 16HBE14o- (16HBE), which was kindly provided by the laboratory of Dr. Dieter C. Gruenert (University of California, San Francisco). 16HBE cells were cultured in MEM (MSKCC core facility), supplemented with 10% fetal bovine serum (FBS)(Omega Scientific, lot number 169905), GlutaMAX (35050, Gibco), and a mixture of penicillin-streptomycin (100X, 10000 U/mL) (15140, Gibco). The media for stable cell line selection were added with 1.5μg/mL puromycin (P7255, Sigma). 16HBE cells were cultured in a 37°C incubator with 5% CO_2. Cells were passaged when 70% confluent, every 3-4 days.

HEK293T cells were purchased from ATCC, and grown in DME high glucose + sodium pyruvate (MSKCC core facility) supplemented with 10% FBS (Omega Scientific, lot number 169905) and a mixture of penicillin-streptomycin (100X, 10000 U/mL) (15140, Gibco). Cells were cultured in a 37°C incubator with 5% CO_2 and passaged when 80-90% confluent, every 3-4 days.

2.2.2 Virus production and purification

For virus production, 90% confluent HEK293T cells cultured in 6-well plate were transfected with 1 μg VSVG, 1 μg pDeltaR8.9 and 1 μg lentiviral construct for

lentivirus production or 1 μg VSVG, 1 μg pCpG gag pol and 1 μg retroviral vector for retrovirus production. DNA constructs were transfected in to cells using Lipofectamine 2000 transfection reagent (11668, Invitrogen) with Opti-MEM (31985, Invitrogen) according to the manufacturer's instruction. The culture media were removed the next day after infection, and the media were collected daily for the following 3 days for virus collection. Virus-containing media were pooled, centrifuged at 1000 rpm for 5 min to remove cell debris, and filtered through 0.45 μm filter, then aliquoted and stored in -80°C. For each batch of virus production, total 3 mL virus-containing media were collected for future use.

2.2.3 Virus infection

$2x10^5$ 16HBE cells were seeded in each well of a 6-well plate and infected on the following day. The original media was removed and 1.5 mL virus-containing media supplemented with 1.5 μL polybrene (8 μg/μL stock, Sigma) was added for spin infection at 2250 rpm for 30 minutes. The viral media were discarded and replaced by regular 16HBE media after centrifugation. Selection was started two days after infection with 1.5 μg/mL puromycin (Sigma). Pooled stable cell lines were established for the future experiments.

2.2.4 Wound healing assay and colony migration assay

For the wound healing assay, $3x10^6$ 16HBE cells were seeded in each well of a 6-well plate (Falcon) and incubated for two days before the experiment. A 1000P tip was used to scratch a wound on the confluent monolayer in the middle of well, and a cell scraper was used to remove half of the cells from the plate. After washing with PBS several times to remove cell debris and adding fresh 16HBE media, the plate was imaged on a time-lapse microscope for 16 hours, with 5 minutes / frame to record the cell migration behaviors.

For the colony migration assay, $2x10^5$ 16HBE cells were seeded in each well of a 6-well plate (Falcon) and incubated for three days before the experiment. After adding fresh 16HBE media, the plate was imaged on a time-lapse microscope for 16 hours, with 5 minutes / frame to record the cell migration behaviors.

2.3 Molecular Biology

2.3.1 RNA extraction and cDNA preparation

Total RNAs were extracted using RNeasy Plus Mini Kit (74134, QIAGEN), following the instructions from the manufacturer. The RNA concentration were measured by Nanodrop and adjusted to 100 ng/μL. cDNA preparation was carried out using 1 μg RNA, 1 μL Oligo dT or Random hexamer primer (IDT technology), and 1.5 μL

RNase-free H2O. The RNA mixtures were heated on PCR machine at 65°C for 5min, then chilled on ice, and added 4 μL or 5X Reaction buffer (Thermo Scientific), 0.5 μL RiboLock RNase inhibitor (EO0381, Thermoscientific), 2μL 10mM dNTP (Sigma), and 1 μL RevertAid reverse transcriptase (EO0441, Thermo Scientific). Then the reverse transcription reactions were performed on the PCR machine using the following program: 25°C for 10 mins, 42°C for 60 mins, 72°C for 10 min, then cooled at 4°C.

2.3.2 Polymerase chain reaction (PCR)

For examining gene expression in cells, each PCR reaction was carried out in a total 20 μL reaction, with 100 ng DNA as template, 0.5 μM forward and reverse primer, 2 μL 10X PCR buffer (without magnesium, Invitrogen), 1 μM dNTPs (Sigma), 1.5 mM $MgCl_2$, 0.2 μL Taq polymerase (10342, Invitrogen), and 9.2 μL H2O. The PCR program was 94°C for 3 mins, followed by 30 cycles of [94°C for 45 secs, 60°C for 30 secs, 72°C for 1 min], then followed by 72°C for 10 min and 4°C. PCR products were run on a 2% TAE gel to check the expression of the gene.

2.3.3 Quantitative polymerase chain reaction (qPCR)

For primer efficiency test, 1 μg cDNA was prepared and diluted to 50%, 25%, and 10%. For regular qPCR, 1 μg cDNA was used per reaction. The total 25 μL reaction

contained 10 μL cDNA, 1.25 μL of 5 μM forward and reverse primers, and 12.5 μL Maxima SYBR Green/ROX qPCR Master Mix (2X) (K0221, Thermo Scientific). After spinning down at 1000 rpm for 1 min, the reactions were carried out on the qPCR machine with the program: 95°C for 10 mins, 40 cycles of [95°C for 15 sec, 60°C for 60 sec] for gene expression detection, then 71 cycles of [60°C for 30 sec, with increase of 0.5°C per cycle] for melting curve detection. The gene expressions were normalized by the expression of GAPDH and HPRT and triplet measurements were used for each sample.

2.4 Biochemistry

2.4.1 Cell lysate preparation

Cells were washed by ice-cold PBS once and lysed using ice-cold RIPA buffer (50mM Tris-HCl pH7.4, 150 mM NaCl, 2 mM EDTA, 1% NP-40, 0.1% SDS) and supplemented with 5 mM Na_3VO_4, 10 mM NaF, 25 mM β-glycerolphosphate, and 1 mM PMSF before use. Lysates were collected using a cell scraper and transferred to 1.5 mL eppendorf for centrifugation at 13,000 rpm for 1 min at 4°C. After centrifugation, appropriate amounts of cell lysates were transferred to a new eppendorf and 5X sample buffer was added (final concentration: 50 mM Tris HCl pH 6.8, 2% SDS, 10% glycerol, 0.1% bromophenol blue, 100mM DTT), then boiled at 100°C for 5 minutes. Lysates were stored at -20°C for future use. Lysates without sample buffer

added were used for protein concentration measurement following the manufacturer's instructions (23225, Pierce™ BCA protein assay kit, ThermoFisher Scientific).

2.4.2 Western bolt analysis

Generally, 15 μg of protein lysates were loaded on 3-8% Tris-Acetate gels, or 4-12% Bis-Tris gels, or 12% Bis-Tris gels (NuPAGE, ThermoFisher Scientific) depending on the molecular weights of the target proteins and run at 120V for approximately 90 minutes in minigel apparatus. After resolving the proteins, the SDS-PAGE was transferred to methanol-activated PVDF membrane (0.45 mm pore size, Millipore) in transfer apparatus with transfer buffer (10X transfer buffer, BP-190, Boston Bioproducts) supplemented with 10% methanol. The transfer was carried out at 0.15A for 2 hours in a 4°C cold room. Membranes were blocked with 5% milk in TBS (10X TBS, 1259, Fisher scientific) containing 0.1% Tween-20 for 30 minutes at room temperature. Primary antibody incubations were carried out in TBS-T at 4°C overnight. Membranes were washed 3 times with TBS-T for 10 minutes, followed by secondary antibody incubation in TBS-T for 1 hour at room temperature. After washing with TBS-T 3x 10 minutes, membranes were incubated with Amersham ECL Western Blotting Detection Reagents (RPN2209, GE Healthcare Life Sciences) for 1 minute and exposed on Fuji medical X-ray film.

2.4.3 Cdc42-GTP pulldown assay

For GST-PAK CRIB protein purification, pGEX-PAK CRIB in BL21 DE3 pLysS strain was grown in 100 mL LB broth supplemented with Ampicillin 50 μg/mL and Chloroamphenicol 25 μg/mL in a 37°C shaking incubator for overnight. The culture was then diluted into 1L pre-warmed (room temperature) LB Ampicillin/Chloroamphenicol and grown in 30°C shaker for 2 hours followed by induction with 0.5 mM IPTG and grown for further 5 hours. The bacteria were pelleted and resuspended in 20 mL 50 mM Tris pH 8.0, then pelleted again, snap frozen in liquid nitrogen and stored overnight at -80°C. The pellet was resuspended in 20 mL GTLB I buffer (50mM Tris pH 8, 40 mM EDTA pH 8, 25% (w/v) sucrose, 1 mM PMSF) containing protease inhibitors and incubated on a rotating wheel at 4°C for 15 minutes. 8 mL GTLB II solution (50 mM Tris pH 8, 100 mM $MgCl_2$, 0.2% (w/v) Triton X-100, 1 mM PMSF) containing protease inhibitors was added and rotated for another 10 minutes at 4°C. Then the solution was sonicated at short bursts on ice to shear the DNA, until no longer viscous, but not opaque, and then centrifuged at 12000 rpm for 45 minutes at 4°C. The supernatant was transferred to a 50 mM Falcon tube and 1 mL of 50% glutathione-agarose bead slurry was added and rotated at 4°C for 1 hour. The beads were then spun down at 2400 rpm and washed 4 times with wash buffer (50 mM Tris pH 7.6, 50 mM NaCl, 5 mM $MgCl_2$, and 1 mM PMSF) containing protease inhibitors. The washed beads were resuspended in 1 mL wash buffer containing 50% glycerol, aliquoted, and stored at -80°C.

For GTP-Cdc42 pulldown, 16HBE cells were cultured to 60-70% confluence in 100 mm dishes and washed with ice-cold PBS. Cells were lysed with 500 μL lysis / wash buffer (50 mM Tris pH7.6, 150 mM NaCl, 10 mM MgCl2, 1% NP-40, 5% glycerol, 1 mM PMSF) containing protease inhibitors. The lysates were centrifuged at 13000 rpm for 4 minutes at 4°C and the protein concentrations were measured for the supernatants. About 50 μg lysates were used, and 5x sample buffer was added and boiled at 100°C for 5 minutes. Approximately 1 μg lysates were incubated with 20 mL GST-Pak1-CRIB beads and rotated on the wheel at 4°C for 1 hour. The lysates and beads were centrifuged at 2600 rpm for 2 minutes at 4°C to pellet the beads and further washed with wash buffer and centrifuged 4 times. After the final wash, 1 mL syringes were used to remove the supernatant carefully. 20 μL of 2x sample buffer was added to the beads, boiled for 5 minutes and then analyzed by western blot.

2.4.4 Immunoprecipitation

Cells grown in 6-well plates were washed with ice-cold PBS and scraped in 500 μL ice-cold lysis buffer (50mM Tris-HCl pH 8, 150 mM NaCl, 0.5% NP-40, 1 mM PMSF) containing protease inhibitors. Cell lysates were centrifuged at 13000 rpm for 15 minutes at 4°C. IgG antibody (0.5 μg / tube) was added to the supernatant and rotated on a wheel for 30 minutes at 4°C. Then 20 mL equilibrated protein G sepharose beads were added to the supernatants and rotated on the wheel for 30 minutes at 4°C to precipitate the IgG antibody. After centrifugation at 2500 rpm for 2

minutes at 4°C, about 30 mL of supernatants were saved and 5x sample buffer was added followed by boiling for 5 min. The rest of the supernatants were incubated with 1 μg antibody on a rotating wheel for 1-2 hours at 4°C, before 20 μL beads were added for another incubation on the wheel for 1 hour at 4°C. The beads were pelleted by centrifugation at 2500 rpm for 2 minutes at 4°C and washed with lysis buffer 5 times. After the last wash and centrifugation, 10 μL of 5x sample buffer was added to the beads and boiled for 5 minutes. Samples were analyzed by western blot.

2.5 Immunofluorescence microscopy

2.5.1 Preparation of coverslips

13 mm round glass coverslips (Fisher Scientific) were treated with nitric acid for 15 minutes and washed with flowing deionized water for 30 minutes. Coverslips were then washed with methanol several times and dried in the hood. Once dry, coverslips were transferred to a glass petri dish and autoclaved for 30 minutes at 180°C.

2.5.2 Fixing and immunostaining

16HBE cells grown on coverslips were washed once with PBS c/m (MSKCC media facility), containing 0.1 mM $CaCl_2$ and 1 mM $MgCl_2$, and fixed with 3.7% (v/v) formaldehyde (Sigma), diluted in PBS, for 10 minutes at room temperature. For immunostaining, the coverslips were washed 3 times in PBS and blocked with BTPA

buffer (0.5% BSA, 0.02% sodium azide, 0.25% Triton X-100 in PBS c/m) for 30 minutes. Following blocking, the coverslips were incubated with primary antibody (diluted in PBS c/m) for 1 hour at room temperate and washed three times with PBS c/m for 5 minutes. Coverslips were then incubated with secondary antibodies and Hoechst (diluted in PBS c/m) for 1 hour at room temperate. Finally, the coverslips were washed 3 times with PBS c/m for 5 minutes and mounted onto microscope slides (Fisher Scientific) using fluorescent mounting media (DakoCytomation).

2.5.3 Microscope

For stained samples, cells were visualized using a Zeiss Axio inverted fluorescence microscope, equipped with a Hamamatsu ORCA-ER digital camera. For time-lapse imaging, the Zeiss Axiovert 200m inverted microscope was used, with culture conditions maintained at 37°C and 5 % CO_2. The AxioVision software by Zeiss was used to image the staining results and time-lapse experiments.

2.5.4 Quantification of tight junction formation

Tight junction integrity was quantified in 16HBE cells with ZO-1 or occludin staining. Twelve non-overlapping images were randomly selected and pictures were taken under 40X magnification, containing approximately 500-600 cells in total. The images were analyzed using ImageJ software. Cells with a continuous staining of ZO-1 or

occludin at cell-cell contacts were counted as cells that have intact tight junctions. Cells with punctate or no staining of ZO-1 or occludin at cell-cell contacts were defined as cells that do not have intact tight junctions. Mitotic cells in the monolayer sometimes have disruption of tight junction staining, and therefore are not included in the quantification. The percentages of cells with intact tight junctions were calculated for each experiment and the quantification results of three independent experiments were shown in a bar chart with error bars corresponding to the SEM (Standard Error of the Mean), calculated in Prism software. An unpaired t-test was used to evaluate statistical significance, with two-tailed p-value and 95% confidence intervals.

2.6 Computational analysis

2.6.1 Wound detection and migration behavior analysis

The movies of wound healing experiments were sent to our collaborator, Dr. Assaf Zaritsky (Dr. Gaudenz Danuser Lab, UTSW) for further analysis. Briefly, the image at time t was parted by 15 x 15 pixels (as a patch) and cross correlation-based motion estimation was applied to give estimations of the velocity field from the image at the next time frame (t + 1). After defining cellular and non-cellular regions, the average velocity for all the cells at time t and distance d toward the wound edge is recorded as (t,d) on the velocity kymograph. The directionality was defined as the absolute ratio of velocity toward the wound and velocity parallel to the wound. A higher value indicates higher directionality, while a lower value indicates cells with less

directionality. The coordination was defined by the fraction of cells migrating in coordinated clusters within the monolayer. By comparing similarity of trajectories of neighboring patches, the similar ones were grouped as a cluster (Zaritsky, Kaplan et al. 2014).

2.6.2 Principle component analysis (PCA)

To compare the difference between kymographs generated in each experiment, the spatial temporal information (the color-coded values) on the kymograph was separated into twelve sections and averaged to twelve values. Each section contains the cell migration information within 60 minutes and 50 μm spaces within the migrating monolayer. The migration behaviors of cells localized within 200 μm behind the wound during the first three hours were analyzed. Therefore, each kymograph had twelve vectors to represent the encoded migration behaviors. Then, the principle component analysis was applied to reduce the twelve vectors into three features (PC1, PC2, and PC3), which encoded magnitude, temporal, and spatial derivatives separately. Therefore, for one experiment, a total of nine numbers including speed PC1-3, directionality PC1-3, and coordination PC1-3 were generated to constitute the migration behaviors of cells. The difference between the control and experimental groups were compared using Wilconxon signed-rank test to evaluate statistical significance.

Chapter 3 – The Role of Rap1 in epithelial collective migration

3.1 Overview

Collective migration is a fundamental process that occurs during development, for example during mammary gland morphogenesis and vascular sprouting, as well as in disease states such as cancer progression. The hallmarks of epithelial collective migration are the maintenance of cell-cell interactions that hold epithelial sheets together during migration, the establishment of multicellular polarity of the actin cytoskeleton within the epithelial sheet to generate protrusion and traction forces, and the modification or clearing of the extracellular matrix (ECM) to generate the migration path. As with single cell migration, Rho GTPases (Rho, Rac, and Cdc42) are involved in collective migration. However, the detailed mechanisms involved in controlling collective migration are unclear.

Rap1, a Ras-related GTPase, is required for apical junction formation in epithelial and endothelial cells and for integrin activation (see section 1.3.2b). Studies also indicate that Rap1 localizes at the leading edge of fibroblasts and controls motility in *Dictyostelium discoideum* (Jeon, Lee et al. 2007). Since Rap1 is an important regulator of cell-cell and cell-ECM interactions (Boettner and Van Aelst 2009), I examined

whether Rap1 also functions in epithelial collective migration and if so, how Rap1 coordinates with Rho GTPases to regulate the migration process.

To examine the regulation of epithelial collective migration, 16HBE14o- human bronchial epithelial cells (abbreviated to 16HBE) were utilized as a model cell line, which forms adherens and tight junctions in culture (Figure 3.1A, B) and migrates collectively after scratching a monolayer (Figure 3.1C) or when seeded in islands (Figure 3.1D). Therefore, these characteristics made 16HBE cells a suitable model to study epithelial collective migration.

In this study, I discovered that Rap1 activates Cdc42 to control the directionality of collective migration, potentially through a mechanism involving the Cdc42 GEF β-PIX and the known scaffold protein IQGAP.

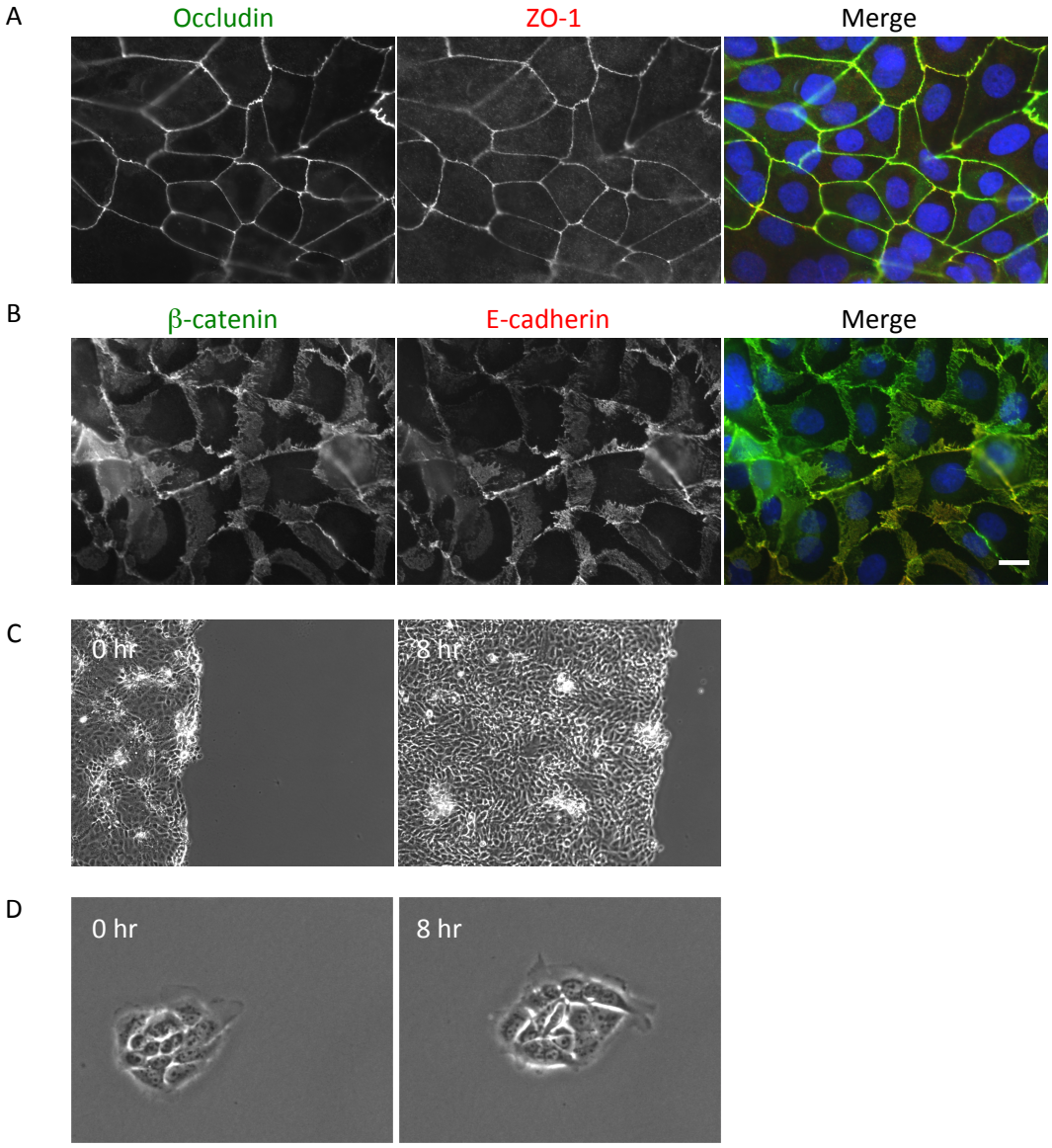

Figure 3.1 Human bronchial epithelial cell line (16HBE) is a suitable model for studying epithelial collective migration.
(A, B) 16HBE cells were seeded sparsely and cultured for three days before being fixed and stained for tight junctions, occludin (green) and ZO-1 (red) (A) and adherens junctions, β-catenin (green) and E-cadherin (red) (B). Hoechst for nuclear staining. Scale bar: 20μm.
(C) 16HBE cells were seeded at high density for two days before scratching and time-lapse microscopic imaging to examine the kinetics for the wound healing assay.
(D) 16HBE cells were seeded at very low density for three days before time-lapse imaging for a colony migration assay.

3.2 Rap1A and Cdc42 control directionality in epithelial collective migration

To study the function of Rap1A in migration, I established 16HBE stable cell lines expressing empty vector, wild-type (WT), constitutive active (V12), or dominant negative (N17) Rap1A (Figure 3.2A) after virus infection and drug selection. Unlike normal 16HBE cells, which form colonies with irregular cell shape when seeded sparsely, stable cell lines expressing WT or V12 Rap1A exhibited a rounded and flattened cell shape, while those expressing N17 Rap1A exhibited colonies with apparent reduced cell-cell adhesion (Figure 3.2B). The stable cell lines were seeded sparsely for colony migration assays and at high density for wound healing assays. Control cells exhibited collective migration in the colony migration assay and sealed the wound in approximately 10 hours in the wound healing assay. While the Rap1A WT- and Rap1A V12-expressing cells did not move, the Rap1A N17-expressing cells exhibited a slower wound closure rate (Figure 3.2 C, D).

Figure 3.2 Expression of different Rap1A constructs (WT, V12, and N17) resulted in migration defects.
(A) Control (pQ) and Rap1A-expressing (WT, V12, and N17) 16HBE stable cell lines were lysed and analyzed by Western blot with indicated antibodies. N=3.
(B) Morphology of control and Rap1A WT, V12, and N17-expressing stable cell lines.
(C) Rap1A WT and Rap1A V12-expressing stable cell lines were seeded sparsely for three days and recorded for colony migration assay.
(D) Control and Rap1A N17-expressing stable cell lines were seeded for two days and recorded for wound healing assay. The gap distances between two wounded edges were measured in ImageJ and calculated in Excel. N=3.

Figure 3.2

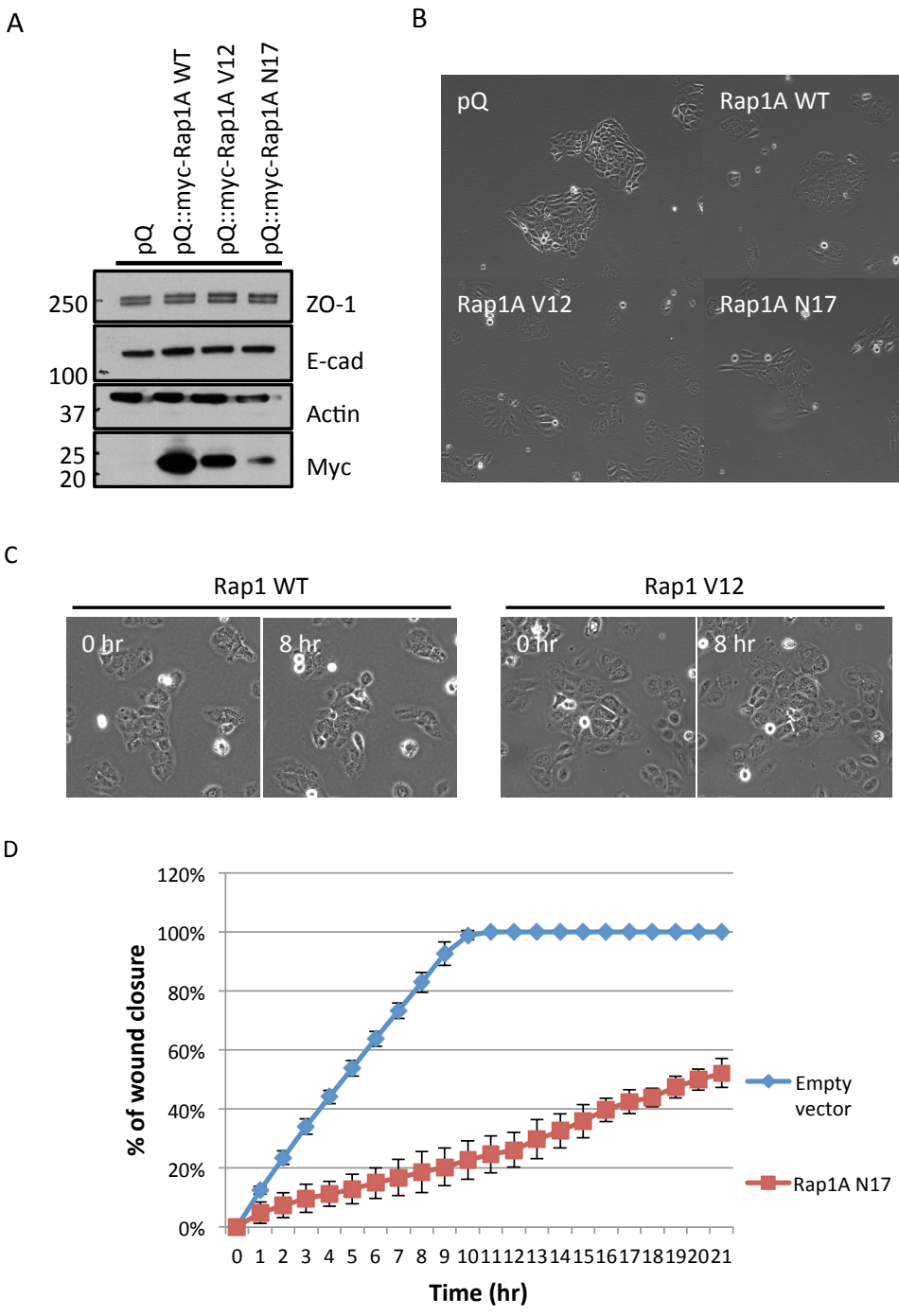
A
pQ
pQ::myc-Rap1A WT
pQ::myc-Rap1A V12
pQ::myc-Rap1A N17
250
100
37
25
20
ZO-1
E-cad
Actin
Myc
B
pQ
Rap1A WT
Rap1A V12
Rap1A N17
C
Rap1 WT
Rap1 V12
0 hr
8 hr
0 hr
8 hr
D
120%
100%
80%
60%
40%
20%
0%
% of wound closure
0 1 2 3 4 5 6 7 8 9 10 11 12 13 14 15 16 17 18 19 20 21
Time (hr)
Empty vector
Rap1A N17

To futher study the role of Rap1 in collective migration, known Rap1 effectors and also Rho GTPases (Rho, Rac, and Cdc42) were examined for potential downstream functions. Rap1 has been reported to have several downstream effectors, including AF6, KRIT1, RIAM, Radil, Rasip1, RapL, RGS14, RASSF1A, RalGDS, ARAP3, and PDZGEF, which regulate cell-matrix adhesion or cell-cell adhesion (Figure 3.3A) (Raaijmakers and Bos 2009). Among these, Radil was found to be required for Rap1A-mediated inside-out activation of integrin signaling and cell adhesion (Liu, Aerbajinai et al. 2012). Radil also mediates Epac1-induced cell spreading of lung carcinoma cells (Ross, Post et al. 2011) and is required for neural crest cell migration during zebrafish development (Smolen, Schott et al. 2007). Therefore, Radil is a possible downstream candidate involved in Rap1-regulated epithelial collective migration. Stable cell lines with Radil-depletion were generated by infection of Radil shRNA-containing viruses and selected by puromycin. Then, the pooled stable cell lines were examined in the wound healing assay. However, cells with stable knockdown of Radil did not cause a delay of wound closure rate (Figure 3.3B, C). Several other individual stable cell lines harboring shRNAs against additional downstream effectors of Rap1, AF6/afadin, Kirt1, and Riam, were also generated to examine if depletion of these effectors caused a migration delay in the wound healing assay. However, none of these led to delayed wound closure after depletion. It is therefore possible that other downstream effectors mediate dominant Rap1-dependent control over collective migration.

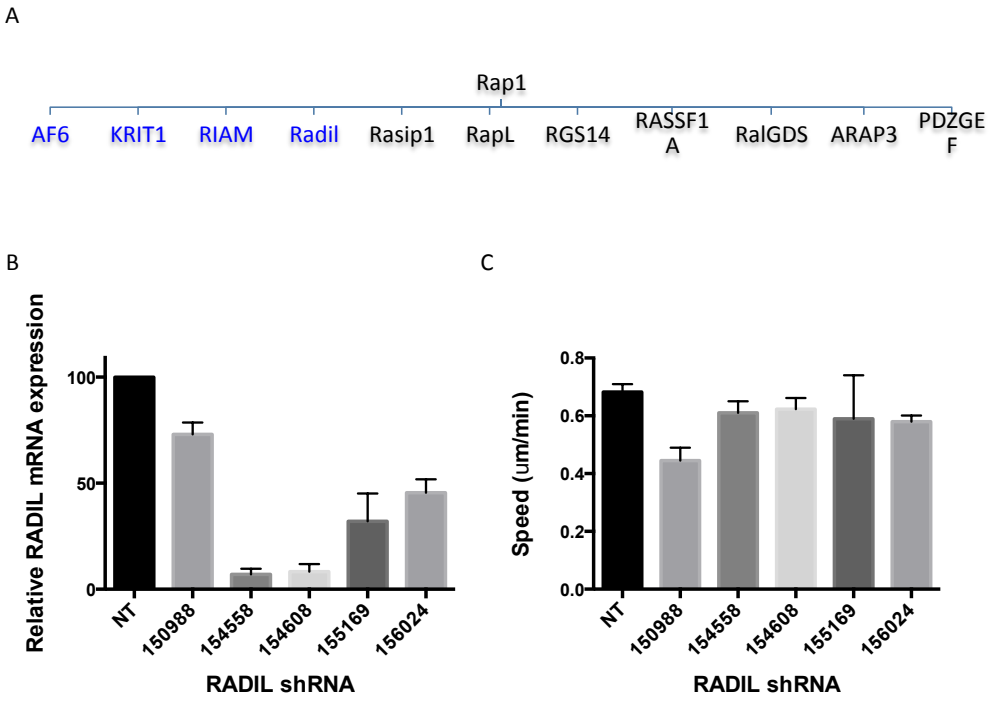

Figure 3.3 Depletion of Radil, a Rap effector, did not cause a migration delay in the wound healing assay.

(A) Figure shows the known downstream effectors of Rap1. Those marked in blue text were examined in the wound healing assay.

(B) Knockdown efficiencies of Radil-depleted stable cell lines were analyzed by qRT-PCR using Radil-specific primer. The mean±SEM is shown. N=3.

(C) Radil-depleted stable cell lines were seeded and recorded for wound healing assay. The speed of migration was measured in ImageJ. The mean±SEM is shown. N=3.

Rho GTPases (Rho, Rac, and Cdc42) are the important regulators of cell migration. It is possible that Rap1 regulates epithelial collective migration through the regulation of Rho GTPases. To examine the role of Rho GTPases in epithelial collective migration, I generated dominant negative Rac1 (Rac1 N17) expressing stable cell lines and Cdc42-depleted stable cell lines after virus infection and drug selection, and quantified collective migration utilizing the colony migration and wound healing assays. Cells expressing dominant negative Rac1 did not move in the colony migration assay (Figure 3.4A, B) and cells with depletion of Cdc42 exhibited significantly reduced wound closure (Figure 3.4B, D). Since the expression of dominant negative Rap1A did not inhibit migration, but slowed the wound closure rate, Rap1A inhibition therefore led to a similar phenotype as Cdc42 depletion, suggesting that Rap1 could regulate collective migration through Cdc42.

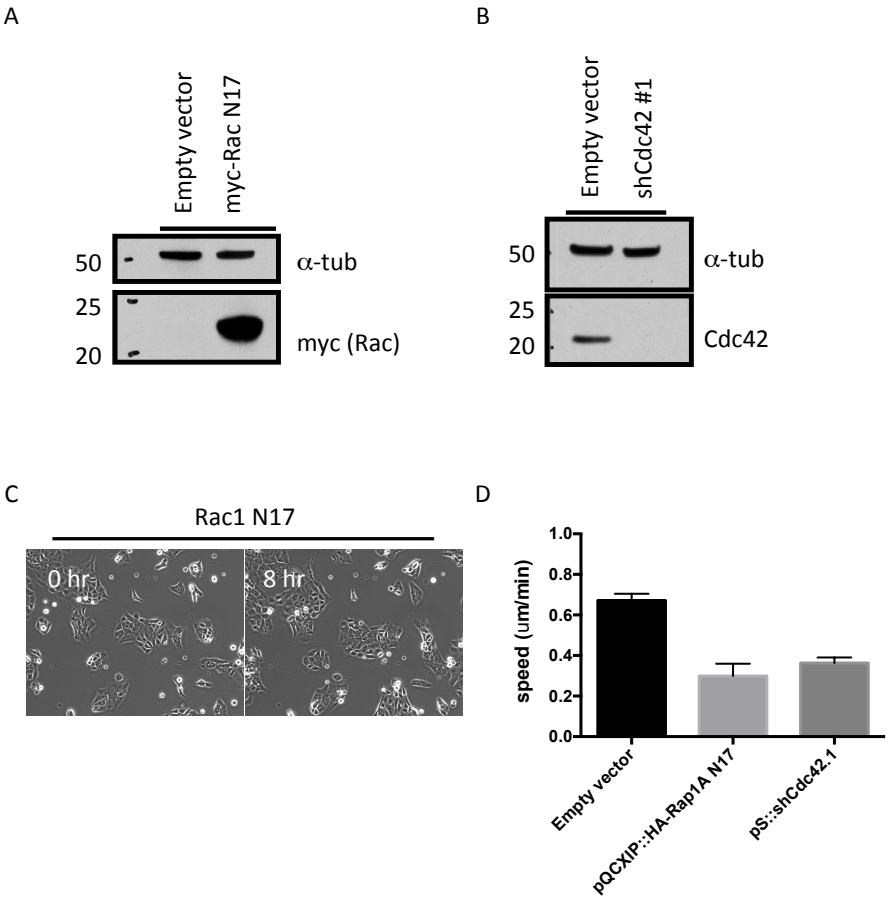

Figure 3.4 Expression of dominant-negative Rac1 (Rac1 N17) or depletion of Cdc42 slows migration speed.

(A, B) Rac1 N17-expressing (A) or Cdc42-depleted (B) stable cell lines were lysed and analyzed by Western blot with indicated antibodies. N=3.

(C) Rac1 N17-expressing stable cell lines were seeded sparsely for three days and recorded for colony migration assay.

(D) Rap1A N17-expressing and Cdc42-depleted stable cell lines were seeded for wound healing assay. Migration speeds were measured in ImageJ. The mean±SEM is shown. N=3.

3.3 Rap1A and Cdc42 control directionality during collective migration

Previous studies have implicated Cdc42 in controlling the directionality of migrating cells (Chou, Burke et al. 2003). The direction of actin polymerization determines the direction of cell migration; such that in collectively migrating cells, actin forms protrusion toward the wound edge. To determine whether directionality was disrupted in Cdc42-depleted cells and in dominant negative Rap1A-expressing cells, the pattern of actin polymerization was examined during collective migration in a wound healing assay, using cells expressing GFP-actin by transfection. For the majority of control cells, both in the front or the back rows, actin polymerization was oriented toward the wound. However, for cells with dominant negative Rap1A expression or Cdc42 depletion, actin polymerization not only appeared in the direction toward the wound, but also toward the direction different from the wound edge. Moreover, the mutant cells in the back rows had a stronger phenotype compared to cells in the front row (Figure 3.5). The results suggested that both Rap1A and Cdc42 controlled directionality during collective migration.

Figure 3.5 Rap1A and Cdc42 determine the direction of actin polymerization.
Control, Rap1A N17-expressing, or Cdc42-depleted stable cell lines were transfected with pEGFP-actin and seeded for wound healing assays.
(A) Phase images show that the selected cells are located at the front of wound edge.
(B) Dynamics of the actin cytoskeleton in control or Cdc42-depleted cells. The yellow arrows indicate the protrusion in the direction of migration. The red arrow indicates the protrusion in the direction opposite to the direction of migration.
(C, D) Quantification of the percentage of cells with protrusions in the same or opposite direction to the migration direction in control, Cdc42-depleted, and Rap1A N17-expressing stable cell lines were located in the front row (C) and the back rows (D). The mean±SD is shown. N=2.

Figure 3.5

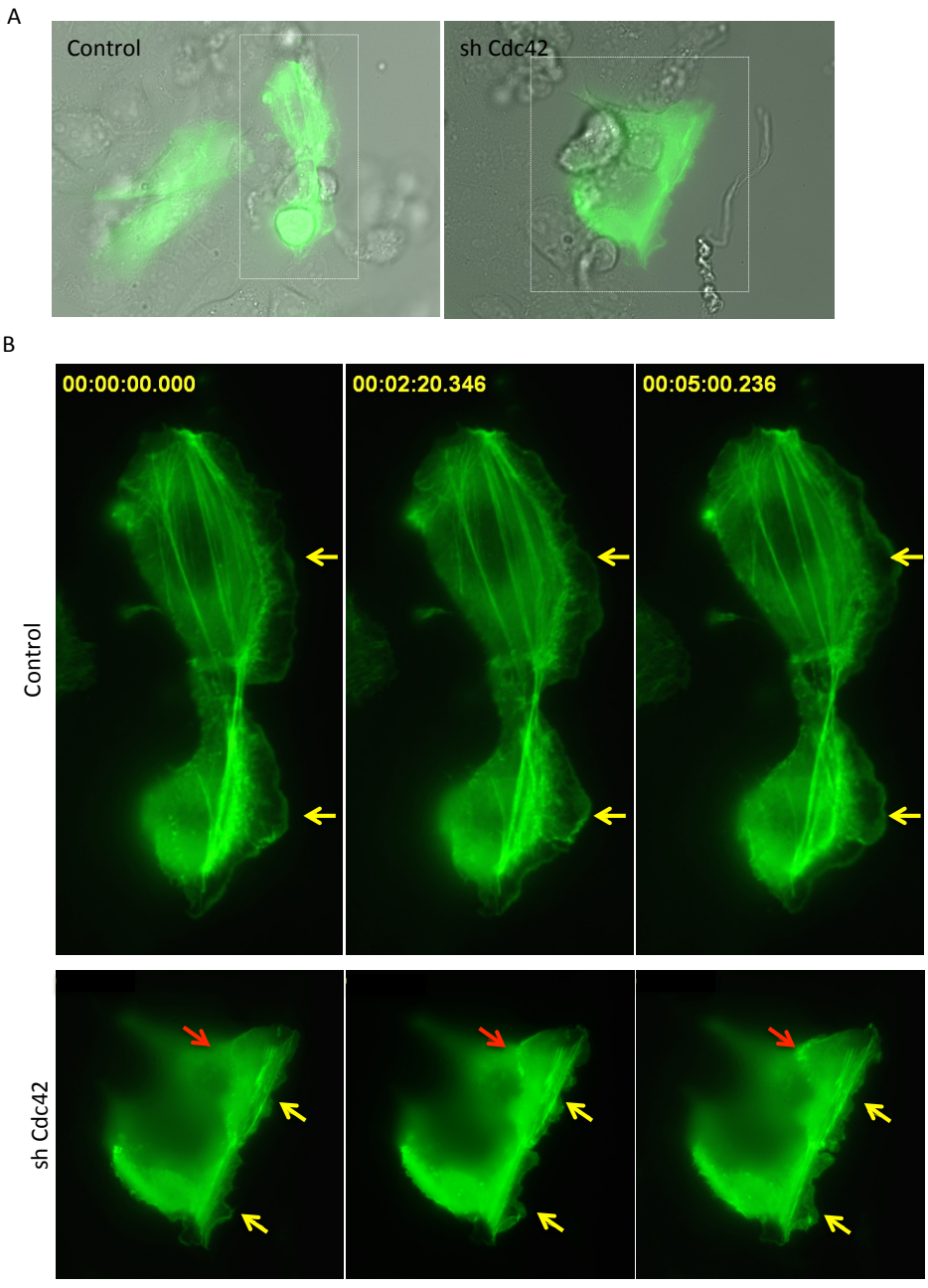
A
Control
sh Cdc42
B
00:00:00.000
00:02:20.346
00:05:00.236
Control
sh Cdc42

Figure 3.5 (Continued)

C

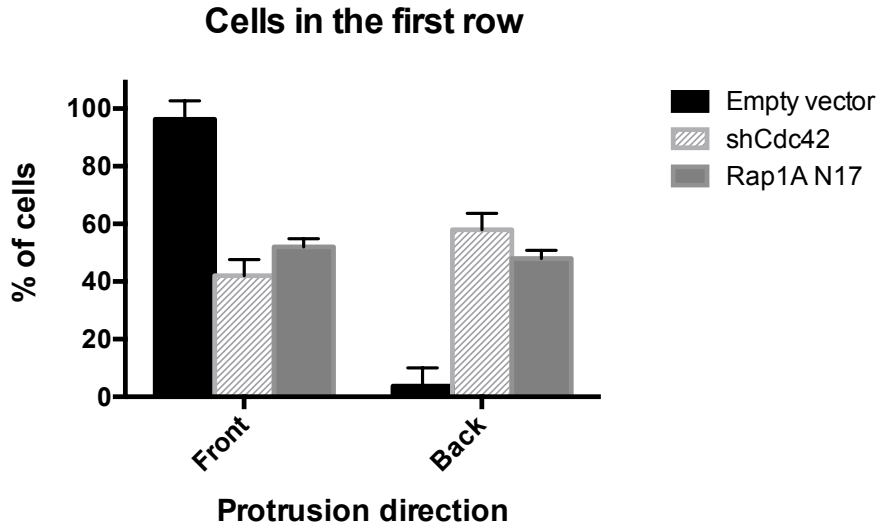

D

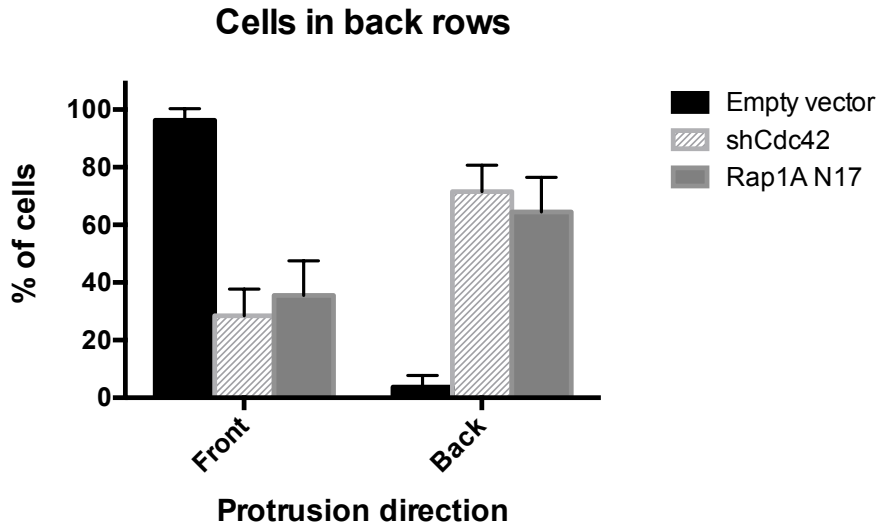

3.4 Rap1A activates Cdc42

In the budding yeast, Bud1, a Rap1A homolog, activates Cdc42 by a mechanism involving a Cdc42 GEF, to determine the position of the budding site where the daughter cell emerges (Park, Bi et al. 1997). However, whether this Rap1-CDC42p GEF-CDC42p axis is conserved from yeast to mammals remains unknown. To investigate whether Rap1A activates Cdc42 in 16HBE cells, I performed GTP-Cdc42 pulldown assays in control, Rap1A WT-, V12- or N17-expressing cells. Using GST-PAK-CRIB beads to pull down active Cdc42 (GTP-Cdc42), I found that expression of wild type and active Rap1A (Rap1A V12) increased the level of GTP-Cdc42 in 16HBE cells, while expression of dominant negative Rap1A (N17) decreased the level of GTP-Cdc42 (Figure 3.6B). This result suggested that expression of Rap1A activates endogenous Cdc42. The GTPγS and GDP loading served as positive and negative controls to test the efficacy of the GST-PAK-CRIB pulldown beads (Figure 3.6A).

How does Rap1 activate Cdc42? Rap1 could activate Cdc42 through a Cdc42 GEF, as occurs in budding yeast. Vav2 is a widely expressed GEF that functions to activate Rac1, RhoA, RhoG, and Cdc42 *in vitro*. It has been reported that Rap1 binds to the PH domain of the DH-PH region of Vav2 to recruit Vav2 to the cell periphery to promote cell spreading (Arthur, Quilliam et al. 2004). Other than Vav2, a published screening result from the Hall lab also suggested that β-PIX, a Rac/Cdc42 dual GEF, might also be involved in collective migration (Omelchenko, Rabadan et al. 2014). Therefore, I generated stable cell lines depleted for Vav2 and β-PIX by infected with shRNA-

containing viruses and selected with puromycin, and then tested them for effects on collective migration. Cells with β-PIX depletion displayed a delayed the wound closure rate, as also found in Cdc42-depleted or Rap1A N17-expressing cells. By contrast, cells with Vav2 depletion appeared similar to controls (Figure 3.7).

The phenotypic similarity between Cdc42- and β-PIX-depleted cells, and dominant negative Rap1A-expressing cells suggested the hypothesis that Rap1A could recruit β-PIX and thereby activate Cdc42 to control epithelial collective migration. However, Rap1 and β-PIX could not be co-immunoprecipitated from HEK cells suggesting that they do not interact directly (Figure 3.8A). Other than a direct interaction, Rap1 may function to activate β-PIX indirectly, for example through a scaffold protein. From the literature, IQGAP1 is reported to interact with both Rap1 and Cdc42 and localize to the leading edge to control directional cell migration (Joyal, Annan et al. 1997, Jeong, Li et al. 2007, Choi, Thapa et al. 2013), which makes it an ideal candidate to be involved in collective migration. IQGAP1 indeed interacted with β-PIX in the HEK cells (Figure 3.8B). Therefore, Rap1 may interact with IQGAP1 in order to activate β-PIX and Cdc42 to regulate the directionality of collective migration.

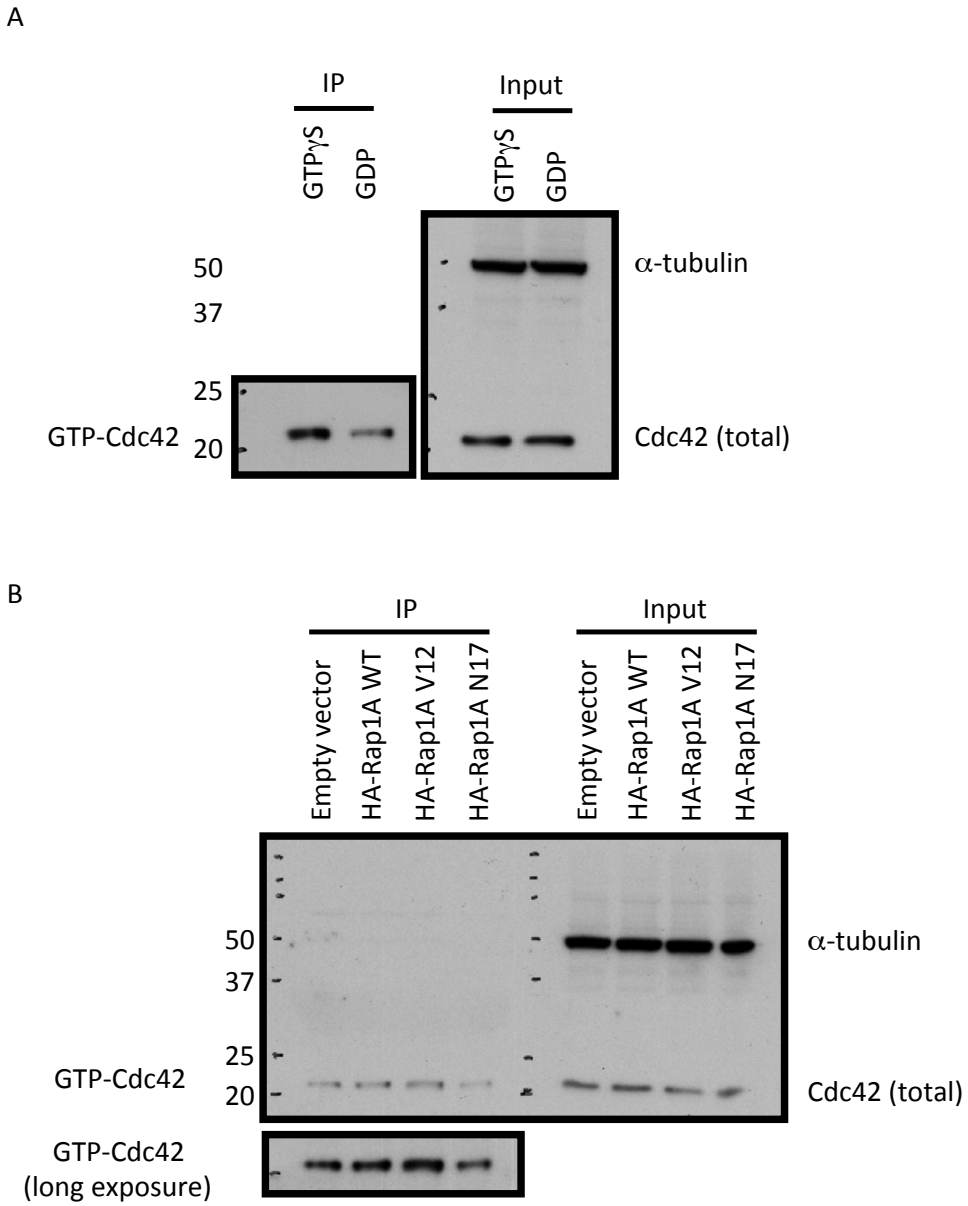

Figure 3.6 Expression of Rap1 WT or V12 in 16HBE cells activates Cdc42.
(A) Control cells were loaded with GTPγS or GDP and lysed. Active Cdc42 was pulled-down by GST-PAK1-PBD beads.
(B) Control, Rap1A WT, V12, or N17-expressing 16HBE stable cell lines were lysed and active Cdc42 pull-down was performed by using GST-PAK1-PBD beads. N=3.

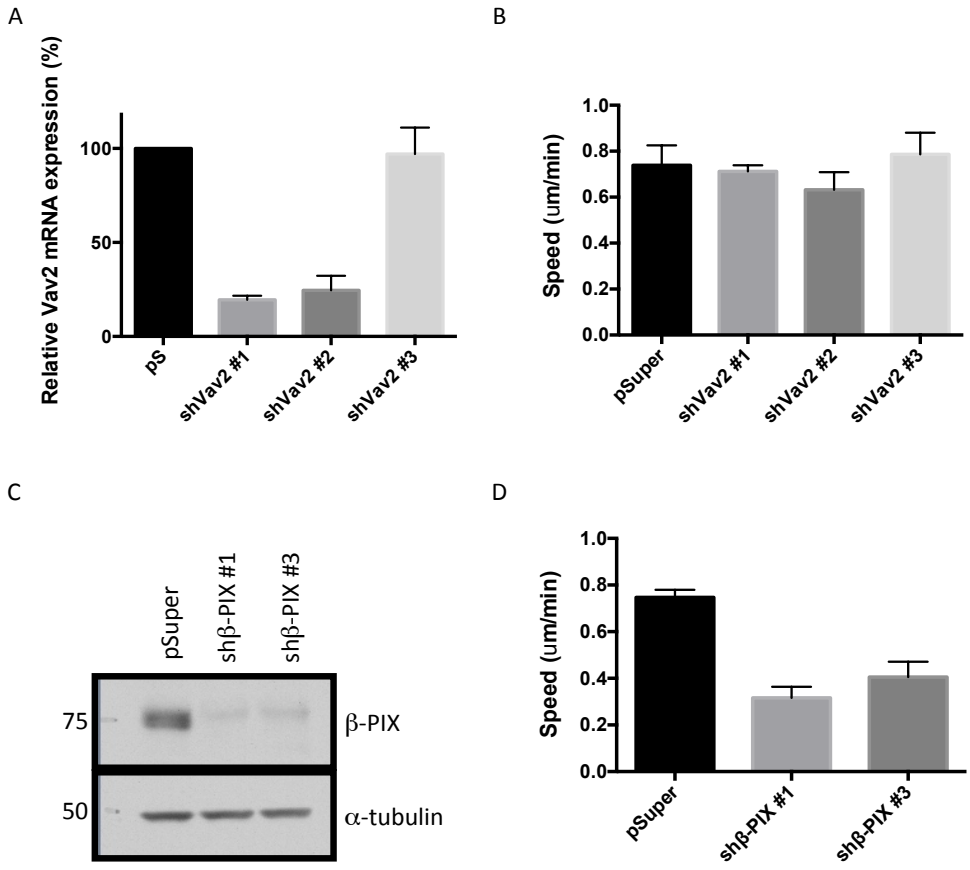

Figure 3.7 β-PIX, not Vav2, is involved in epithelial collective migration.
(A) Knockdown efficiencies of Vav2-depleted stable cell lines were analyzed by qRT-PCR using Vav2-specific primer.
(B) Vav2-depleted stable cell lines were seeded for wound healing assay. Migration speeds were measured in ImageJ.
(C) Knockdown efficiency of β-PIX depleted stable cell lines were analyzed by Western blot.
(D) β-PIX-depleted stable cell lines were seeded for wound healing assay. Migration speeds were measured in ImageJ.

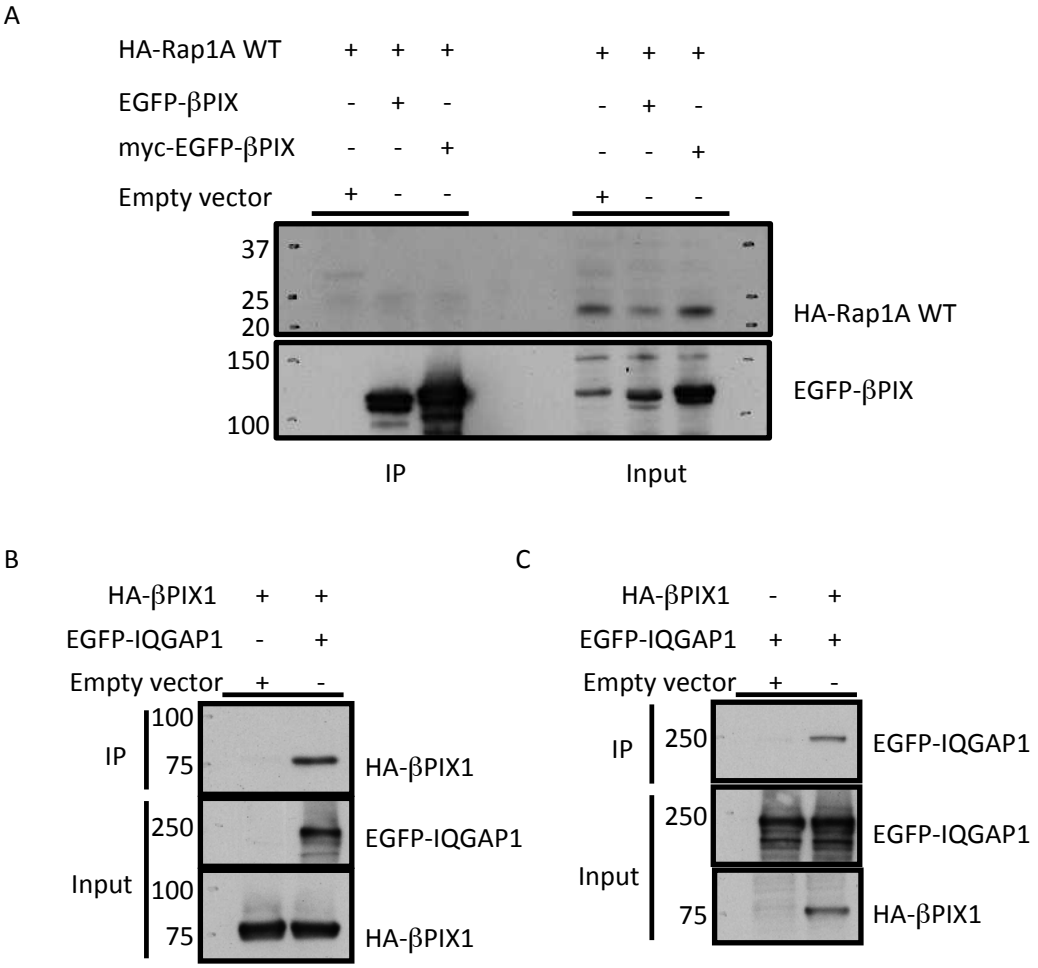

Figure 3.8 β-PIX interacts with IQGAP1, but not with Rap1A.
(A) HA-tagged Rap1IX WT and empty vector, EGFP-tagged β-PIX or myc- and EGFP-tagged β-PIX were co-expressed in HEK293T cells. EGFP-β-PIX was precipitated with a GFP antibody but HA-tagged Rap1A was not detected in the precipitant. N=3.
(B) HA-tagged β-PIX and empty vector or EGFP-tagged IQGAP1 were co-expressed in HEK293T cells. By using EGFP antibody to precipitate the lysate, co-precipitation of β-PIX was detected using a HA antibody. N=3.
(C) EGFP-tagged IQGAP1 and empty vector or HA-tagged β-PIX were co-expressed in HEK293T cells. By using HA antibody to precipitate the lysate, co-precipitation of IQGAP1 was detected using a GFP antibody. N=3.

3.5 Rap1 and junction formation

It is known that Rap1 is involved in regulating cell-cell adhesion (Boettner and Van Aelst 2009, Pannekoek, Kooistra et al. 2009). Consistent with previous studies, tight junctions were disrupted by expression of dominant negative Rap1A. Moreover, cells with wild type or constitutive active Rap1A expression also exhibited discontinuous ZO-1 staining (Figure 3.9). However, the ZO-1 and E-cadherin expression levels determined by western did not change in the mutant Rap1A-expressing cells (Figure 3.2A), indicating that the junction phenotype was caused by ZO-1 mislocalization rather than downregulation in those samples.

To further investigate the downstream effectors of Rap1A in controlling junction formation, cells were infected with lentiviruses encoding shRNA targeting AF6/afadin, Kirt1, Riam, and Radil, and stable cell lines were selected and examined for cell-cell adhesion phenotypes. Among these stable cell lines, depletion of AF6, but not the other Rap effectors, disrupted tight junction formation, while adherens junctions, analyzed by E-cadherin localization, remain intact in 16HBE cells (Figure 3.10). AF6 was also found to localize to tight junctions, suggesting altogether that Rap1 controls tight junction formation through AF6 in 16HBE cells, which agrees with a similar result published previously (Zhadanov, Provance et al. 1999).

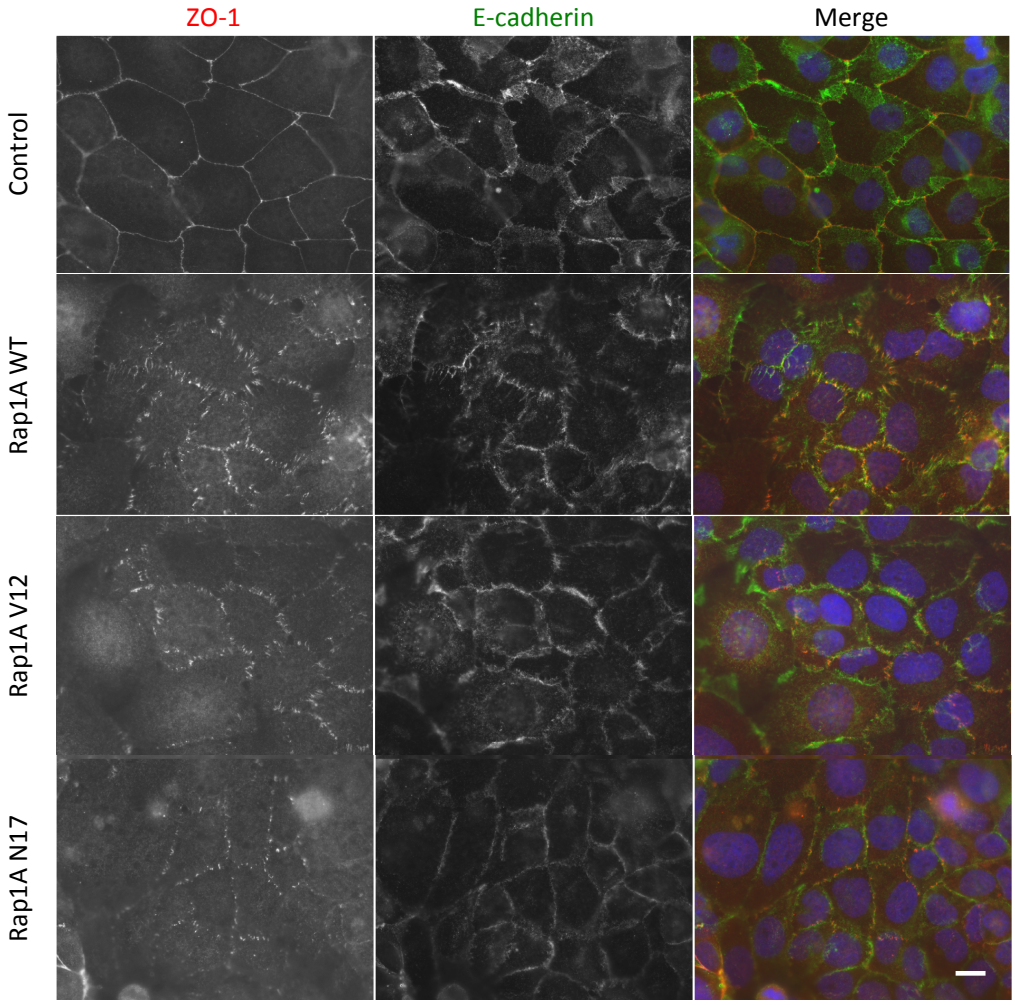

Figure 3.9 Expression of Rap1A construct (WT, V12, or N17) disrupts the tight junction formation in 16HBE cells.
Control, Rap1A WT, V12, or N17-expressing 16HBE stable cell lines were seeded sparsely for three days and then fixed and stained for ZO-1 (red) and E-cadherin (green). The nuclei were stained with Hoechst. Scale bar: 20μm.

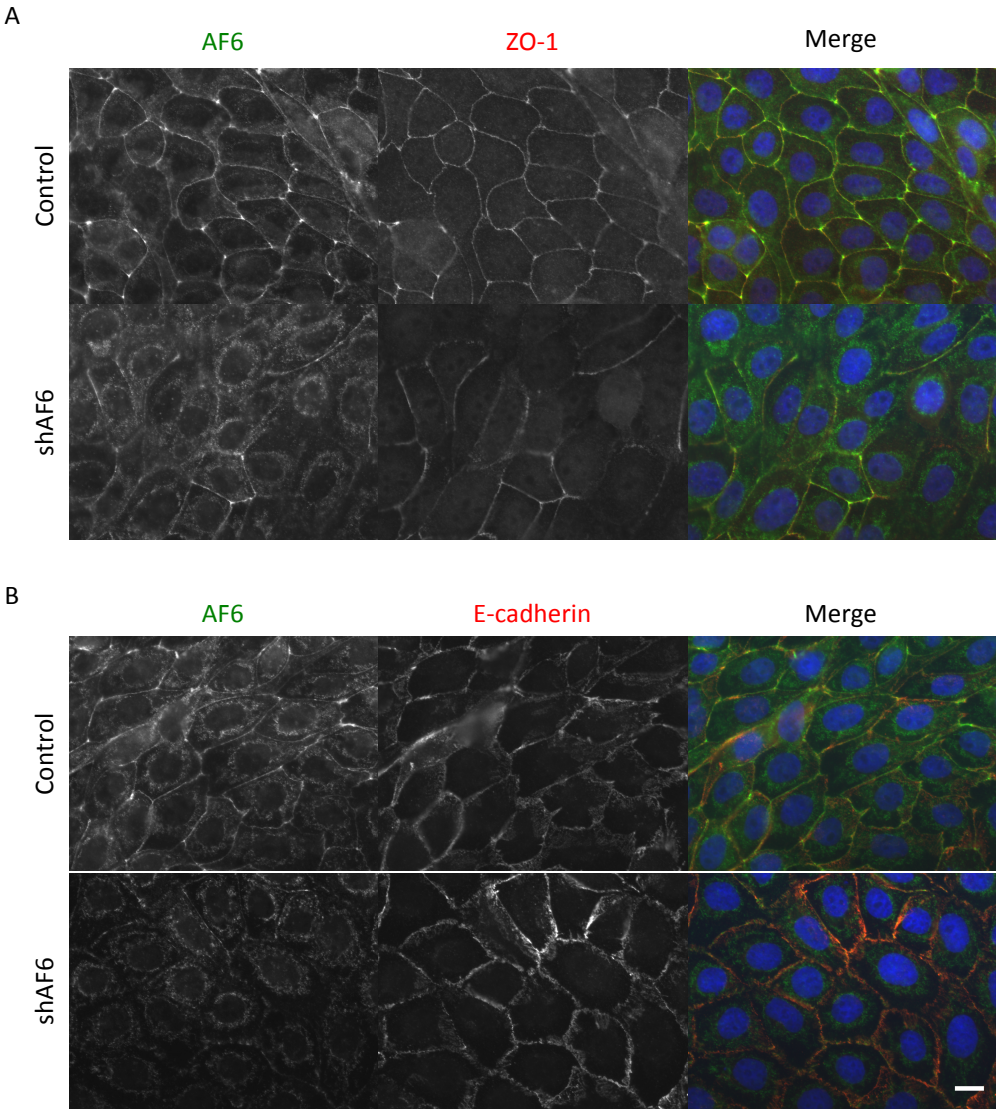

Figure 3.10 AF6 is required for tight junction formation, but not for adherens junction formation.
Control or AF6-depleted 16HBE cells were seeded at low density and cultured for three days before being fixed and stained for AF6 (green) and ZO-1 (red) in (A) or AF6 (green) and E-cadherin (red) in (B). The nuclei were stained for Hoechst. Scale bar: 20 μm.

3.6 Discussion

To examine the function of Rap1A in epithelial collective migration, I established stable cell lines with dominant negative Rap1A expression. Functional studies with these cells revealed that wound closure, which is mediated by collective migration in 16HBE cells, was delayed, and tight junctions were disrupted by loss of Rap1A function, demonstrating that key aspects of collective migration – cell adhesions and cell movement – require Rap1. Further experiments demonstrated that both Rap1A and Cdc42 control the directionality of cell movement and actin polymerization during collective migration, suggesting that Rap1 and Cdc42 may act in the same pathway to controlling directionality during collective migration.

The relationship between Rap1 and Cdc42 was first demonstrated in budding yeast. Bud1/Rsr1, the homolog of Rap1 in budding yeast, determines the position of the bud site. Bud1/Rsr1 activates CDC42p, the homolog of Cdc42, through CDC24p, a CDC42p GEF in yeast (Park, Bi et al. 1997). Whether this Rap1-CDC42p GEF-CDC42p axis is conserved from yeast to mammals remains unknown. I have shown that Rap1 activates Cdc42, and that β-PIX, a Cdc42/Rac GEF, is also involved in controlling directionality during collective migration. I also found that IQGAP1, a Cdc42 and Rap1 interacting scaffold protein, could bind to β-PIX when expressed in HEK cells. However, due to a lack of further experiments to demonstrate that IQGAP1, β-PIX, Rap1, and Cdc42 can indeed form a complex, it remains unclear as

present if these proteins collaborate directly to control collective migration, although this is a compelling model (Figure 3.11).

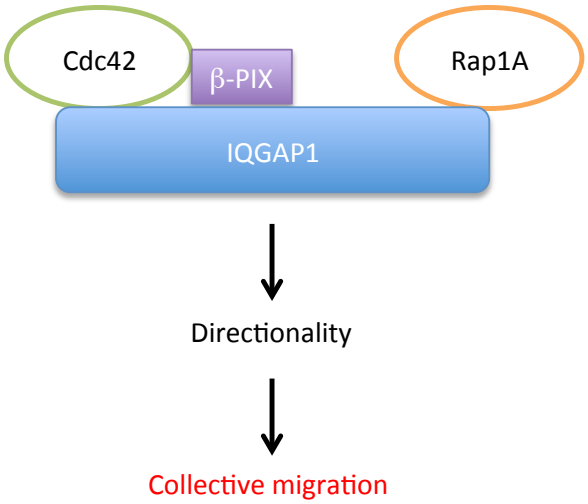

Figure 3.11 Model for Rap1A and Cdc42 controlled directionality in epithelial collective migration.
The current data suggests that Rap1A interacts with IQGAP1, while IQGAP1 binds to β-PIX and Cdc42 concomitantly and thus facilitates Rap1 activation of Cdc42 via β-PIX. Together, Rap1A, β-PIX, and Cdc42 control the directionality of epithelial collective migration.

It is also possible that Rap1A activates Cdc42 through another Cdc42 GEF in addition to, or instead of, β-PIX, in light of the current lack of evidence for a direct interaction of Rap1A and β-PIX. To address this possibility, I conducted a GEF screen in order to identify other potential GEFs involved in collective migration, which is described in Chapter 4. Alternatively, it is also possible that Rap1A sequesters a Cdc42 GAP and thus facilitates Cdc42 activation. These possible mechanisms require further examination.

The results of the experiments reported in this chapter demonstrate that Rap1A controls directionality during collective migration. However, experiments aimed at finding the downstream effectors of Rap1A did not succeed, as depletion of four candidate effectors, AF6, Kirt1, Riam, and Radil, did not inhibit wound closure. There are several additional Rap1 effectors that have been reported in the literature, such as Rasip1, RapL, RGS14, RASSF1A, RalGDS, ARAP3, and PDZGEF, which could potentially be involved in Rap1-dependent regulation of directionality during collective migration. Further experiments are therefore needed to identify the key downstream effector of Rap1A that regulate collective migration.

Chapter 4 – Guanine Nucleotide Exchange Factors (GEFs) involved in epithelial collective migration

4.1 Overview

Rho GTPases (Rho, Rac, and Cdc42) are the master regulators of migration in single cells and control junction formation in epithelial cells. However, in epithelial collective migration, how Rho GTPases participate in regulating migration while maintaining junctions, and which GEFs are involved in regulating collective migration, remain unknown. In this study, the role of Rho GTPases in epithelial collective migration and their regulation by GEFs was examined by systematic functional screening. To achieve this, time-lapse imaging analyses of epithelial wound closure, using 16HBE cells that migrate collectively, were examined computationally for cells with loss-of-function for Rho GTPases (Rho, Rac, and Cdc42), as well as for any of 80 GEFs, whose expression levels were knocked-down by shRNA-mediated gene silencing. The GEF shRNA screen targeted 80 GEFs, with 3 shRNAs per gene, resulting in the construction of more than 200 pooled stable cell lines in total. 16HBE cells harboring shRNAs that knocked-down their targets by more than two-fold were examined for migration behavior and junction formation. The time-lapse cell migration movies of each were examined computationally in a collaborative effort by Dr. Assaf Zaritsky and Dr. Gaudenz Danuser, at UT Southwestern.

4.2 RhoA, Rac1, and Cdc42 are involved in epithelial collective migration

RhoA, Rac1, and Cdc42 are the three well-characterized members in the Rho GTPase family. Their functions in migration are mostly studied in the single fibroblast system. They are also involved in junction formation and maintenance, which contributes to cell-cell adhesion during collective migration. Several studies suggest that Rho GTPases regulate collective migration (see section 1.4.3); however the detailed mechanisms are largely unknown in the field. To address this question, 16HBE cells were infected with viruses harboring RhoA, Rac1, or Cdc42 shRNAs and examined for migration and junction phenotypes. After puromycin selection, pooled stable cell lines were established and seeded for wound healing assays to monitor migration behaviors, immunostainining to examine tight junctions (via staining for ZO-1), and qRT/PCR or Western blotting to determine the knockdown efficiency.

Confluent 16HBE cells exhibited a sharp, continuous ZO-1 staining pattern lining the cell periphery, which indicated intact tight junctions, and band-like E-cadherin staining in between cells, which represented adherens junctions. As previously reported, in stable cell lines with depletion of RhoA, Rac1, or Cdc42, the ZO-1 localization at cell-cell contacts was lost or discontinuous, which indicated severe tight junction defects(Jou, Schneeberger et al. 1998, Wallace, Durgan et al. 2010, Wallace, Magalhaes et al. 2011). The peripheral E-cadherin localization was largely maintained,

but despite weakened intensity in the RhoA-, Rac1-, or Cdc42-depleted cells (Figure 4.1).

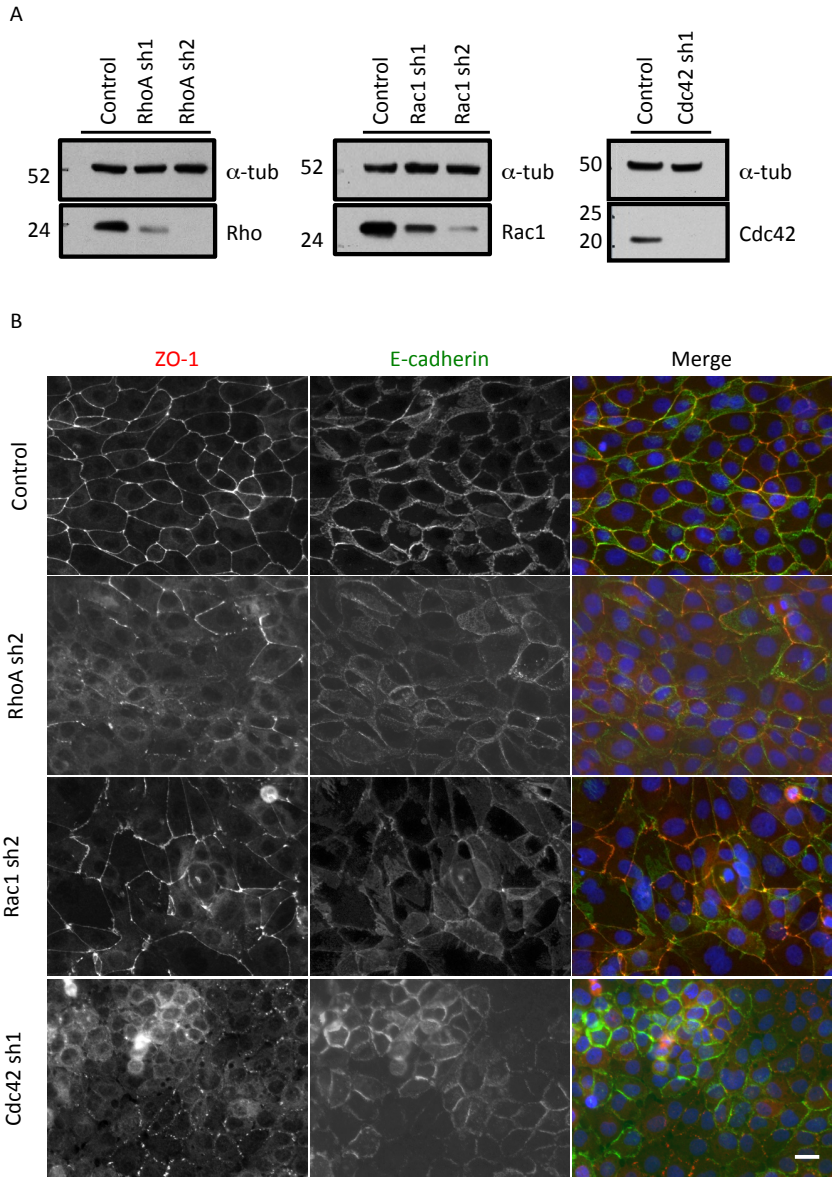

Figure 4.1 RhoA, Rac1, and Cdc42 are required for tight junction formation.
(A) Control, RhoA-, Rac1-, and Cdc42-depleted 16HBE stable cell lines were lysed and analyzed by Western blot for indicated antibodies. N=3.
(B) Indicated stable cell lines were seeded sparsely, grown for three days before being fixed and stained for E-cadherin (green) and ZO-1 (red). Hoechst used for nuclear staining. Scale bar: 20μm.

Stable cell lines with depletion of RhoA, Rac1 or Cdc42 exhibited different migration phenotypes. Downregulation of Rac1 or Cdc42 caused a significant delay in the wound healing rate, however, surprisingly depletion of RhoA did not change the wound healing rate (Figure 4.2A). We further utilized a computational program to analyze the migration behaviors of Rho GTPase-depleted cells located within 200 μm behind the wound edge during the first 3 hours of imaging. The analyses generated corresponding kymographs to represent the spatial and temporal changes of GTPase-depleted cells in speed, directionality, and coordination during migration (Figure 4.2B). The speed was indicated the local velocity of movement. The directionality was the ratio between the local velocity perpendicular to the wound and the velocity parallel to the wound. The coordination was the fraction of cells that migrate as clusters with similar migration trajectories. In the speed kymograph of control cells, the analysis indicated that the front row cells initially had higher speed compared to the cells in the back row. Subsequently, the back row cells caught up with the speed of the front row cells at later time points. This difference in the response time between the front and back row cells created the diagonal line in the speed kymograph shown in Figure 4.2B. In the directionality and coordination kymographs, a similar trend could be found, in that the front row cells displayed higher directionality/coordination initially but the back row cells caught up at later time points. For Rac1 or Cdc42-depleted cells, the speed, directionality, and coordination decreased in both front row and back row cells. On the contrary, in RhoA-depleted cells, the directionality and coordination did not change significantly compared with control cells. However, the spatial and temporal pattern in the speed kymograph was different in RhoA-depleted

cells. It showed that the front row and back row cells migrated simultaneously in response to the wound, which created a vertical line on the kymograph, instead of the diagonal line, which was observed in the control. Examining the migration behavior in a particle image velocimetry (PIV) analysis further supported the finding that RhoA-depleted cells had a similar vector magnitude in both the front and the back row cells, while the control cells had larger vectors in the front cells than in the back cells (Figure 4.2C). In conclusion, we found that the depletion of Rac1 or Cdc42 decreased the speed, directionality, and coordination; however, depletion of RhoA did not change the migration speed, but caused the front row and back row cells to migrate simultaneously.

Figure 4.2 Depletion of Rac1, Cdc42, and RhoA disrupted epithelial collective migration.
(A) Control, Rac1-, Cdc42-, or RhoA-depleted stable cell lines were seeded and recorded for wound healing assay. The speed of migration at the leading edge was measured in ImageJ. The mean±SEM is shown. ns: $p>0.05$, *:$p\leq0.05$, ****: $p\leq0.0001$.
(B) The speed, directionality and coordination kymographs were generated after computational analysis from movies of control, Rac-1, Cdc42-, or RhoA-depleted cells in wound healing assay. The unit in speed kymograph was μm/hr. The directionality was the ratio between velocity perpendicular- and the velocity parallel- to the wound. The coordination was the fraction of cells that migrate as clusters with similar migration trajectories. Figure shows the representative kymographs from one experiment. Total of three independent experiments were performed.
(C) The images were generated from snapshots of migration movies from control and RhoA-depleted after PIV analysis cells from two consecutive images (t, t+5 min). The vector magnitude and direction indicates the speed and directionality of movement in the migrating monolayer.

Figure 4.2

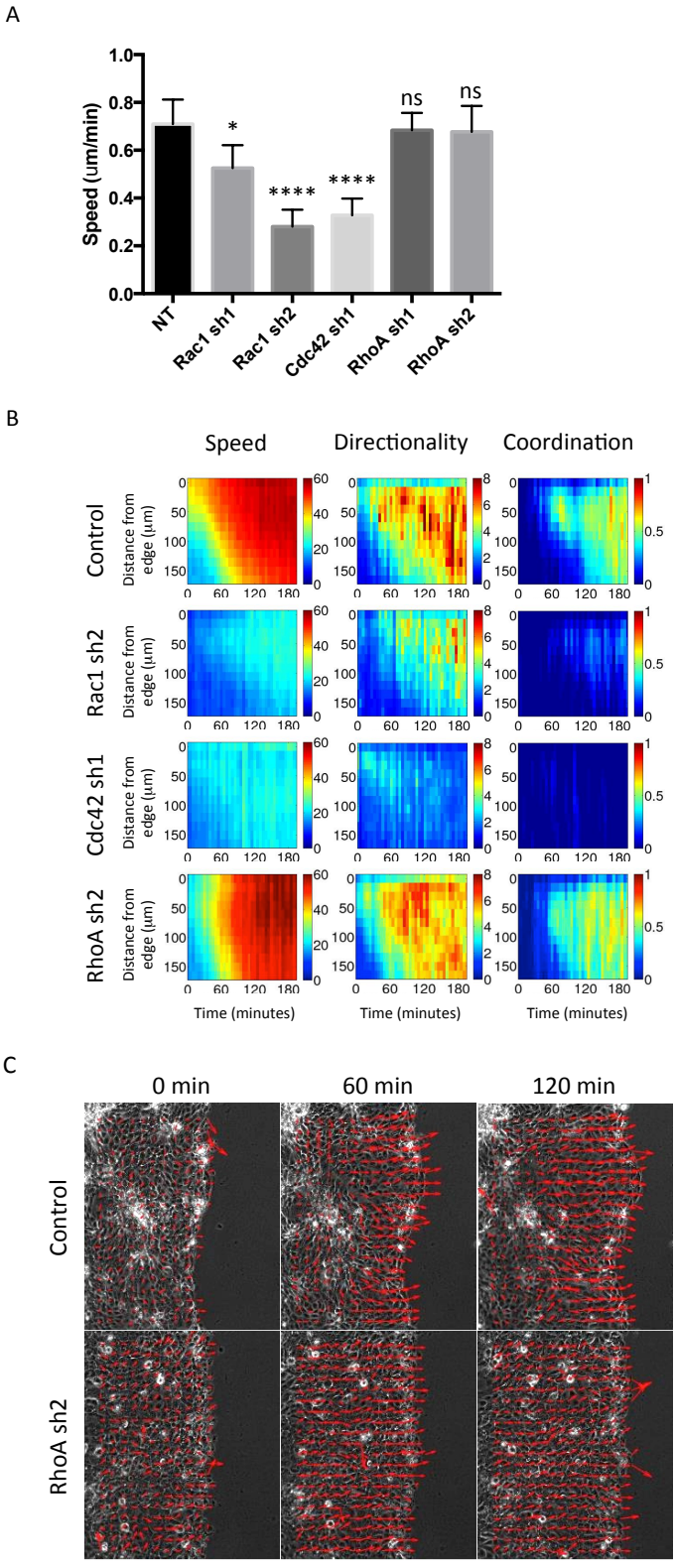
A
Speed (um/min)
1.0
0.8
0.6
0.4
0.2
0.0
*
****
****
ns
ns
NT
Rac1 sh1
Rac1 sh2
Cdc42 sh1
RhoA sh1
RhoA sh2
B
Speed
Directionality
Coordination
Control
Rac1 sh2
Cdc42 sh1
RhoA sh2
Distance from edge (μm)
Time (minutes)
C
0 min
60 min
120 min
Control
RhoA sh2

4.3 Screening of Rho GEFs

In total, there were 258 shRNAs targeting 80 GEFs in the shRNA library utilized for this study. Most GEFs were targeted by three independent shRNAs, while ARHGEF25, FGD6, FGD5, KALRN, ARHGEF38, and ARHGEF39 had six different targeting shRNAs in the library. Since all GEFs may not be expressed in 16HBE cells that were used for the migration analyses, prior to conducting the screen the GEF expression profile in 16HBE cells was determined by quantitative RT-PCR. Surprisingly, the PCR results indicated there were 75 GEFs out of 80 total expressed in 16HBE cells, with the exception of MCF2, FGD2, FGD5, PLEKHG7, and ARHGEF38.

After establishing more than 250 stable cell lines harboring specific shRNAs, knockdown efficiencies of individual hairpins were determined by qRT-PCR or Western blotting. The results were plotted in Figure 4.3 and summarized in Table 4.1. The shRNAs that depleted more than 50% of the transcript for a given gene were selected for further migration analysis. There were 11 genes for which the primers were not functional in the qRT-PCR reaction, however, the shRNAs targeting these genes were still included in the migration analysis. Together, we analyzed a total of 60 GEFs (49 validated GEFs + 11 non-validated GEFs) for their migration and junction phenotypes.

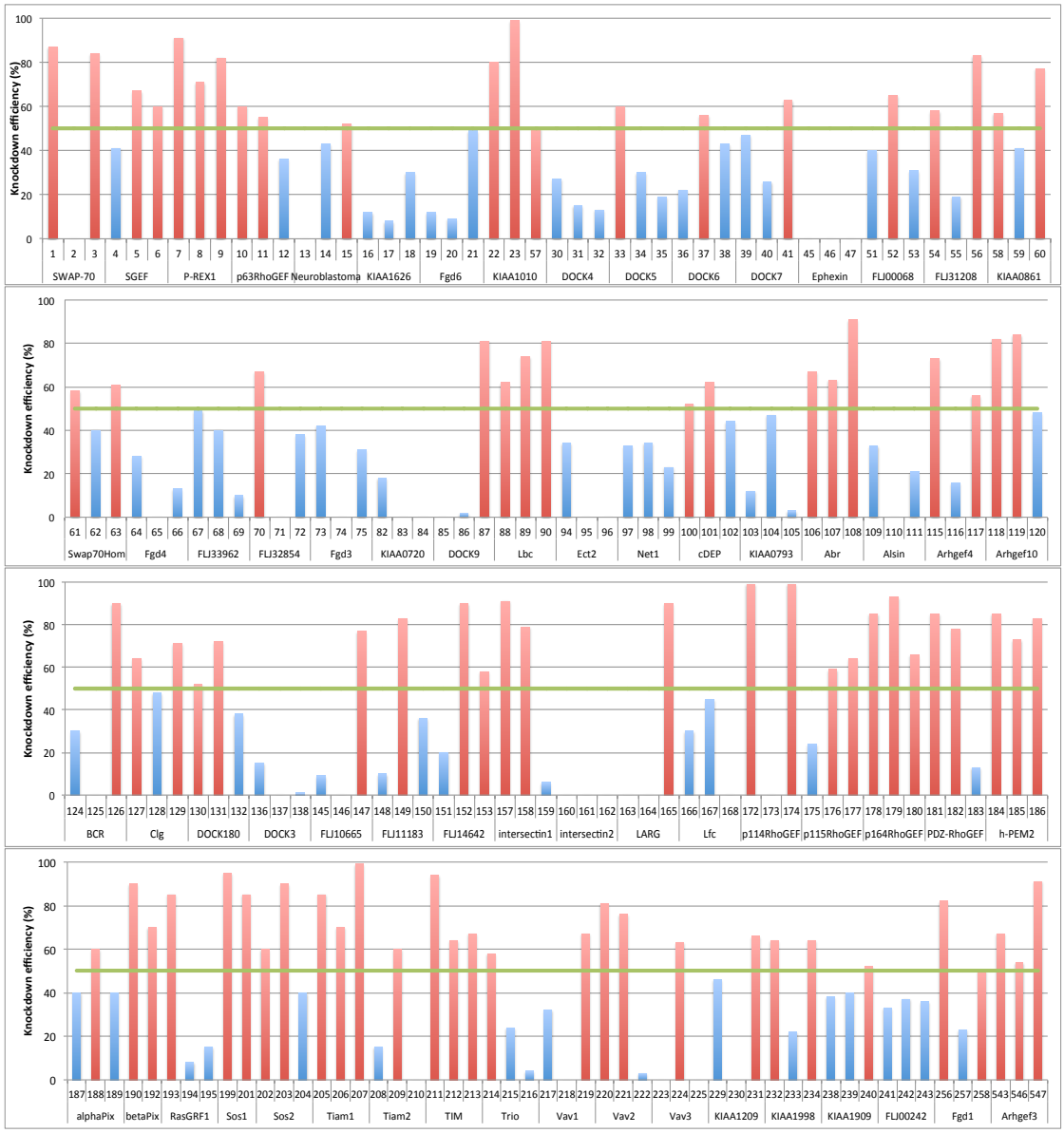

Figure 4.3 Knockdown efficiency of indicated genes for Rho GEF shRNAs. Stable cell lines harboring shRNA targeting Rho GEF were generated, lysed and analyzed for qRT-PCR or Western blot for the target genes. The threshold of knockdown efficiency was arbitrarily selected at 50% (green line). Migration movies from stable cell lines with more than 50% depletion of target gene (red) were selected for further computational analysis. The stable cell lines with less than 50% depletion of target gene were discarded (blue). Some shRNAs were unable to deplete the target gene, which were labeled as 0% knockdown efficiency in the figure.

Table 4.1 Summary of shRNA screen.
In total 75 genes were analyzed in 16HBE cells. Valid shRNA indicated the stable cell lines harboring the shRNA depleted more than 50% of its target gene.

Valid shRNA	Gene names	Total number
3	ABR, AKAP13, ARHGEF17, ARHGEF3, ARHGEF5, ARHGEF9, PREX1, TIAM1, ARHGEF25	9
2	ARHGEF1, ARHGEF10, ARHGEF11, ARHGEF18, ARHGEF28, ARHGEF39, ARHGEF4, β-PIX, DEF6, DOCK1, FARP1, ITSN1, MCF2L2, PLEKHG2, SGEF, SOS1, SOS2, SPATA13, SWAP70, TUBA, VAV2	21
1	α-PIX, ARHGEF12, ARHGEF16, BCR, DOCK5, DOCK6, DOCK7, DOCK9, FGD1, FGD6, PLEKHG1, PLEKHG4, PLEKHG4B, PLEKHG6, RASGRF1, TIAM2, TRIO, VAV1, VAV3	19
0	ALSIN, ARHGEF10L, ARHGEF40, DOCK3, DOCK4, ECT2, FARP2, FGD3, FGD4, GEF-H1, INTERSECTIN2, NET1, NGEF, PLEKHG3, PLEKHG5	15
Non-validated	ARHGEF15, DOCK2, DOCK8, DOCK10, DOCK11, ECT2L, KALRN, MCF2L, OBSCN, PREX2, RASGRF2	11

To summarize the screen results, for migration phenotype, we found that cells depleted of SOS1 had a significant delay in the wound healing rate and a decreased speed, directionality, and coordination by computational analysis (described in section 4.4). Cells with ARHGEF11, ARHGEF28 or ARHGEF3 depletion did not change the migration speed, but increased the directionality (described in section 4.5). Moreover, ARHGEF18-depleted cells had a similar migration phenotype as RhoA-depleted cells, in which cells in the front and in the back rows migrated simultaneously (described in section 4.5). For junction phenotypes, other than ARHGEF18 and SOS1, which were previously identified by the Hall lab (Xu, Jin et al. 2013, Durgan, Tao et al. 2015), additional GEFs were discovered that are required for tight junction formation, including BCR, PLEKHG2, PLEKHG6, ARHGEF28. Interestingly, those GEFs with

tight junction defects also exhibited the collective migration phenotypes, which were further analyzed computationally (described in section 4.7).

4.4 β-PIX, SOS1 in epithelial collective migration

In a previous study, β-PIX was found to regulate epithelial collective migration (Figure 3.7). Therefore, we considered β-PIX as a positive control in our screen. In agreement with the previous observation, β-PIX-depleted cells displayed decreased migration speed, directionality, and coordination using computational analysis (Figure 4.4).

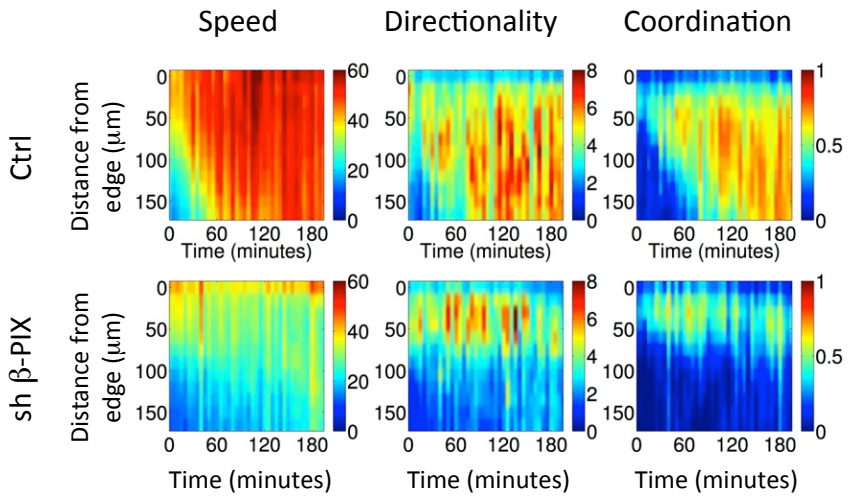

Figure 4.4 β-PIX was required for epithelial collective migration.
Control and stable cell lines with β-PIX depletion were seeded and recorded for wound healing assay. The movies were analyzed by computational program and the speed, directionality, and coordination kymographs were generated after analysis. The unit in speed kymograph was μm/hr. The directionality was the ratio between velocity perpendicular- and the velocity parallel- to the wound. The coordination was the fraction of cells that migrate as clusters with similar migration trajectories. This figure shows the representative kymographs from one experiment. A total of three independent experiments were performed.

Other than β-PIX, depletion of SOS1 also led to a strong migration delay in the wound healing assay (Figure 4.5A, B). However, depletion of the most closely-related GEF, SOS2, did not cause this migration delay (Figure 4.5C, D). By computational analysis, we found SOS1 depletion resulted in decrease in speed, directionality, and coordination on the kymographs (Figure 4.6B).

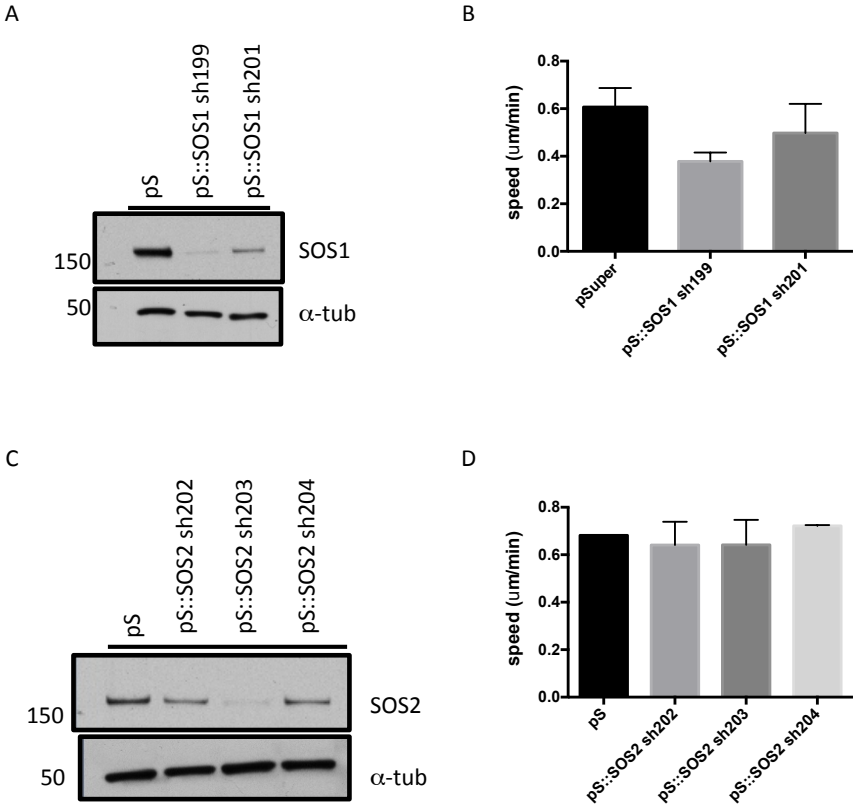

Figure 4.5 SOS1, but not SOS2, functions in epithelial collective migration.
(A, C) Control, stable cell lines with SOS1-depletion (A) or SOS2-depletion (B) were lysed and analyzed for Western blot with indicated antibodies. Representative results of three independent experiments are shown.
(B, D) Control, stable cell lines with SOS1-depletion (C) or SOS2-depletion (D) were seeded for wound healing assay. The speed of migration was measured in ImageJ. The mean±SEM is shown. N=3.

SOS1 is a Ras and Rac dual GEF, which contains a DH-PH domain for activation of Rac and a REM/Cdc25 domain for Ras activation. From the previous results, we already knew that Rac1 is involved in collective migration. To understand whether SOS1 controls the Ras or Rac pathway in collective migration, I expressed dominant-negative H-Ras (H-Ras N17) in 16HBE cells. However, the cells did not survive due to the high expression of H-Ras N17. Therefore, inhibitors of Ras downstream effectors were utilized to examine of the Ras signaling pathway is involved in collective migration (Figure 4.6A). Addition of GSK1120212 (GSK) or PD0325901 (PD), which are inhibitors of MEK1/2 that functions downstream of Ras, or SCH772984 (ERKi), an inhibitor of ERK that functions downstream of MEK, to the cells, each resulted in decreased speed, directionality and coordination in collective migration (Figure 4.6B). These results suggested that the Ras pathway, in addition to Rac1, is also involved in regulating collective migration.

Since Rac1 is also required for proper collective migration, it was unclear whether SOS1 regulates collective migration through the Rac or Ras pathway. The structure of SOS1 indicated that the DH-PH domain of SOS1 was required for Rac activation, while the REM/Cdc25 domain was for required for Ras activation. Ideally, the question of which pathway SOS1 regulates during collective migration could be answered by performing rescue experiments using SOS1 shRNA-resistant constructs with DH-PH domain mutation, or REM/Cdc25 domain deletion, in SOS1-depelted cells and testing their migration phenotypes. However, due to the relatively large size

of SOS1, retrovirus particles could not be efficiently produced to perform these rescue experiments.

In summary, cells with both Rac1 depletion or treated with inhibitors of Ras effectors showed decreased migration speed, directionality, and coordination in collective migration, which suggests that SOS1 could regulate collective migration through both Rac and Ras signaling.

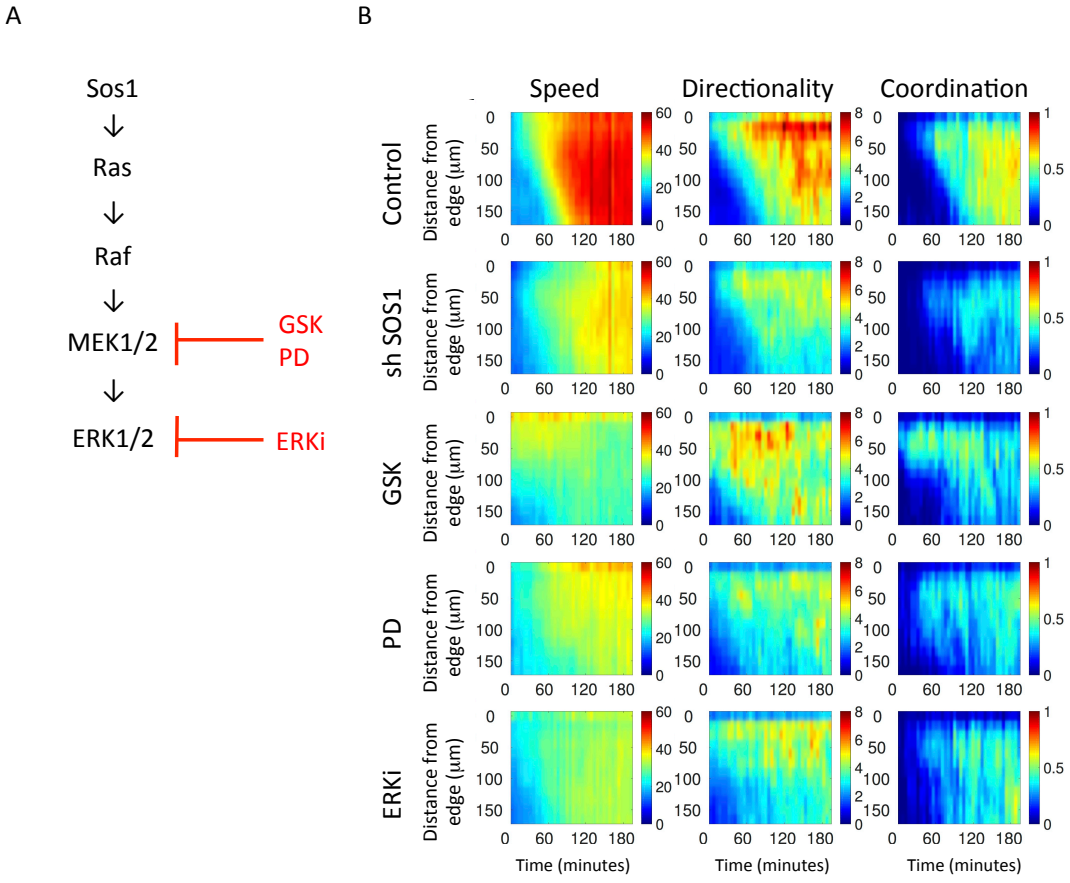

Figure 4.6 SOS1 and its downstream Ras pathway regulated epithelial collective migration.
(A) Schematic figure indicated the SOS1-RAS pathway. GSK: GSK1120212, PD: PD0325901, ERKi: SCH772984
(B) Control and stable cell lines with SOS1-depletion or inhibitor treatments were seeded and recorded for wound healing assay. The movies were analyzed by computational program and the speed, directionality, and coordination kymographs were generated after analysis. The unit in speed kymograph was μm/hr. The directionality was the ratio between velocity perpendicular- and the velocity parallel-to the wound. The coordination was the fraction of cells that migrate as clusters with similar migration trajectories.This figure shows the representative kymographs from one experiment. A total of three independent experiments were performed.

4.5 Rho-specific GEFs, ARHGEF3, ARHGEF11, ARHGEF18, and ARHGEF28 in epithelial collective migration

RhoA-depleted cells exhibited an unusual phenotype compared to loss-of-function for Rac or Cdc42, with front and back rows of cells migrating simultaneously. We further examined if any Rho-specific GEFs might have emerged in the screen whose knockdown could phenocopy loss of RhoA, in order to identify a potential signaling pathway regulating Rho in collective migration (Figure 4.2B).

By using computational analyses, we found that depletion of ARHGEF18 had a similar phenotype to RhoA depletion, as the front row and back row cells migrated simultaneously, and thus displayed a vertically-oriented straight line on the speed kymograph (Figure 4.7A). Other than ARHGEF18, we found that cells depleted for the addition Rho GEFs ARHGEF3, ARHGEF11, and ARHGEF28 exhibited a different migration phenotype, with evidence for increased directionality (Figure 4.7B). The PIV figures of control and ARHGEF11-depleted cells further supported the result that cells with depletion of ARHGEF11 had increased directionality compared to control cells (Figure 4.7C). Altogether, we found that depletion of ARHGEF18 had a similar phenotype to depletion of RhoA in speed; however, depletion of ARHGEF3, ARHGEF11, or ARHGEF28 instead increased directionality, which was different from the RhoA phenotype.

Figure 4.7 ARHGEF18, ARHGEF3, ARHGEF11 and ARHGEF28 are required for epithelial collective migration.
(A, B) Control and stable cell lines with (A) ARHGEF18-depletion or (B) ARHGEF3-, ARHGEF11, or ARHGEF18-depletion were seeded and recorded for wound healing assay. The movies were analyzed by computational program and the speed, directionality, and coordination kymographs were generated after analysis. This figure shows the representative kymographs from one experiment. The unit in speed kymograph was μm/hr. The directionality was the ratio between velocity perpendicular- and the velocity parallel- to the wound. The coordination was the fraction of cells that migrate as clusters with similar migration trajectories.A total of three independent experiments were performed.
(C) Images generated from snapshots of migration movies from control and ARHGEF11-depleted cells after PIV analysis. The vector magnitude and direction indicates the speed and directionality of movement in the migrating monolayer.

Figure 4.7

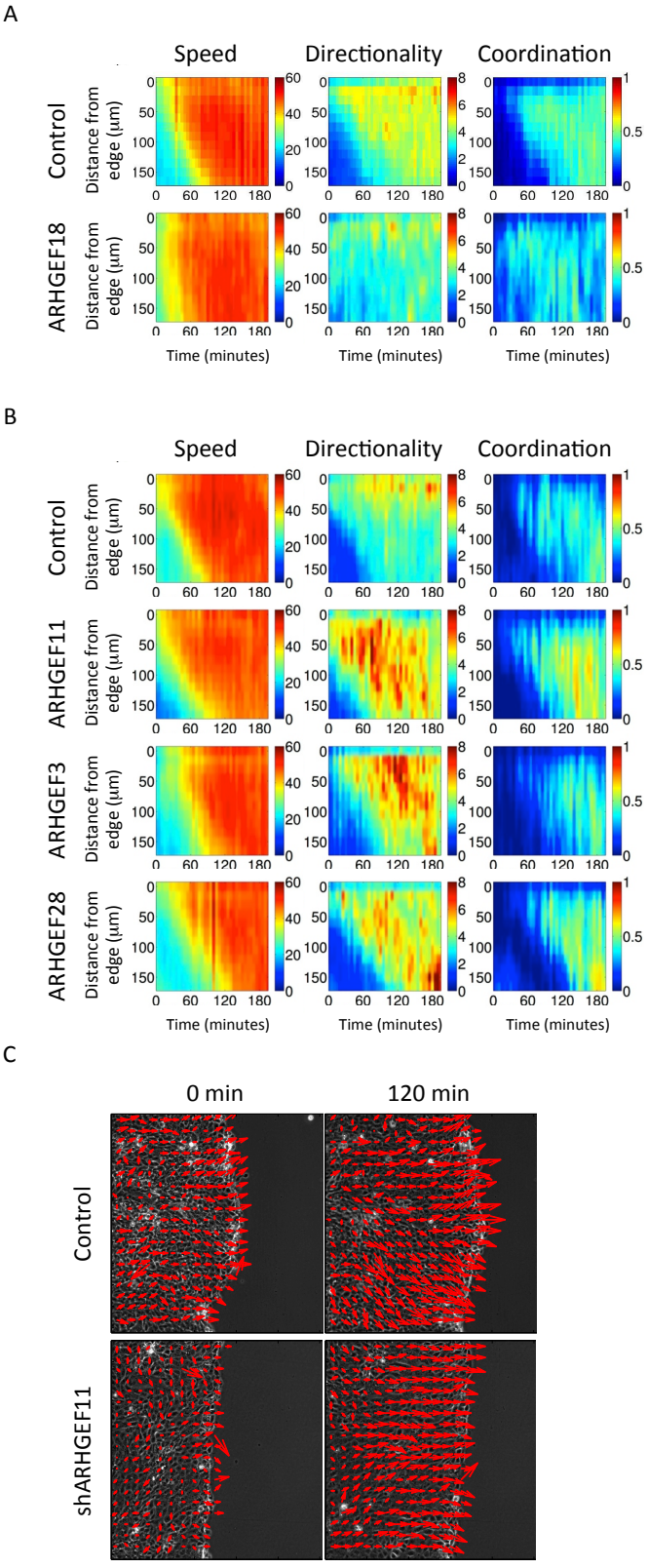
A
Speed
Directionality
Coordination
Control
ARHGEF18
Distance from edge (μm)
Time (minutes)
B
Speed
Directionality
Coordination
Control
ARHGEF11
ARHGEF3
ARHGEF28
Distance from edge (μm)
Time (minutes)
C
0 min
120 min
Control
shARHGEF11

4.6 Rho pathway in collective migration

One well-known downstream effector of Rho is Rho-kinase, or ROCK, which is known to lead to activation of myosin light chain to induce actomyosin contraction in cells (Figure 1.3). To understand whether this known pathway that is activated by Rho signaling is required for collective migration, 16HBE cells were treated with inhibitors, including the ROCK inhibitor Y27632 and the myosin II inhibitor Blebbistatin, and the effects on collective migration were examined and compared to loss-of-function for RhoA, or the Rho GEFs identified in the screen. For each of these follow-up experiments, analyses were performed three times to validate the reproducibility of phenotypes, and each experiment was examined quantitatively to determine phenotypes in three categories, speed, directionality, and coordination, displayed in the representative kymographs. In order to compare different experimental replicates, the spatial temporal information (the color-coded values) on the kymographs were separated into twelve sections and averaged into twelve values. Therefore, each kymograph had twelve vectors representing the encoded migration behaviors. Then, principle component analysis was applied to reduce the twelve vectors into three features (PC1, PC2, and PC3), which encoded magnitude, temporal, and spatial derivatives separately. Therefore, for each individual experiment, a total of nine values including speed PC1-3, directionality PC1-3, and coordination PC1-3 were generated to constitute the migration behaviors of cells. To compare the different experimental results, high-dimensional similarity analysis was introduced to represent

the similarity between two treatments, which was color-coded in the matrix (Figure 4.8A).

We compared the migration results of Rho, Rho GEF depletion, and Rho effectors inhibition in Figure 4.8A. As shown in the figure, the migration behaviors of cells with long-term blebbistatin 10μM treatment were similar to cells with depletion of RhoA or ARHGEF18, which together form a blue cluster in the matrix. The other similarity cluster was formed by cells with depletion of ARHGEF3, ARHGEF28 and ARHGEF11. The migration behaviors of cells with long-term Y27632 treatments were highly similar to cells with long-term blebbistatin treatment, but not as similar to cells with depletion of RhoA. ARHGEF3 or ARHGEF28-depleted cells had moderate similarity to cells with long-term blebbistatin treatment, but not to RhoA-depleted cells. Together, the results suggested that ARHGEF18 regulated RhoA and its downstream effector, myosin, to control epithelial collective migration, while ARHGEF3, ARHGEF11, and ARHGEF28 may function differently in regulating this process (Figure 4.8B).

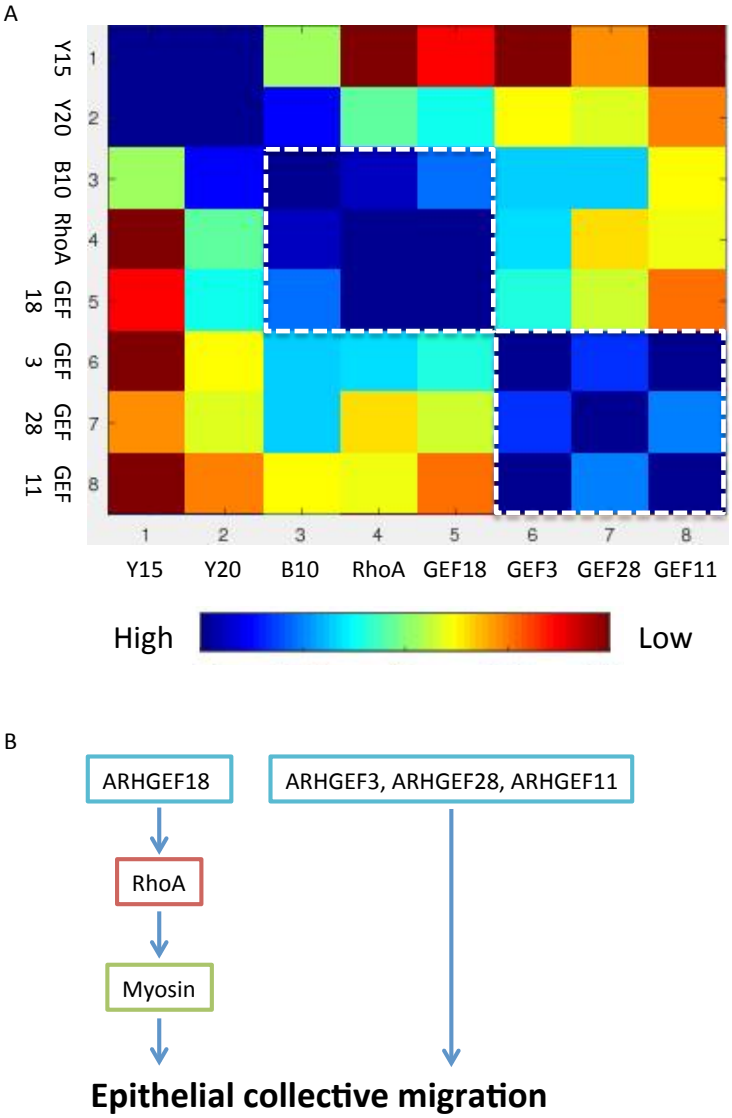

Figure 4.8 Cell monolayers with different perturbations exhibited distinct migration behaviors.
(A) Pair-wise distance matrix analysis of the migration behaviors of long-term Y27632 15uM (Y15), 20uM (Y20) or Blebbistatin 10uM (B10) treatments, and RhoA-, ARHGEF18- (GEF18), ARHGEF3- (GEF3), ARHGEF28- (GEF28), and ARHGEF11- (GEF11) depleted cells. The marked regions indicate the high similarity regions in the matrix.
(B) Schematic pathway plotted the relationships of Rho GEFs, RhoA, myosin, and epithelial collective migration.

4.7 Tight junctions and collective migration

One important characteristic of epithelial collective migration is that the cells are connected together during movement. In epithelial cell sheets, cells are connected through tight junctions, adherens junctions, gap junctions and desmosomes. The cadherin-based adherens junctions are important for maintaining collective migration. However, whether the integrity of the other junctional structures is required for effective collective migration is not clear. Previously, we identified that ARHGEF18 (p114 RhoGEF), a Rho-specific GEF, and SOS1, a Rac/Ras duel GEF, were required for tight junction formation (Xu, Jin et al. 2013, Durgan, Tao et al. 2015). To identify in the screen that additional GEFs might also be required for tight junction formation, junction phenotypes in GEF-depleted cells were quantified by ZO-1 immunostaining.

In addition to ARHGEF18 and SOS1, which were shown previously to be tight junction regulators, I further identified that BCR, PLEKHG6, ARHGEF28, which are Rho-specific GEFs, and PLEKHG2 (CLG), a Cdc42 and Rac duel GEF, are also required for tight junction formation, as depletion of those GEFs induced failure to localize ZO-1, a tight junction component, at cell-cell contacts (Figure 4.9A). Quantification of these results is shown in Figure 4.9B. To examine if cells with tight junction defects also have collective migration defects, we analyzed the migration behaviors of those GEF-depleted cells using principle component analysis, which categorized the migration behaviors in speed PC1-3, directionality PC1-3, and coordination PC1-3. The results are presented in Figure 4.9C. In addition to cells with

depletion of ARHGEF28, which had more significant migration defects described in section 4.5, cells with depletion of BCR, PLEKHG2, or PLEKHG6 all exhibited certain degrees of collective migration defects in directionality and coordination. Therefore, we concluded that cells with disrupted tight junctions also have collective migration defects.

Figure 4.9 Cells have tight junction defects also have collective migration defects. Control, shBCR, shPLEKHG2 hairpin 1, 2, shPLEKHG6 or shARHGEF28 hairpin 1, 2 stably infected 16HBE cells examined for tight junction and migration assay.
(A) Control or shPLEKHG6 16HBE stable cell lines were seeded at low density for 3 days and then fixed and stained for ZO-1 (red) and nuclei (blue). Scale bar: 20 μm.
(B) Quantification of tight junction phenotypes for indicated stable cell lines from 3 independent experiments. Counted cells >600 per sample/experiment. Error bars indicate Mean±SEM, ****: $p<0.0001$.
(C) Stable cell lines were seeded for wound healing assay. Table of migration phenotypes for cells with tight junction defects. Statistics via Wilcoxon signed rank test: $p \leq 0.01$: *, $p \leq 0.001$: **, $p \leq 0.0001$: ***. Number of arrows indicates to the p-value.

Figure 4.9

A

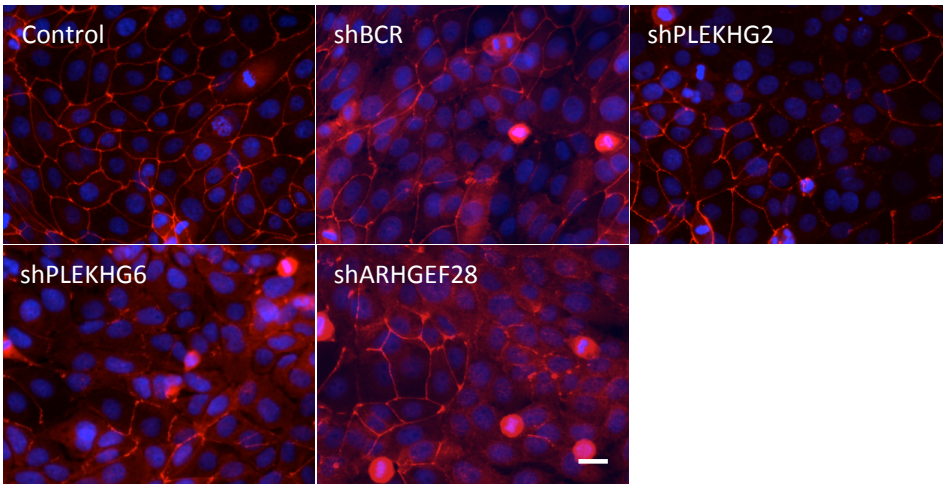

B

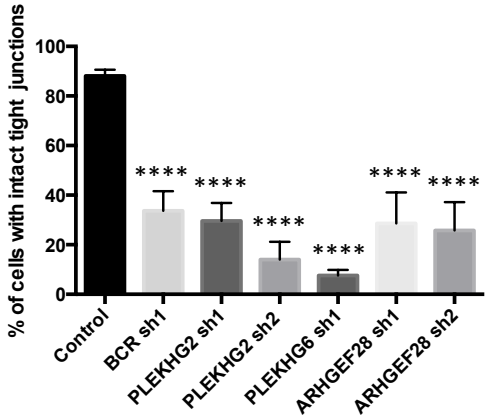

C

Gene	Speed			Directionality			Coordination		
	PC1	PC2	PC3	PC1	PC2	PC3	PC1	PC2	PC3
BCR	-	-	-	-	-	-	-	↓	-
PLEKHG2	-	-	-	-	-	-	-	↑	-
PLEKHG6	-	-	-	↑↑	-	-	-	-	-
ARHGEF28	-	-	-	↑↑↑	↑	↑	↑↑↑	↑	↑↑

4.8 Discussion

Collective migration is an important biological process yet little is known about how cells coordinately regulate such movements. While Rho GTPases are critical regulators of the cytoskeleton and are known to play distinct roles in single cell migration, how they control cell movements in epithelial sheets, where the individual cells are also connected by cell-cell junctions, is less clear. To examine this question, a systematic screening approach was utilized to quantitatively determine the effects of depletion of individual Rho GTPases on collective migration, and to identify potential key GEFs that mediate signaling in this context.

These studies identified that depletion of Rac or Cdc42, but not RhoA, induced a significant delay in collective migration in a wound healing assay (Figure 4.2A). Further computational analysis confirmed this finding. For Rac1- or Cdc42-depleted cells, both the front and the back row cells showed reduced migration speed, directionality, and coordination. In single cell migration, it has been reported that Rac is required for lamellipodia formation while Cdc42 is required for filopodia formation (Nobes and Hall 1995), and both are important for organizing the actin cytoskeleton during migration. Therefore, it was not surprising that depletion of Rac1 or Cdc42 disrupted collective migration, as their depletion also inhibited single cell migration. The remaining migration ability in the depleted cell lines may be contributed by incomplete knockdown of Rac1 or Cdc42, or cell division in the confluent monolayer.

Depletion of RhoA did not decrease the migration speed; instead, it induced the front row and back row to migrate simultaneously. In the speed kymograph of control cells, the front row cells migrated faster (responding to the wound earlier) compared to the back row cells, which created a diagonal line on the kymograph. However, for RhoA-depleted cells, the front and the back row cells migrated simultaneously toward the wound, which created a straight line on the speed kymograph (Figure 4.2B). There are two possible hypotheses to explain the phenotype. First, the Rho-depleted front row cells responded slower than control cells, but the back row cells remained unaffected. Therefore, the front and the back row cells migrated simultaneously in RhoA-depleted cells. Second, the coordination between the front and the back row cells may be changed by RhoA depletion. This effect could be caused by the loss of an inhibitory signal in the back row cells, and thus the back row cells behave like the front row cells. Alternatively, signal transduction between the leaders and followers could be faster; therefore the followers have similar speed as the leaders.

In order to identify the Rho GEFs that control epithelial collective migration, I established and screened more than 200 stable cell lines which harbor shRNA hairpins targeting 75 expressed GEFs in 16HBE cells, to examine their effects on migration behavior. Excluding the shRNA hairpins that depleted less than 50% of its target gene, I generated more than 2600 movies and sent these for further computational analysis for examining the collective migration behaviors in the screen and the follow-up hit evaluation experiments. In addition to β-PIX, which was already known for its function in collective migration (Omelchenko, Rabadan et al. 2014), we identified

SOS1, ARHGEF18, ARHGEF3, ARHGEF11, and ARHGEF28 as regulators of epithelial collective migration.

The screening results identified SOS1, a Ras/Rac duel GEF, as an important regulator of collective migration. Follow-up studies utilizing inhibitors of Ras effectors suggest that the Ras pathway is indeed involved in collective migration. However, it is possible that SOS1 also functions as a Rac GEF in the context of epithelial collective migration. Both Ras and Rac have been reported to be involved in collective migration (see section 1.3.2 and section 1.4.3). 16HBE cells with dominant-negative Rac1 expression or strong inhibition of Rac1 did not migrate (Figure 3.4C). However, SOS1-depleted cells still migrated, only with reduced speed. These results could suggest that SOS1 regulate Ras activity in migration, or that residual SOS1 activity in the knockdown cells is sufficient to activate Rac for migration. Further experiments are needed to clarify whether SOS1 functions as a Rac1 or Ras GEF in collective migration. Expressing SOS1 with deletion of the Ras or Rac activation domain and looking for rescue of the migration phenotype in SOS1-depleted cells would help answer this question.

The results of the screen and follow-up experiments also demonstrate that depletion of ARHGEF18 and long-term blebbistatin treatment had a similar migration phenotype to depletion of RhoA, suggesting that ARHGEF18 may function in the same pathway, potentially upstream of RhoA to control collective migration. The involvement of myosin further suggests that force generation might be required for RhoA-regulated

epithelial collective migration. However, cells with inhibition of the upstream myosin effector, ROCK, using Y27632, did not have a similar migration phenotype as cells with RhoA depletion. This may due to an off-target effect of Y27632. Other than ROCK, Y27632 also inhibits protein kinase C-related protein kinase 2 (PRK-2) at a similar IC50 (Davies, Reddy et al. 2000).

Interestingly, depletion of other Rho-specific GEFs, ARHGEF3, ARHGEF11, and ARHGEF28 resulted in different migration phenotypes. One of the key steps in migration is forming focal adhesions at the front of the cells to generate traction forces and release of adhesions in the rear of cells to permit cell movement. The assembly of focal adhesions requires Rho activity (Ridley and Hall 1992). Moreover, it has been reported that ARHGEF11 (also named PDZ-RhoGEF) and ARHGEF28 (also known as p190RhoGEF or Rgnef) are located at focal adhesion complexes and regulate adhesion formation (Iwanicki, Vomastek et al. 2008, Miller, Lawson et al. 2013). However, there is currently no report to suggest that ARHGEF3 is related to focal adhesion. Since depletion of ARHGEF3, ARHGEF11, and ARHGEF28 had similar phenotypes in collective migration, it is possible that they regulate RhoA in a similar, but non-redundant manner. Migration experiments for inhibitors that target focal adhesion kinase would help to test this hypothesis. Thus, combined with the results from ARHGEF18 depletion, I hypothesize that ARHGEF3, ARHGEF11, and ARHGEF28 locally control RhoA activity at focal adhesions, while ARHGEF18 regulates RhoA activity broadly in epithelial collective migration.

In this study, I identified that BCR, PLEKHG6, ARHGEF28, which are Rho-specific GEFs, and PLEKHG2 (CLG), a Cdc42 and Rac duel GEF, are required for tight junction formation (Figure 4.9A). Among them, we were most excited about the finding of PLEKHG2. We already knew that Cdc42 and its downstream effectors, PAK4 and Par6, regulate tight junction formation (Wallace, Durgan et al. 2010). However, the GEF involved in controlling Cdc42 activities in tight junction formation was unknown. My finding that depletion of PLEKHG2 caused tight junction defects provided a candidate for the GEF that activates Cdc42 in controlling tight junction formation.

Finally, cells with tight junction defects also exhibited collective migration defects, suggesting that the integrity of tight junctions is important for collective migration. Moreover, the integrity of tight junctions is known to affect the stability of adherens junctions, which are required for epithelial collective migration. Therefore, depletion of these particular GEFs may also lead to changes in adherens junctions that could contribute to collective migration defects. Further experiments addressing the integrity and dynamics of adherens junctions in the context of these knockdowns may inform on this possibility.

Chapter 5 - Conclusion and future directions

5.1 Thesis overview

Collective migration is a complex biological process involving the coordinated movement of groups of cells with stable or transient cell connections. Collective migration plays important roles in development and adulthood, for example during mammary gland morphogenesis, epidermal wound closure, wound healing, vascular sprouting, and neural crest migration, and also in disease progression, for example to mediate the spread of cancer cells through collective invasion.

Small GTPases control many distinct cellular behaviors including morphogenesis, proliferation, differentiation, cell division, and migration. They function as molecular switches, which are activated by GEFs and inactivated by GAPs. The Ras superfamily of small GTPases is composed of five subfamilies, which are Ras, Rho, Rab, Ran, and Arf. Among them, members of the Ras and Rho families have been suggested to be involved in the regulation of collective migration.

Rap GTPases belong to the Ras family, which mainly function in cell-cell and cell-ECM interactions, the two important connections in collective migration. However, whether Rap proteins regulate collective migration was unknown. In my studies, I have found that Rap1A controls epithelial collective migration. Expressing dominant

negative Rap1A disrupted the direction of actin-rich protrusions in migrating cells and, therefore, the directionality of the migrating monolayer. Since Rho GTPases are master regulators in migration, I have shown that Rap1A activates Cdc42, and provided a possible mechanism whereby a Cdc42 GEF, β-PIX, and a scaffold protein, IQGAP1, may be involved in Rap1A-dependent regulation.

Rho GTPases (Rho, Rac, and Cdc42) are known to control single cell migration. However, the detailed functions of Rho GTPases in epithelial collective migration were unclear. Combining biological approaches and computational analysis, we have demonstrated that Rac1 and Cdc42 are required for speed, directionality, and coordination in epithelial collective migration, while depletion of RhoA induced the front and the back row cells to migrate simultaneously, without significantly affecting the would healing rate.

Since Rho GTPases are activated by their GEFs, one interesting question is what are the GEFs that regulate the activities of Rho GTPases in the context of epithelial collective migration. In the human genome, approximately 80 GEFs exist to control Rho GTPases under distinct conditions. After conducting a comprehensive screen targeting 80 GEFs and performing a detailed computational analysis of their migration behaviors, we have identified that SOS1, a Ras/Rac duel GEF, controls speed, directionality, and coordination in epithelial collective migration. Furthermore, from the results of inhibitor treatments against Ras downstream effectors, we propose that SOS1 regulates Ras activity in epithelial collective migration. Other than SOS1, we

also discovered that ARHGEF18 controls RhoA and its downstream effector, myosin, in epithelial collective migration. Depletion of ARHGEF3, ARHGEF11, and ARHGEF28, Rho specific GEFs, also induce migration defects but these defects are different from those caused by RhoA-depletion. Finally, the cells with tight junction defects have collective migration defects suggesting that the integrity of tight junctions is required for epithelial collective migration.

Below, I discuss potential future directions for understanding the detailed mechanisms of epithelial collective migration.

5.2 Mechanism of Cdc42 activation by Rap1A in epithelial collective migration

As described in chapter 3 (section 3.5), I used an *in vitro* pull-down assay to demonstrate that Rap1A activates Cdc42. This mechanism is conserved in budding yeast, where Bub1 (Rap1 homolog in yeast) activates Cdc42 through Cdc24p (Cdc42 GEF in yeast) to determine the budding site (Park, Bi et al. 1997). However, the hypothesis that Rap1 activates Cdc42 would be strengthened by expressing a fluorescence resonance energy transfer (FRET)-based Cdc42 biosensor in control and Rap1A-depleted cells. By comparing Cdc42 activity within control and Rap1A-depleted cells in a wound healing assay, our hypothesis would be supported if the level

of Cdc42 activity was decreased in Rap1A-depleted cells when compared with control cells in migrating sheets.

In section 3.5, I proposed a possible mechanism whereby Rap1A activates Cdc42, through β-PIX and IQGAP1. However, due to lack of direct binding evidence between Rap1A and β-PIX, it is possible that Rap1A activates Cdc42 through other Cdc42 GEFs. In the GEF screen described in chapter 4, I had validated 49 GEFs with efficient shRNAs to deplete gene expression (knockdown more than 50% of target gene). Among them, no novel Cdc42 GEF was identified for controlling epithelial collective migration. However, because some Cdc42 GEFs did not have suitable shRNAs to efficiently knockdown the gene expression (Table 4.1), it is still possible that Rap1A regulates one of these other Cdc42 GEFs to activate Cdc42 in cells. Other than activating Cdc42 through a GEF, Rap1A may function through inhibiting a Cdc42 GAP and thus facilitating Cdc42 activation. Therefore, the detailed mechanism about how does Rap1A activate Cdc42 requires further examination.

5.3 Regulation of Rho GTPases in collective migration

From the GEF screen results, we confirmed that β-PIX, a Rac/Cdc42 GEF, and discovered that SOS1, a Ras/Rac GEF, function in epithelial collective migration. However, because for some GEFs we did not have proper reagents to deplete gene expression, it is possible that we missed some GEFs that also regulate collective

migration in 16HBE cells. Additionally, because of the high degree of structural and functional similarities between different GEFs, it is possible that some GEFs exhibit functional redundancy with the others. Therefore, the effect of depleting one specific GEF may be compensated by other related GEFs, which also reduces the opportunity to find novel GEFs that are required for collective migration. The possible solution for this issue is to deplete the GEFs in the same subfamily at the same time; this may, therefore, avoid the redundancy problem in the screen.

Rho has been shown to be required for tail retraction during single cell migration (Worthylake, Lemoine et al. 2001). On the other hand, Rho activity had also been found at the front of lamellipodia in migrating cells, where it may contribute to mDia1-mediated actin polymerization and/or myosin II-mediated retraction (Machacek, Hodgson et al. 2009). Moreover, RhoA controls actomyosin activity and is important in force generation in cells. Therefore, during collective migration, RhoA may function in the front row, in the back rows, and in between cells, to transmit force in the migrating monolayer. It has been reported that in the MDCK collective migration model, which forms finger structures where the leader cells drag the follower cells when migrating, that RhoA is required to control the formation of fingers (Reffay, Parrini et al. 2014). Therefore, it is possible that in the 16HBE collective migration model, RhoA activity is high in the front row cells in order to generate force for migration, and ARHGEF18 is required to activate RhoA in the front. To test this hypothesis in future experiments, a FRET-based RhoA biosensor is needed, to examine RhoA activity in the migrating monolayer, especially in the front

row cells. Furthermore, to study force generation and transmission in the monolayer, 16HBE cells could be cultured on soft micro-pillars, which function as independent force sensors for mapping force generation. Combined with RhoA-depletion and RhoA GEF-depletion tools, this would allow us to understand the detailed mechanism of the function of RhoA during epithelial collective migration.

REFERENCES

Ahearn, I. M., K. Haigis, D. Bar-Sagi and M. R. Philips (2012). "Regulating the regulator: post-translational modification of RAS." Nat Rev Mol Cell Biol **13**(1): 39-51.

Arber, S., F. A. Barbayannis, H. Hanser, C. Schneider, C. A. Stanyon, O. Bernard and P. Caroni (1998). "Regulation of actin dynamics through phosphorylation of cofilin by LIM-kinase." Nature **393**(6687): 805-809.

Arthur, W. T., L. A. Quilliam and J. A. Cooper (2004). "Rap1 promotes cell spreading by localizing Rac guanine nucleotide exchange factors." J Cell Biol **167**(1): 111-122.

Bianco, A., M. Poukkula, A. Cliffe, J. Mathieu, C. M. Luque, T. A. Fulga and P. Rorth (2007). "Two distinct modes of guidance signalling during collective migration of border cells." Nature **448**(7151): 362-365.

Boettner, B., E. E. Govek, J. Cross and L. Van Aelst (2000). "The junctional multidomain protein AF-6 is a binding partner of the Rap1A GTPase and associates with the actin cytoskeletal regulator profilin." Proc Natl Acad Sci U S A **97**(16): 9064-9069.

Boettner, B. and L. Van Aelst (2009). "Control of cell adhesion dynamics by Rap1 signaling." Curr Opin Cell Biol **21**(5): 684-693.

Bos, J. L. (2005). "Linking Rap to cell adhesion." Curr Opin Cell Biol **17**(2): 123-128.

Bristow, J. M., M. H. Sellers, D. Majumdar, B. Anderson, L. Hu and D. J. Webb (2009). "The Rho-family GEF Asef2 activates Rac to modulate adhesion and actin dynamics and thereby regulate cell migration." J Cell Sci **122**(Pt 24): 4535-4546.

Broders-Bondon, F., P. Paul-Gilloteaux, E. Gazquez, J. Heysch, M. Piel, R. Mayor, J. D. Lambris and S. Dufour (2016). "Control of the collective migration of enteric neural crest cells by the Complement anaphylatoxin C3a and N-cadherin." Dev Biol **414**(1): 85-99.

Brugnera, E., L. Haney, C. Grimsley, M. Lu, S. F. Walk, A. C. Tosello-Trampont, I. G. Macara, H. Madhani, G. R. Fink and K. S. Ravichandran (2002). "Unconventional Rac-GEF activity is mediated through the Dock180-ELMO complex." Nat Cell Biol **4**(8): 574-582.

Burridge, K. and E. S. Wittchen (2013). "The tension mounts: stress fibers as force-generating mechanotransducers." J Cell Biol **200**(1): 9-19.

Cai, D., S. C. Chen, M. Prasad, L. He, X. Wang, V. Choesmel-Cadamuro, J. K. Sawyer, G. Danuser and D. J. Montell (2014). "Mechanical feedback through E-cadherin promotes direction sensing during collective cell migration." Cell **157**(5): 1146-1159.

Carmona-Fontaine, C., E. Theveneau, A. Tzekou, M. Tada, M. Woods, K. M. Page, M. Parsons, J. D. Lambris and R. Mayor (2011). "Complement fragment C3a controls mutual cell attraction during collective cell migration." Dev Cell **21**(6): 1026-1037.

Carr, H. S., Y. Zuo, W. Oh and J. A. Frost (2013). "Regulation of focal adhesion kinase activation, breast cancer cell motility, and amoeboid invasion by the RhoA guanine nucleotide exchange factor Net1." Mol Cell Biol **33**(14): 2773-2786.

Chapnick, D. A. and X. Liu (2014). "Leader cell positioning drives wound-directed collective migration in TGFbeta-stimulated epithelial sheets." Mol Biol Cell **25**(10): 1586-1593.

Cheung, K. J., V. Padmanaban, V. Silvestri, K. Schipper, J. D. Cohen, A. N. Fairchild, M. A. Gorin, J. E. Verdone, K. J. Pienta, J. S. Bader and A. J. Ewald (2016). "Polyclonal breast cancer metastases arise from collective dissemination of keratin 14-expressing tumor cell clusters." Proc Natl Acad Sci U S A **113**(7): E854-863.

Choi, S., N. Thapa, A. C. Hedman, Z. Li, D. B. Sacks and R. A. Anderson (2013). "IQGAP1 is a novel phosphatidylinositol 4,5 bisphosphate effector in regulation of directional cell migration." EMBO J **32**(19): 2617-2630.

Chou, J., N. A. Burke, A. Iwabu, S. C. Watkins and A. Wells (2003). "Directional motility induced by epidermal growth factor requires Cdc42." Exp Cell Res **287**(1): 47-56.

Chrzanowska-Wodnicka, M., G. C. White, 2nd, L. A. Quilliam and K. J. Whitehead (2015). "Small GTPase Rap1 Is Essential for Mouse Development and Formation of Functional Vasculature." PLoS One **10**(12): e0145689.

Cote, J. F. and K. Vuori (2002). "Identification of an evolutionarily conserved superfamily of DOCK180-related proteins with guanine nucleotide exchange activity." J Cell Sci **115**(Pt 24): 4901-4913.

Cote, J. F. and K. Vuori (2006). "In vitro guanine nucleotide exchange activity of DHR-2/DOCKER/CZH2 domains." Methods Enzymol **406**: 41-57.

Cullere, X., S. K. Shaw, L. Andersson, J. Hirahashi, F. W. Luscinskas and T. N. Mayadas (2005). "Regulation of vascular endothelial barrier function by Epac, a cAMP-activated exchange factor for Rap GTPase." Blood **105**(5): 1950-1955.

Dachsel, J. C., S. P. Ngok, L. J. Lewis-Tuffin, A. Kourtidis, R. Geyer, L. Johnston, R. Feathers and P. Z. Anastasiadis (2013). "The Rho guanine nucleotide exchange factor Syx regulates the balance of dia and ROCK activities to promote polarized-cancer-cell migration." Mol Cell Biol **33**(24): 4909-4918.

Dambly-Chaudiere, C., N. Cubedo and A. Ghysen (2007). "Control of cell migration in the development of the posterior lateral line: antagonistic interactions between the chemokine receptors CXCR4 and CXCR7/RDC1." BMC Dev Biol **7**: 23.

David, N. B., D. Sapede, L. Saint-Etienne, C. Thisse, B. Thisse, C. Dambly-Chaudiere, F. M. Rosa and A. Ghysen (2002). "Molecular basis of cell migration in the fish lateral line: role of the chemokine receptor CXCR4 and of its ligand, SDF1." Proc Natl Acad Sci U S A **99**(25): 16297-16302.

Davies, S. P., H. Reddy, M. Caivano and P. Cohen (2000). "Specificity and mechanism of action of some commonly used protein kinase inhibitors." Biochem J **351**(Pt 1): 95-105.

de Beco, S., C. Gueudry, F. Amblard and S. Coscoy (2009). "Endocytosis is required for E-cadherin redistribution at mature adherens junctions." Proc Natl Acad Sci U S A **106**(17): 7010-7015.

Der, C. J., T. G. Krontiris and G. M. Cooper (1982). "Transforming genes of human bladder and lung carcinoma cell lines are homologous to the ras genes of Harvey and Kirsten sarcoma viruses." Proc Natl Acad Sci U S A **79**(11): 3637-3640.

Dona, E., J. D. Barry, G. Valentin, C. Quirin, A. Khmelinskii, A. Kunze, S. Durdu, L. R. Newton, A. Fernandez-Minan, W. Huber, M. Knop and D. Gilmour (2013). "Directional tissue migration through a self-generated chemokine gradient." Nature **503**(7475): 285-289.

Dube, N., M. R. Kooistra, W. J. Pannekoek, M. J. Vliem, V. Oorschot, J. Klumperman, H. Rehmann and J. L. Bos (2008). "The RapGEF PDZ-GEF2 is required for maturation of cell-cell junctions." Cell Signal **20**(9): 1608-1615.

Durgan, J., G. Tao, M. S. Walters, O. Florey, A. Schmidt, V. Arbelaez, N. Rosen, R. G. Crystal and A. Hall (2015). "SOS1 and Ras regulate epithelial tight junction formation in the human airway through EMP1." EMBO Rep **16**(1): 87-96.

Eden, S., R. Rohatgi, A. V. Podtelejnikov, M. Mann and M. W. Kirschner (2002). "Mechanism of regulation of WAVE1-induced actin nucleation by Rac1 and Nck." Nature **418**(6899): 790-793.

Egan, S. E., B. W. Giddings, M. W. Brooks, L. Buday, A. M. Sizeland and R. A. Weinberg (1993). "Association of Sos Ras exchange protein with Grb2 is implicated in tyrosine kinase signal transduction and transformation." Nature **363**(6424): 45-51.

Ehrlich, J. S., M. D. Hansen and W. J. Nelson (2002). "Spatio-temporal regulation of Rac1 localization and lamellipodia dynamics during epithelial cell-cell adhesion." Dev Cell **3**(2): 259-270.

Eva, A., G. Vecchio, C. D. Rao, S. R. Tronick and S. A. Aaronson (1988). "The predicted DBL oncogene product defines a distinct class of transforming proteins." Proc Natl Acad Sci U S A **85**(7): 2061-2065.

Ewald, A. J., A. Brenot, M. Duong, B. S. Chan and Z. Werb (2008). "Collective epithelial migration and cell rearrangements drive mammary branching morphogenesis." Dev Cell **14**(4): 570-581.

Ewald, A. J., R. J. Huebner, H. Palsdottir, J. K. Lee, M. J. Perez, D. M. Jorgens, A. N. Tauscher, K. J. Cheung, Z. Werb and M. Auer (2012). "Mammary collective cell migration involves transient loss of epithelial features and individual cell migration within the epithelium." J Cell Sci **125**(Pt 11): 2638-2654.

Farooqui, R. and G. Fenteany (2005). "Multiple rows of cells behind an epithelial wound edge extend cryptic lamellipodia to collectively drive cell-sheet movement." J Cell Sci **118**(Pt 1): 51-63.

Fata, J. E., H. Mori, A. J. Ewald, H. Zhang, E. Yao, Z. Werb and M. J. Bissell (2007). "The MAPK(ERK-1,2) pathway integrates distinct and antagonistic signals from TGFalpha and FGF7 in morphogenesis of mouse mammary epithelium." Dev Biol **306**(1): 193-207.

Fischer, K. R., A. Durrans, S. Lee, J. Sheng, F. Li, S. T. Wong, H. Choi, T. El Rayes, S. Ryu, J. Troeger, R. F. Schwabe, L. T. Vahdat, N. K. Altorki, V. Mittal and D. Gao (2015). "Epithelial-to-mesenchymal transition is not required for lung metastasis but contributes to chemoresistance." Nature **527**(7579): 472-476.

Francis, S. A., X. Shen, J. B. Young, P. Kaul and D. J. Lerner (2006). "Rho GEF Lsc is required for normal polarization, migration, and adhesion of formyl-peptide-stimulated neutrophils." Blood **107**(4): 1627-1635.

Friedl, P. and D. Gilmour (2009). "Collective cell migration in morphogenesis, regeneration and cancer." Nat Rev Mol Cell Biol **10**(7): 445-457.

Gaggioli, C., S. Hooper, C. Hidalgo-Carcedo, R. Grosse, J. F. Marshall, K. Harrington and E. Sahai (2007). "Fibroblast-led collective invasion of carcinoma cells with differing roles for RhoGTPases in leading and following cells." Nat Cell Biol **9**(12): 1392-1400.

Gale, N. W., S. Kaplan, E. J. Lowenstein, J. Schlessinger and D. Bar-Sagi (1993). "Grb2 mediates the EGF-dependent activation of guanine nucleotide exchange on Ras." Nature **363**(6424): 88-92.

Gerhardt, H., M. Golding, M. Fruttiger, C. Ruhrberg, A. Lundkvist, A. Abramsson, M. Jeltsch, C. Mitchell, K. Alitalo, D. Shima and C. Betsholtz (2003). "VEGF guides angiogenic sprouting utilizing endothelial tip cell filopodia." J Cell Biol **161**(6): 1163-1177.

Goitre, L., E. Trapani, L. Trabalzini and S. F. Retta (2014). "The Ras superfamily of small GTPases: the unlocked secrets." Methods Mol Biol **1120**: 1-18.

Goldfarb, M., K. Shimizu, M. Perucho and M. Wigler (1982). "Isolation and preliminary characterization of a human transforming gene from T24 bladder carcinoma cells." Nature **296**(5856): 404-409.

Gomez, N. and P. Cohen (1991). "Dissection of the protein kinase cascade by which nerve growth factor activates MAP kinases." Nature **353**(6340): 170-173.

Haas, P. and D. Gilmour (2006). "Chemokine signaling mediates self-organizing tissue migration in the zebrafish lateral line." Dev Cell **10**(5): 673-680.

Hall, A. (2009). "The cytoskeleton and cancer." Cancer Metastasis Rev **28**(1-2): 5-14.

Hall, A., C. J. Marshall, N. K. Spurr and R. A. Weiss (1983). "Identification of transforming gene in two human sarcoma cell lines as a new member of the ras gene family located on chromosome 1." Nature **303**(5916): 396-400.

Han, D. D., D. Stein and L. M. Stevens (2000). "Investigating the function of follicular subpopulations during Drosophila oogenesis through hormone-dependent enhancer-targeted cell ablation." Development **127**(3): 573-583.

Hart, M. J., A. Eva, T. Evans, S. A. Aaronson and R. A. Cerione (1991). "Catalysis of guanine nucleotide exchange on the CDC42Hs protein by the dbl oncogene product." Nature **354**(6351): 311-314.

Hellstrom, M., L. K. Phng, J. J. Hofmann, E. Wallgard, L. Coultas, P. Lindblom, J. Alva, A. K. Nilsson, L. Karlsson, N. Gaiano, K. Yoon, J. Rossant, M. L. Iruela-Arispe, M. Kalen, H. Gerhardt and C. Betsholtz (2007). "Dll4 signalling through Notch1 regulates formation of tip cells during angiogenesis." Nature **445**(7129): 776-780.

Hobbs, G. A., C. J. Der and K. L. Rossman (2016). "RAS isoforms and mutations in cancer at a glance." J Cell Sci **129**(7): 1287-1292.

Hogan, C., N. Serpente, P. Cogram, C. R. Hosking, C. U. Bialucha, S. M. Feller, V. M. Braga, W. Birchmeier and Y. Fujita (2004). "Rap1 regulates the formation of E-cadherin-based cell-cell contacts." Mol Cell Biol **24**(15): 6690-6700.

Hogg, N. A., C. J. Harrison and C. Tickle (1983). "Lumen formation in the developing mouse mammary gland." J Embryol Exp Morphol **73**: 39-57.

Huebner, R. J., N. M. Neumann and A. J. Ewald (2016). "Mammary epithelial tubes elongate through MAPK-dependent coordination of cell migration." Development **143**(6): 983-993.

Iwanicki, M. P., T. Vomastek, R. W. Tilghman, K. H. Martin, J. Banerjee, P. B. Wedegaertner and J. T. Parsons (2008). "FAK, PDZ-RhoGEF and ROCKII cooperate to regulate adhesion movement and trailing-edge retraction in fibroblasts." J Cell Sci **121**(Pt 6): 895-905.

Jaffe, A. B. and A. Hall (2005). "Rho GTPases: biochemistry and biology." Annu Rev Cell Dev Biol **21**: 247-269.

Jakobsson, L., C. A. Franco, K. Bentley, R. T. Collins, B. Ponsioen, I. M. Aspalter, I. Rosewell, M. Busse, G. Thurston, A. Medvinsky, S. Schulte-Merker and H. Gerhardt (2010). "Endothelial cells dynamically compete for the tip cell position during angiogenic sprouting." Nat Cell Biol **12**(10): 943-953.

Jeon, T. J., D. J. Lee, S. Merlot, G. Weeks and R. A. Firtel (2007). "Rap1 controls cell adhesion and cell motility through the regulation of myosin II." J Cell Biol **176**(7): 1021-1033.

Jeong, H. W., Z. Li, M. D. Brown and D. B. Sacks (2007). "IQGAP1 binds Rap1 and modulates its activity." J Biol Chem **282**(28): 20752-20762.

Jou, T. S., E. E. Schneeberger and W. J. Nelson (1998). "Structural and functional regulation of tight junctions by RhoA and Rac1 small GTPases." J Cell Biol **142**(1): 101-115.

Joyal, J. L., R. S. Annan, Y. D. Ho, M. E. Huddleston, S. A. Carr, M. J. Hart and D. B. Sacks (1997). "Calmodulin modulates the interaction between IQGAP1 and Cdc42. Identification of IQGAP1 by nanoelectrospray tandem mass spectrometry." J Biol Chem **272**(24): 15419-15425.

Karnoub, A. E., D. K. Worthylake, K. L. Rossman, W. M. Pruitt, S. L. Campbell, J. Sondek and C. J. Der (2001). "Molecular basis for Rac1 recognition by guanine nucleotide exchange factors." Nat Struct Biol **8**(12): 1037-1041.

Katagiri, K., A. Maeda, M. Shimonaka and T. Kinashi (2003). "RAPL, a Rap1-binding molecule that mediates Rap1-induced adhesion through spatial regulation of LFA-1." Nat Immunol **4**(8): 741-748.

Kawasaki, Y., R. Sato and T. Akiyama (2003). "Mutated APC and Asef are involved in the migration of colorectal tumour cells." Nat Cell Biol **5**(3): 211-215.

Kiyokawa, E., Y. Hashimoto, S. Kobayashi, H. Sugimura, T. Kurata and M. Matsuda (1998). "Activation of Rac1 by a Crk SH3-binding protein, DOCK180." Genes Dev **12**(21): 3331-3336.

Kiyokawa, E., Y. Hashimoto, T. Kurata, H. Sugimura and M. Matsuda (1998). "Evidence that DOCK180 up-regulates signals from the CrkII-p130(Cas) complex." J Biol Chem **273**(38): 24479-24484.

Knox, A. L. and N. H. Brown (2002). "Rap1 GTPase regulation of adherens junction positioning and cell adhesion." Science **295**(5558): 1285-1288.

Kobielak, A., H. A. Pasolli and E. Fuchs (2004). "Mammalian formin-1 participates in adherens junctions and polymerization of linear actin cables." Nat Cell Biol **6**(1): 21-30.

Komander, D., M. Patel, M. Laurin, N. Fradet, A. Pelletier, D. Barford and J. F. Cote (2008). "An alpha-helical extension of the ELMO1 pleckstrin homology domain mediates direct interaction to DOCK180 and is critical in Rac signaling." Mol Biol Cell **19**(11): 4837-4851.

Krugmann, S., S. Andrews, L. Stephens and P. T. Hawkins (2006). "ARAP3 is essential for formation of lamellipodia after growth factor stimulation." J Cell Sci **119**(Pt 3): 425-432.

Kulesa, P. M. and R. McLennan (2015). "Neural crest migration: trailblazing ahead." F1000Prime Rep **7**: 02.

Lafuente, E. M., A. A. van Puijenbroek, M. Krause, C. V. Carman, G. J. Freeman, A. Berezovskaya, E. Constantine, T. A. Springer, F. B. Gertler and V. A. Boussiotis (2004). "RIAM, an Ena/VASP and Profilin ligand, interacts with Rap1-GTP and mediates Rap1-induced adhesion." Dev Cell **7**(4): 585-595.

Laurin, M. and J. F. Cote (2014). "Insights into the biological functions of Dock family guanine nucleotide exchange factors." Genes Dev **28**(6): 533-547.

Lee, H. S., C. J. Lim, W. Puzon-McLaughlin, S. J. Shattil and M. H. Ginsberg (2009). "RIAM activates integrins by linking talin to ras GTPase membrane-targeting sequences." J Biol Chem **284**(8): 5119-5127.

Leevers, S. J., H. F. Paterson and C. J. Marshall (1994). "Requirement for Ras in Raf activation is overcome by targeting Raf to the plasma membrane." Nature **369**(6479): 411-414.

Li, N., A. Batzer, R. Daly, V. Yajnik, E. Skolnik, P. Chardin, D. Bar-Sagi, B. Margolis and J. Schlessinger (1993). "Guanine-nucleotide-releasing factor hSos1 binds to Grb2 and links receptor tyrosine kinases to Ras signalling." Nature **363**(6424): 85-88.

Li, Z., M. Hannigan, Z. Mo, B. Liu, W. Lu, Y. Wu, A. V. Smrcka, G. Wu, L. Li, M. Liu, C. K. Huang and D. Wu (2003). "Directional sensing requires G beta gamma-

mediated PAK1 and PIX alpha-dependent activation of Cdc42." Cell **114**(2): 215-227.

Liu, L., W. Aerbajinai, S. M. Ahmed, G. P. Rodgers, S. Angers and C. A. Parent (2012). "Radil controls neutrophil adhesion and motility through beta2-integrin activation." Mol Biol Cell **23**(24): 4751-4765.

Lorenowicz, M. J., J. van Gils, M. de Boer, P. L. Hordijk and M. Fernandez-Borja (2006). "Epac1-Rap1 signaling regulates monocyte adhesion and chemotaxis." J Leukoc Biol **80**(6): 1542-1552.

Machacek, M., L. Hodgson, C. Welch, H. Elliott, O. Pertz, P. Nalbant, A. Abell, G. L. Johnson, K. M. Hahn and G. Danuser (2009). "Coordination of Rho GTPase activities during cell protrusion." Nature **461**(7260): 99-103.

Matsubayashi, Y., M. Ebisuya, S. Honjoh and E. Nishida (2004). "ERK activation propagates in epithelial cell sheets and regulates their migration during wound healing." Curr Biol **14**(8): 731-735.

McDonald, J. A., E. M. Pinheiro and D. J. Montell (2003). "PVF1, a PDGF/VEGF homolog, is sufficient to guide border cells and interacts genetically with Taiman." Development **130**(15): 3469-3478.

McGregor, J. R., R. Xi and D. A. Harrison (2002). "JAK signaling is somatically required for follicle cell differentiation in Drosophila." Development **129**(3): 705-717.

McKeown, S. J., A. S. Wallace and R. B. Anderson (2013). "Expression and function of cell adhesion molecules during neural crest migration." Dev Biol **373**(2): 244-257.

McLennan, R., L. Dyson, K. W. Prather, J. A. Morrison, R. E. Baker, P. K. Maini and P. M. Kulesa (2012). "Multiscale mechanisms of cell migration during development: theory and experiment." Development **139**(16): 2935-2944.

McLennan, R., L. J. Schumacher, J. A. Morrison, J. M. Teddy, D. A. Ridenour, A. C. Box, C. L. Semerad, H. Li, W. McDowell, D. Kay, P. K. Maini, R. E. Baker and P. M. Kulesa (2015). "VEGF signals induce trailblazer cell identity that drives neural crest migration." Dev Biol **407**(1): 12-25.

McLennan, R., J. M. Teddy, J. C. Kasemeier-Kulesa, M. H. Romine and P. M. Kulesa (2010). "Vascular endothelial growth factor (VEGF) regulates cranial neural crest migration in vivo." Dev Biol **339**(1): 114-125.

Miki, H., T. Sasaki, Y. Takai and T. Takenawa (1998). "Induction of filopodium formation by a WASP-related actin-depolymerizing protein N-WASP." Nature **391**(6662): 93-96.

Miller, N. L., C. Lawson, E. G. Kleinschmidt, I. Tancioni, S. Uryu and D. D. Schlaepfer (2013). "A non-canonical role for Rgnef in promoting integrin-stimulated focal adhesion kinase activation." J Cell Sci **126**(Pt 21): 5074-5085.

Montell, D. J. (2003). "Border-cell migration: the race is on." Nat Rev Mol Cell Biol **4**(1): 13-24.

Montell, D. J., P. Rorth and A. C. Spradling (1992). "slow border cells, a locus required for a developmentally regulated cell migration during oogenesis, encodes Drosophila C/EBP." Cell **71**(1): 51-62.

Moore, R., E. Theveneau, S. Pozzi, P. Alexandre, J. Richardson, A. Merks, M. Parsons, J. Kashef, C. Linker and R. Mayor (2013). "Par3 controls neural crest

migration by promoting microtubule catastrophe during contact inhibition of locomotion." Development **140**(23): 4763-4775.

Moumen, M., A. Chiche, S. Cagnet, V. Petit, K. Raymond, M. M. Faraldo, M. A. Deugnier and M. A. Glukhova (2011). "The mammary myoepithelial cell." Int J Dev Biol **55**(7-9): 763-771.

Murphy, A. M. and D. J. Montell (1996). "Cell type-specific roles for Cdc42, Rac, and RhoL in Drosophila oogenesis." J Cell Biol **133**(3): 617-630.

Ng, M. R., A. Besser, G. Danuser and J. S. Brugge (2012). "Substrate stiffness regulates cadherin-dependent collective migration through myosin-II contractility." J Cell Biol **199**(3): 545-563.

Nikolic, D. L., A. N. Boettiger, D. Bar-Sagi, J. D. Carbeck and S. Y. Shvartsman (2006). "Role of boundary conditions in an experimental model of epithelial wound healing." Am J Physiol Cell Physiol **291**(1): C68-75.

Nobes, C. D. and A. Hall (1995). "Rho, rac, and cdc42 GTPases regulate the assembly of multimolecular focal complexes associated with actin stress fibers, lamellipodia, and filopodia." Cell **81**(1): 53-62.

Omelchenko, T., M. A. Rabadan, R. Hernandez-Martinez, J. Grego-Bessa, K. V. Anderson and A. Hall (2014). "beta-Pix directs collective migration of anterior visceral endoderm cells in the early mouse embryo." Genes Dev **28**(24): 2764-2777.

Oubaha, M., M. I. Lin, Y. Margaron, D. Filion, E. N. Price, L. I. Zon, J. F. Cote and J. P. Gratton (2012). "Formation of a PKCzeta/beta-catenin complex in endothelial cells promotes angiopoietin-1-induced collective directional migration and angiogenic sprouting." Blood **120**(16): 3371-3381.

Pannekoek, W. J., M. R. Kooistra, F. J. Zwartkruis and J. L. Bos (2009). "Cell-cell junction formation: the role of Rap1 and Rap1 guanine nucleotide exchange factors." Biochim Biophys Acta **1788**(4): 790-796.

Parada, L. F., C. J. Tabin, C. Shih and R. A. Weinberg (1982). "Human EJ bladder carcinoma oncogene is homologue of Harvey sarcoma virus ras gene." Nature **297**(5866): 474-478.

Park, H. O., E. Bi, J. R. Pringle and I. Herskowitz (1997). "Two active states of the Ras-related Bud1/Rsr1 protein bind to different effectors to determine yeast cell polarity." Proc Natl Acad Sci U S A **94**(9): 4463-4468.

Peng, J., B. J. Wallar, A. Flanders, P. J. Swiatek and A. S. Alberts (2003). "Disruption of the Diaphanous-related formin Drf1 gene encoding mDia1 reveals a role for Drf3 as an effector for Cdc42." Curr Biol **13**(7): 534-545.

Pizon, V., P. Chardin, I. Lerosey, B. Olofsson and A. Tavitian (1988). "Human cDNAs rap1 and rap2 homologous to the Drosophila gene Dras3 encode proteins closely related to ras in the 'effector' region." Oncogene **3**(2): 201-204.

Prasad, M. and D. J. Montell (2007). "Cellular and molecular mechanisms of border cell migration analyzed using time-lapse live-cell imaging." Dev Cell **12**(6): 997-1005.

Price, L. S., A. Hajdo-Milasinovic, J. Zhao, F. J. Zwartkruis, J. G. Collard and J. L. Bos (2004). "Rap1 regulates E-cadherin-mediated cell-cell adhesion." J Biol Chem **279**(34): 35127-35132.

Pruitt, W. M., A. E. Karnoub, A. C. Rakauskas, M. Guipponi, S. E. Antonarakis, A. Kurakin, B. K. Kay, J. Sondek, D. P. Siderovski and C. J. Der (2003). "Role of the

pleckstrin homology domain in intersectin-L Dbl homology domain activation of Cdc42 and signaling." Biochim Biophys Acta **1640**(1): 61-68.

Quiros, M. and A. Nusrat (2014). "RhoGTPases, actomyosin signaling and regulation of the epithelial Apical Junctional Complex." Semin Cell Dev Biol **36**: 194-203.

Raaijmakers, J. H. and J. L. Bos (2009). "Specificity in Ras and Rap signaling." J Biol Chem **284**(17): 10995-10999.

Reffay, M., M. C. Parrini, O. Cochet-Escartin, B. Ladoux, A. Buguin, S. Coscoy, F. Amblard, J. Camonis and P. Silberzan (2014). "Interplay of RhoA and mechanical forces in collective cell migration driven by leader cells." Nat Cell Biol **16**(3): 217-223.

Ridley, A. J. (2011). "Life at the leading edge." Cell **145**(7): 1012-1022.

Ridley, A. J. (2015). "Rho GTPase signalling in cell migration." Curr Opin Cell Biol **36**: 103-112.

Ridley, A. J. and A. Hall (1992). "The small GTP-binding protein rho regulates the assembly of focal adhesions and actin stress fibers in response to growth factors." Cell **70**(3): 389-399.

Ridley, A. J., H. F. Paterson, C. L. Johnston, D. Diekmann and A. Hall (1992). "The small GTP-binding protein rac regulates growth factor-induced membrane ruffling." Cell **70**(3): 401-410.

Rojas, A. M., G. Fuentes, A. Rausell and A. Valencia (2012). "The Ras protein superfamily: evolutionary tree and role of conserved amino acids." J Cell Biol **196**(2): 189-201.

Rorth, P. (2002). "Initiating and guiding migration: lessons from border cells." Trends Cell Biol **12**(7): 325-331.

Rorth, P. (2012). "Fellow travellers: emergent properties of collective cell migration." EMBO Rep **13**(11): 984-991.

Ross, S. H., A. Post, J. H. Raaijmakers, I. Verlaan, M. Gloerich and J. L. Bos (2011). "Ezrin is required for efficient Rap1-induced cell spreading." J Cell Sci **124**(Pt 11): 1808-1818.

Rossman, K. L., C. J. Der and J. Sondek (2005). "GEF means go: turning on RHO GTPases with guanine nucleotide-exchange factors." Nat Rev Mol Cell Biol **6**(2): 167-180.

Rossman, K. L., D. K. Worthylake, J. T. Snyder, D. P. Siderovski, S. L. Campbell and J. Sondek (2002). "A crystallographic view of interactions between Dbs and Cdc42: PH domain-assisted guanine nucleotide exchange." EMBO J **21**(6): 1315-1326.

Rozakis-Adcock, M., R. Fernley, J. Wade, T. Pawson and D. Bowtell (1993). "The SH2 and SH3 domains of mammalian Grb2 couple the EGF receptor to the Ras activator mSos1." Nature **363**(6424): 83-85.

Sahai, E. and C. J. Marshall (2002). "ROCK and Dia have opposing effects on adherens junctions downstream of Rho." Nat Cell Biol **4**(6): 408-415.

Santos, E., S. R. Tronick, S. A. Aaronson, S. Pulciani and M. Barbacid (1982). "T24 human bladder carcinoma oncogene is an activated form of the normal human homologue of BALB- and Harvey-MSV transforming genes." Nature **298**(5872): 343-347.

Serres, E., F. Debarbieux, F. Stanchi, L. Maggiorella, D. Grall, L. Turchi, F. Burel-Vandenbos, D. Figarella-Branger, T. Virolle, G. Rougon and E. Van Obberghen-Schilling (2014). "Fibronectin expression in glioblastomas promotes cell cohesion, collective invasion of basement membrane in vitro and orthotopic tumor growth in mice." Oncogene **33**(26): 3451-3462.

Shih, C. and R. A. Weinberg (1982). "Isolation of a transforming sequence from a human bladder carcinoma cell line." Cell **29**(1): 161-169.

Shimono, Y., Y. Rikitake, K. Mandai, M. Mori and Y. Takai (2012). "Immunoglobulin superfamily receptors and adherens junctions." Subcell Biochem **60**: 137-170.

Silver, D. L. and D. J. Montell (2001). "Paracrine signaling through the JAK/STAT pathway activates invasive behavior of ovarian epithelial cells in Drosophila." Cell **107**(7): 831-841.

Simian, M., Y. Hirai, M. Navre, Z. Werb, A. Lochter and M. J. Bissell (2001). "The interplay of matrix metalloproteinases, morphogens and growth factors is necessary for branching of mammary epithelial cells." Development **128**(16): 3117-3131.

Smola, H., H. J. Stark, G. Thiekotter, N. Mirancea, T. Krieg and N. E. Fusenig (1998). "Dynamics of basement membrane formation by keratinocyte-fibroblast interactions in organotypic skin culture." Exp Cell Res **239**(2): 399-410.

Smolen, G. A., B. J. Schott, R. A. Stewart, S. Diederichs, B. Muir, H. L. Provencher, A. T. Look, D. C. Sgroi, R. T. Peterson and D. A. Haber (2007). "A Rap GTPase interactor, RADIL, mediates migration of neural crest precursors." Genes Dev **21**(17): 2131-2136.

Sun, P., Y. Yuan, A. Li, B. Li and X. Dai (2010). "Cytokeratin expression during mouse embryonic and early postnatal mammary gland development." Histochem Cell Biol **133**(2): 213-221.

Suzuki, A., C. Ishiyama, K. Hashiba, M. Shimizu, K. Ebnet and S. Ohno (2002). "aPKC kinase activity is required for the asymmetric differentiation of the premature junctional complex during epithelial cell polarization." J Cell Sci **115**(Pt 18): 3565-3573.

Szabo, A. and R. Mayor (2016). "Modelling collective cell migration of neural crest." Curr Opin Cell Biol **42**: 22-28.

Tambe, D. T., C. C. Hardin, T. E. Angelini, K. Rajendran, C. Y. Park, X. Serra-Picamal, E. H. Zhou, M. H. Zaman, J. P. Butler, D. A. Weitz, J. J. Fredberg and X. Trepat (2011). "Collective cell guidance by cooperative intercellular forces." Nat Mater **10**(6): 469-475.

Theveneau, E., L. Marchant, S. Kuriyama, M. Gull, B. Moepps, M. Parsons and R. Mayor (2010). "Collective chemotaxis requires contact-dependent cell polarity." Dev Cell **19**(1): 39-53.

Totsukawa, G., Y. Yamakita, S. Yamashiro, D. J. Hartshorne, Y. Sasaki and F. Matsumura (2000). "Distinct roles of ROCK (Rho-kinase) and MLCK in spatial regulation of MLC phosphorylation for assembly of stress fibers and focal adhesions in 3T3 fibroblasts." J Cell Biol **150**(4): 797-806.

Valentin, G., P. Haas and D. Gilmour (2007). "The chemokine SDF1a coordinates tissue migration through the spatially restricted activation of Cxcr7 and Cxcr4b." Curr Biol **17**(12): 1026-1031.

Vanni, C., A. Parodi, P. Mancini, V. Visco, C. Ottaviano, M. R. Torrisi and A. Eva (2004). "Phosphorylation-independent membrane relocalization of ezrin following association with Dbl in vivo." Oncogene **23**(23): 4098-4106.

Vasioukhin, V., C. Bauer, M. Yin and E. Fuchs (2000). "Directed actin polymerization is the driving force for epithelial cell-cell adhesion." Cell **100**(2): 209-219.

Vetter, I. R. and A. Wittinghofer (2001). "The guanine nucleotide-binding switch in three dimensions." Science **294**(5545): 1299-1304.

Wakayama, Y., S. Fukuhara, K. Ando, M. Matsuda and N. Mochizuki (2015). "Cdc42 mediates Bmp-induced sprouting angiogenesis through Fmnl3-driven assembly of endothelial filopodia in zebrafish." Dev Cell **32**(1): 109-122.

Wallace, S. W., J. Durgan, D. Jin and A. Hall (2010). "Cdc42 regulates apical junction formation in human bronchial epithelial cells through PAK4 and Par6B." Mol Biol Cell **21**(17): 2996-3006.

Wallace, S. W., A. Magalhaes and A. Hall (2011). "The Rho target PRK2 regulates apical junction formation in human bronchial epithelial cells." Mol Cell Biol **31**(1): 81-91.

Wang, S., T. Watanabe, K. Matsuzawa, A. Katsumi, M. Kakeno, T. Matsui, F. Ye, K. Sato, K. Murase, I. Sugiyama, K. Kimura, A. Mizoguchi, M. H. Ginsberg, J. G. Collard and K. Kaibuchi (2012). "Tiam1 interaction with the PAR complex promotes talin-mediated Rac1 activation during polarized cell migration." J Cell Biol **199**(2): 331-345.

Wang, X., L. He, Y. I. Wu, K. M. Hahn and D. J. Montell (2010). "Light-mediated activation reveals a key role for Rac in collective guidance of cell movement in vivo." Nat Cell Biol **12**(6): 591-597.

Watanabe, N., L. Bodin, M. Pandey, M. Krause, S. Coughlin, V. A. Boussiotis, M. H. Ginsberg and S. J. Shattil (2008). "Mechanisms and consequences of agonist-induced talin recruitment to platelet integrin alphaIIbbeta3." J Cell Biol **181**(7): 1211-1222.

Watanabe, N., T. Kato, A. Fujita, T. Ishizaki and S. Narumiya (1999). "Cooperation between mDia1 and ROCK in Rho-induced actin reorganization." Nat Cell Biol **1**(3): 136-143.

Watson, C. J. and W. T. Khaled (2008). "Mammary development in the embryo and adult: a journey of morphogenesis and commitment." Development **135**(6): 995-1003.

Wennerberg, K., K. L. Rossman and C. J. Der (2005). "The Ras superfamily at a glance." J Cell Sci **118**(Pt 5): 843-846.

Williams, J. M. and C. W. Daniel (1983). "Mammary ductal elongation: differentiation of myoepithelium and basal lamina during branching morphogenesis." Dev Biol **97**(2): 274-290.

Wolf, K., Y. I. Wu, Y. Liu, J. Geiger, E. Tam, C. Overall, M. S. Stack and P. Friedl (2007). "Multi-step pericellular proteolysis controls the transition from individual to collective cancer cell invasion." Nat Cell Biol **9**(8): 893-904.

Worthylake, R. A., S. Lemoine, J. M. Watson and K. Burridge (2001). "RhoA is required for monocyte tail retraction during transendothelial migration." J Cell Biol **154**(1): 147-160.

Xu, X., D. Jin, J. Durgan and A. Hall (2013). "LKB1 controls human bronchial epithelial morphogenesis through p114RhoGEF-dependent RhoA activation." Mol Cell Biol **33**(14): 2671-2682.

Yamada, T., T. Sakisaka, S. Hisata, T. Baba and Y. Takai (2005). "RA-RhoGAP, Rap-activated Rho GTPase-activating protein implicated in neurite outgrowth through Rho." J Biol Chem **280**(38): 33026-33034.

Yang, N., O. Higuchi, K. Ohashi, K. Nagata, A. Wada, K. Kangawa, E. Nishida and K. Mizuno (1998). "Cofilin phosphorylation by LIM-kinase 1 and its role in Rac-mediated actin reorganization." Nature **393**(6687): 809-812.

Yoon, S. and R. Seger (2006). "The extracellular signal-regulated kinase: multiple substrates regulate diverse cellular functions." Growth Factors **24**(1): 21-44.

Zaritsky, A., D. Kaplan, I. Hecht, S. Natan, L. Wolf, N. S. Gov, E. Ben-Jacob and I. Tsarfaty (2014). "Propagating waves of directionality and coordination orchestrate collective cell migration." PLoS Comput Biol **10**(7): e1003747.

Zhadanov, A. B., D. W. Provance, Jr., C. A. Speer, J. D. Coffin, D. Goss, J. A. Blixt, C. M. Reichert and J. A. Mercer (1999). "Absence of the tight junctional protein AF-6 disrupts epithelial cell-cell junctions and cell polarity during mouse development." Curr Biol **9**(16): 880-888.